CALIFORNIA
AIR RESOURCES BOARD

Natural and Working Lands Carbon Inventory

Appendix B: Technical Documentation

2025 Edition

About this Document

This document is designed to complement and expand upon the methods provided in the 2025 NWL Carbon Inventory main report. It is primarily structured by carbon pool (biomass, soil, harvested wood products), with a cross-cutting methodology section at the beginning and a section about wetland greenhouse gas (GHG) fluxes toward the end. Where appropriate, methods are further stratified by land type or soil type. Each section includes a brief comparison with 2018 methodologies, as well as in-depth details on spatial and temporal analyses, uncertainty analyses, and quality assurance and quality control steps. The document concludes with a future work section that highlights ongoing methodological needs and opportunities for advancement.

Contact Information

For questions, contact:

The Nature-Based Strategies Section
California Air Resources Board

nbs@arb.ca.gov

Table of Contents

Overview and Cross-Cutting Methodology

The NWL Carbon Inventory quantifies biomass and soil carbon stocks and stock change across all lands in California, regardless of ownership or management. It also tracks carbon stored in harvested wood products (HWP) as well as greenhouse gas (GHG) fluxes from wetlands.

Estimates for the 2025 NWL Carbon Inventory were produced for the years 2001-2022, with defined reporting intervals for 2001-2013 and 2014-2022 to align with the 2022 Scoping Plan, where appropriate. This section outlines methodology that is pertinent to all land types and reporting categories, including methodological criteria, land cover characterization, and regional assessments.

Methods Criteria

All decisions regarding updates to the NWL Carbon Inventory were made in relation to standardized criteria set forth by CARB (Appendix Table 1). These criteria helped to ensure that the methods and data used were appropriate to meet the goals of the NWL Carbon Inventory, were as rigorous and comprehensive as possible, and are reproducible for others.

Appendix Table 1 - Criteria used to assess methodological updates for the 2025 NWL Carbon Inventory.

Criteria	Details
Spatial Scale	• Have accuracy optimized to statewide scales while also providing sufficient accuracy at the county scale • Ensure wall-to-wall coverage within the state boundary with no double counting
Temporal Scale	• Use available historical data, at least to 2001 • Be as up to date as possible
Spatial Resolution	• Be as spatially explicit as possible, at least to the resolution of ecosystem boundaries • Permit analysis at different stratifications, such as by ownership, management action type, land type, or ecoregion
Temporal Resolution	• Produce annualized values that can be reported very 3-5 years
Thematic Resolution	• Include as many carbon pools and fluxes as possible • Capture at minimum aboveground biomass carbon • Be generally consistent with IPCC GHG inventory guidelines
Sensitivity	• Be sufficiently sensitive to quantify changes as a result of management and other major drivers of change, including climate change • Prioritize assessing directionality and general magnitude of change through time

Practical Criteria	• Generate transparent, repeatable methods that use free or low-cost tools • Prioritize base data that has reasonable expectation of sustainment and openness for use by state staff • Use models that are publicly available and open source • Use base data that require as little pre-processing for state staff as possible • Use base data that have a proven basis in reality and, where applicable, are validated with error or accuracy

Land Cover Classification and Mapping

Land Cover Definitions

The IPCC guidelines define six broad land cover categories, which the NWL Carbon Inventory has adopted: forest land, grassland, cropland, developed land, other land, and wetland. Shrublands were also reported as a distinct land cover category for the NWL Carbon Inventory. Land cover definitions were modified to fit the needs of the NWL Carbon Inventory and in some cases, additional land cover subdivisions were made and used for analysis based on land management, dominant vegetation type, or other factors (Appendix Table 2).

Appendix Table 2 - Land cover categories, their definitions, and subdivisions used in the NWL Carbon Inventory.

Land Cover	NWL Carbon Inventory Definition	Subdivision
Forest land	Forest lands include areas exhibiting ≥10% canopy cover of live trees, but that do not meet the criteria for wetlands or developed lands. Forested wetlands, such as montane meadows or riparian zones, are reported under the wetlands land class.	None
Shrubland	Shrublands include areas exhibiting ≥10% canopy cover of live shrubs and <10% live tree cover that do not meet the criteria for wetlands or developed lands. Shrub-dominated wetlands, such as montane meadows or riparian zones, are reported under the wetlands land class.	Chaparral
Grassland	Grasslands are ecosystems dominated by herbaceous plants with less than 10% tree or shrub cover, but that do not meet the criteria for wetlands or developed lands. This includes rangelands as well as irrigated pastures that fall outside the cropland definition. Herbaceous-dominated wetlands, such as vernal pools, are reported under the wetlands class.	None
Cropland	Croplands encompass all land managed for crop production, including annual and perennial crops, rice fields, crop-pasture rotations, and temporary fallow land. Agroforestry systems, including alley cropping and windbreaks, are considered cropland instead of forest as long as the dominant land use is crop production.	Annual; Perennial; Rice. Within perennial: Almond; Walnut; Pistachio; Vineyard; Citrus; Other Perennial
Developed land	Developed land encompasses areas where humans have built structures, installed energy infrastructure, or created roads. These areas span urban, suburban, exurban, and rural settings, including	Urban; Wildland-Urban Interface; Roads & Energy Infrastructure

	the wildland urban interface. Developed lands may support residential, transportation, manufacturing, and commercial, infrastructure of any size, as well as parks, golf courses, or other maintained green spaces that are surrounded by the built environment. Wetlands and croplands located within census-designated urban areas are classified according to their underlying land type rather than as developed land. The soil in developed lands may be sealed or unsealed.	
Other land	Other lands include areas of sparse vegetation such as sand dunes, bare soil, rock, ice/snow, and land areas that do not fall within the other categories. This also includes unvegetated areas that experience intermittent or partial inundation (e.g., beaches), which lack the hydrologic or soil characteristics needed to be classified as wetland.	None
Wetland	Wetlands are defined as uncultivated land where soils are inundated by water for all or portions of a year, and include coastal wetlands and inland wetlands on mineral soils. Wetlands where the water table has been artificially changed or created through human activity, such as rewetted soils, are also considered wetlands.	Freshwater Mineral Wetlands; Vernal Pools; Montane Meadows; Saline Salt Marshes; Brackish Salt Marshes; Seasonal Organic Wetlands; Freshwater Organic Wetlands; Managed Brackish Wetlands; Rewetted Organic Wetlands

The definitions used for the NWL Carbon Inventory generally aligned with the IPCC (2006) as well as California's Climate Smart Lands Strategy (CNRA, 2022) and Nature-Based Solutions Climate Targets (CNRA, 2024) (Appendix Table 3). However, there were a few exceptions. Namely, the IPCC combines shrublands with forest lands, whereas the 2025 NWL Carbon Inventory treated shrublands as a separate category. In addition, IPCC guidance allows for the inclusion of areas within the Forest Land category where current vegetation structure falls below forest land thresholds but could potentially reach those thresholds in situ; the NWL Carbon Inventory did not apply this provision and instead classified land based on observed vegetation characteristics in any given year. The NWL Carbon Inventory also classified wetlands differently from the Climate Smart Lands Strategy and the development of the Nature-Based Solutions Climate Targets, which both drew heavily from CARB's 2018 NWL Carbon Inventory. For the latter, areas were classified as wetland only if they met hydrologic criteria and were not otherwise classified as another land cover type. For example, forest- and shrub-dominated riparian areas were classified as forest land or shrubland rather than wetland. In contrast, the 2025 NWL Carbon Inventory classified all areas exhibiting wetland hydrology as wetlands, regardless of dominant vegetation or land use characteristics. The updated 2025 NWL Carbon Inventory land cover definitions and maps are being used to report on progress toward the Nature-Based Solutions Climate Targets.

Appendix Table 3 - Land cover categories as defined by the IPCC (2006) and the Climate Smart Lands Strategy (CNRA, 2022).

Land Cover	IPCC Definition	Climate Smart Lands Strategy
Forest land	This category includes all land with woody vegetation consistent with thresholds used to define Forest Land in the national greenhouse gas inventory. It also includes systems with a vegetation structure that currently fall below, but in situ could potentially reach the threshold values used by a country to define the Forest Land category.	Land exhibiting greater than or equal to 10% canopy cover comprised of live trees. The Forest classification also includes riparian forests, which are forest or woodland areas exhibiting greater than or equal to 10% canopy cover comprised of live trees adjacent to a body of water such as a river, stream, lake, or pond.
Shrubland	N/A	Land exhibiting greater than or equal to 10% canopy cover comprised of shrubs or chapparal. These lands are dominated by woody plants but lack tree cover. Riparian willow scrub, woodlands, upland riparian areas, and mixed riparian areas exhibiting greater than or equal to 10% canopy cover comprised of shrubs that do not meet the requirements for a forest are also included in this land cover type.
Grassland	This category includes rangelands and pasture land that are not considered Cropland. It also includes systems with woody vegetation and other non-grass vegetation such as herbs and bushes that fall below the threshold values used in the Forest Land category. The category also includes all grassland from wild lands to recreational areas as well as agricultural and silvopastoral systems, consistent with national definitions.	Areas dominated by grasses or herbaceous vegetation and exhibiting tree or shrub canopy cover below 10%. This encompasses all types of grasslands, including wild lands, recreational areas, and agricultural or livestock related grasslands, such as rangeland or pastureland, that are not classified as croplands.
Cropland	This category includes cropped land, including rice fields, and agro-forestry systems where the vegetation structure falls below the thresholds used for the Forest Land category.	Areas planted in annual or perennial crops and fallow land. This includes irrigated pasture.
Developed land	This category includes all developed land, including transportation infrastructure and human settlements of any size, unless they are already included under other categories. This should be consistent with national definitions.	All developed land such as urban area, human developments in non-urban areas, and transportation infrastructure (e.g., roadways) that traverses either urban or non-urban areas. Includes native and introduced trees and related vegetation in the urban and near-urban areas, including, but not limited to, urban watersheds, soils and related habitats, street trees, park trees, residential trees, natural riparian habitats, and trees on other private and public properties.
Other land	This category includes bare soil, rock, ice, and all land areas that do not fall into any of the other five categories. It allows the total of	Areas characterized primarily by low levels of vegetation, typically resulting from harsh growing conditions. This includes deserts,

	identified land areas to match the national area, where data are available.	barren areas, beaches and dunes, bare rock, ice/snow.
Wetland	This category includes areas of peat extraction and land that is covered or saturated by water for all or part of the year (peatlands and other wetland types) and that does not fall into the Forest Land, Cropland, Grassland or Settlements Developed Land) categories. It includes reservoirs as a managed sub-division and natural rivers and lakes as unmanaged sub-divisions.	Land that is covered or saturated by water for all or portions of a year, and do not fall within other categories. This includes coastal wetlands, drained delta wetlands, freshwater wetlands, floodplains, mountain meadows, vernal pools, alkali sinks and meadows.

Transition Categories

To quantify the magnitude and direction of carbon stock change or reallocation that occurs with conversion from one land cover category to another, the IPCC disaggregates land cover categories into land remaining in that category and land converted from one category to another over time (Appendix Table 4). The 2025 NWL Carbon Inventory estimated land area and carbon stock change associated with each of these land cover transition categories between 2001-2022 and reported them for the periods 2001-2013 and 2014-2022.

Appendix Table 4 - IPCC codes for land cover and land cover transition sub-categories.

IPCC Category	Code	Sub-Category
3B1 Forest Land	3B1a	Forest Land remaining Forest Land
3B1 Forest Land	3B1bi	Cropland Converted to Forest Land
3B1 Forest Land	3B1bii	Grassland Converted to Forest Land
3B1 Forest Land	3B1biii	Wetland Converted to Forest Land
3B1 Forest Land	3B1biv	Developed land Converted to Forest Land
3B1 Forest Land	3B1bv	Other Land Converted to Forest Land
3B2 Cropland	3B2a	Cropland remaining Cropland
3B2 Cropland	3B2bi	Forest Land Converted to Cropland
3B2 Cropland	3B2bii	Grassland Converted to Cropland
3B2 Cropland	3B2biii	Wetland Converted to Cropland
3B2 Cropland	3B2biv	Developed land Converted to Cropland
3B2 Cropland	3B2bv	Other Land Converted to Cropland
3B3 Grassland	3B3a	Grassland remaining Grassland
3B3 Grassland	3B3bi	Forest Land Converted to Grassland
3B3 Grassland	3B3bii	Cropland Converted to Grassland
3B3 Grassland	3B3biii	Wetland Converted to Grassland
3B3 Grassland	3B3biv	Developed land Converted to Grassland
3B3 Grassland	3B3bv	Other Land Converted to Grassland
3B4 Wetland	3B4a	Wetland remaining Wetland
3B4 Wetland	3B4b	Land Converted to Wetland
3B5 Developed Land	3B5a	Developed land remaining Developed land
3B5 Developed Land	3B5bi	Forest Land Converted to Developed land
3B5 Developed Land	3B5bii	Cropland Converted to Developed land
3B5 Developed Land	3B5biii	Grassland Converted to Developed land

3B5 Developed Land	3B5biv	Wetland Converted to Developed land
3B5 Developed Land	3B5bv	Other Land Converted to Developed land
3B6 Other Land	3B6a	Other Land remaining Other Land
3B6 Other Land	3B6bi	Forest Land Converted to Other Land
3B6 Other Land	3B6bii	Cropland Converted to Other Land
3B6 Other Land	3B6biii	Grassland Converted to Other Land
3B6 Other Land	3B6biv	Wetland Converted to Other Land
3B6 Other Land	3B6bv	Developed land Converted to Other Land

To distinguish recent conversions ("land converted to") from long-established land cover ("land remaining"), a 20-year transition (equilibrium) period was adopted by the 2025 NWL Carbon Inventory following IPCC guidance (IPCC, 2006). This represents a departure from the 2018 NWL Carbon Inventory approach, which applied a year-to-year land cover transition method without an explicit equilibrium period. Under the 20-year transition framework, when land converts from one category to another—for example, forest land to grassland—the associated carbon pools are assumed to adjust gradually toward the carbon stock of the new land cover type over time. During this transition window, land is reported as "land converted to" the new category; after the 20 years, once equilibrium is assumed to be reached, it is reported as "land remaining" in that category (Appendix Table 5). If a pixel undergoes an additional land cover change within the 20-year period, the transition clock resets, reflecting adjustment toward a new equilibrium.

Appendix Table 5 - Example land cover change scenarios and how their transition status would be classified using the IPCC 20-year transition approach for inventory years 2001-2022.

Example Scenario	Conversion Year(s)	Land Cover	Sub-Category Classification
A - No Conversion	None	Grassland	Grassland remaining grassland for all years
B - One Conversion	2012	2001-2011: Forest Land; 2012-2022: Grassland	2001-2011: Forest land remaining Forest Land; 2012-2022: Forest Land converted to Grassland
C - Two Conversions	2010 and 2015	2001-2009: Forest Land; 2010-2014: Grassland; 2015-2022: Shrubland	2001-2009: Forest land remaining Forest Land; 2010-2014: Forest Land converted to Grassland; 2015-2022: Grassland converted to Shrubland

Adopting this convention helped ensure that the often slow, post-conversion changes in carbon stocks were captured and reported under the appropriate "land converted to" category rather than prematurely classified as "land remaining" in the new category. This is

particularly important for tracking soil carbon and dead organic matter (e.g., dead wood), which are strongly affected by legacy effects of land cover change. The same 20-year equilibrium convention was used for all carbon pools and land cover transitions, ensuring that changes in biomass and soil carbon were consistently represented across the inventory.

Mapping

The previous 2018 NWL Carbon Inventory mapped lands in three segments—forests and other natural lands (FONL), cropland, and developed land—each built separately using distinct data sources and resolutions. Because spatial boundaries depended on input data coverage, they did not perfectly align, and the 2018 edition did not reconcile these differences; however, any double-counting or under-counting was assumed to be minimal.

In contrast to the 2018 NWL Carbon Inventory, the 2025 edition used an approach that classified California lands into seven main land cover categories (defined in the Land Cover Definitions section above), while ensuring consistent boundaries and eliminating overlaps. This process improved accuracy for the 2025 edition, eliminating unclassified lands (about 1% of the state in the 2018 edition) that had remained outside the scope at that time. The sections below describe the datasets used to map each land cover category for the 2025 NWL Carbon Inventory, and the subsequent Classification Hierarchy section explains how land cover maps were combined and prioritized.

Forest Land, Shrubland, Other Land, and Grassland

Land cover maps for forest land, shrubland, other land and grassland were all derived from LANDFIRE using LANDFIRE-C. LANDFIRE-C modeling from the 2018 NWL Carbon Inventory was updated to support new LANDFIRE products for the years 2016, 2020, and 2022. This included LANDFIRE Existing vegetation type (EVT), existing vegetation cover (EVC), and existing vegetation height (EVH) (LANDFIRE, 2022b,c,d). New data layers required crosswalks to properly interface with existing LANDFIRE-C architecture, and these approaches differed by land type. In forests, compatibility was achieved through the previous inventory method. New LANDFIRE EVT classes were crosswalked to existing classes in LANDFIRE-C. A crosswalk in this context is a mapping or reference table that defines how data elements from one version of a LANDFIRE dataset correspond to data elements in an earlier vintage of the same LANDFIRE dataset. This relied on the existing crosswalk structure, spatial comparison of overlap in undisturbed pixels, and expert opinion. The resulting LANDFIRE-C derived land cover maps were used for forest land, shrubland, other land and grassland. LANDFIRE-C land cover maps were also used to categorize remaining unclassified pixels into developed land and cropland.

Cropland

For 2001–2013, cropland land cover was derived from the USDA Cropland Data Layer (CDL), a national, raster-based crop classification dataset. Annual CDL products were

processed for 2008–2013, while the 2008 CDL map was used as a static proxy for earlier years (2001–2007) to ensure complete temporal coverage. CDL rasters were clipped to the California boundary, reclassified into aggregated annual and perennial land cover classes.

For 2014–2022, cropland land cover was derived from the California Department of Water Resources (DWR) statewide crop mapping dataset. Year-specific crop polygons were rasterized to a 30-m grid using a standardized classification scheme that aggregates detailed crop types into annual and perennial land cover classes. DWR crop mapping data were available for selected years within this period; for years without DWR maps (2015 and 2017), the nearest preceding DWR map was used to maintain temporal continuity. All DWR-based outputs were standardized to a consistent spatial resolution and projection.

Developed Land

Urban areas are specific regions delineated by the U.S. Census Bureau according to housing unit and population density. The Census Bureau updates its urban area map every 10 years. The NWL Carbon Inventory used the 2010 census-delineated urban area map for 2001-2019 and the merged 2010 and 2020 census-delineated urban area maps for 2020-2022. WUI areas are regions outside or bordering urban areas in which there is some amount of impervious surface present, as mapped by the National Land Cover Database (NLCD) impervious surface product integrated into LANDFIRE-C Landcover mapping. R&E areas were mapped by U.S. Census Bureau Topologically Integrated Geographic Encoding and Referencing system (TIGER) lines and data from the Office of Energy Infrastructure Safety, some of which is confidential data. Roads and energy infrastructure data from 2022 were used for 2001-2022.

Wetland

Land cover mapping of wetland categories relied on the California Aquatic Resources Inventory (CARI) and additional maps of rewetting activities in the Delta. As with the previous inventory, CARI was crosswalked into IPCC relevant categories of Inland Wetland Mineral Soils and Coastal Wetlands based on “major class” and “wetland type” properties. Updated from the previous inventory, IPCC rewetted organic soils were identified using maps of rewetting activities in the Delta provided by the Delta Conservancy. Inland wetland mineral soils were further disaggregated into managed freshwater mineral wetlands, unmanaged freshwater mineral wetlands, and vernal pools using “wetland type” and “anthropogenic modifier” properties. Additionally, montane meadows were extracted from other mineral wetlands by setting unmanaged freshwater mineral wetlands in the Sierra and Klamath ecoregions to a separate category. This approach was taken in the absence of a suitable montane meadows map but is likely an overestimate of current montane meadows extent. Coastal wetlands were further disaggregated into saline salt marshes, brackish salt marshes, managed brackish wetlands, and freshwater organic wetlands using the “Salinity_modifier” and “Anthropogenic_modifier” properties of CARI. Seasonal organic

wetlands were further identified as any freshwater wetland on Histosol soils—other than rewetted organic wetlands—in the Delta ecoregion.

Classification Hierarchy

To generate complete land cover maps for the State of California for all years in the 2025 NWL Carbon Inventory, individual land cover maps (described in the Mapping section above) were combined using a hierarchical decision framework. Under this framework, land cover maps were combined for each year, and where overlaps occurred, a prioritization scheme was used to determine which land cover category took precedence (Appendix Table 6). In these areas of overlap, land cover categories that were assigned higher priority values overwrote land cover categories with lower priority values. For example, if a pixel was covered by both the developed land census urban area map (Priority 2) and the forest, shrubland, and other land map (Priority 1), it was designated as developed land. The resulting land cover maps contained a unique land cover value for each 30-meter pixel within California. For reporting purposes, two additional datasets containing primary and secondary roads and energy infrastructure were added to the land cover map and overlaid over forest land, shrubland and other lands. See the Biomass Carbon Methodological Details, Soil Carbon Methodological Details, and GHG Flux Methodological Details sections for more information on how the land cover maps were used to quantify and report on carbon trends.

Appendix Table 6 - Classification hierarchy by priority value

IPCC Land Cover Category	Land Cover Dataset Name	Priority
Cropland	Delta Rice	7
Cropland & Grassland	Perennial Crops and Grasslands	6
Wetland	Delta Wetlands	5
Wetland	CARI Wetlands	4
Cropland	Annual Crops	3
Developed Land	Census Urban Areas	2
Forest, Shrubland, Other Land	Forest, Shrubland, Other Lands	1

Comparison with the CARB AB 32 Inventory

The NWL Carbon Inventory addresses the carbon (CO_2) component of the agriculture, forestry, and other land use (AFOLU) sector (IPCC, 2006). In a complementary effort, CARB's AB 32 GHG Inventory addresses GHG emissions from other select categories of agriculture, as well as from the industry, transportation, electric power, commercial and residential, and recycling and waste sectors. Together, these inventories offer a more complete accounting of California's emissions and removals related to natural and working lands (NWL; Appendix Table 7) and provide a consistent basis for tracking progress toward California's climate goals.

Appendix Table 7 - Mapping of NWL-related IPCC categories and sub-categories to CARB's NWL Carbon Inventory and AB 32 GHG Inventory.

IPCC Category	Code	Sub-Category	CARB Inventory
3A1 – Enteric Fermentation	3A1ai-3A1j	All livestock types	AB 32 GHG Inventory
3A2 – Manure Management	3A2ai-3A2j	All livestock types	AB 32 GHG Inventory
3B1 – Forest Land	3B1a	Forest Land remaining Forest Land	NWL Carbon Inventory
3B1 – Forest Land	3B1bi-3B1bv	Land converted to Forest Land	NWL Carbon Inventory
3B2 - Cropland	3B2a	Cropland remaining Cropland	NWL Carbon Inventory
3B2 - Cropland	3B2bi-3B2bv	Land converted to Cropland	NWL Carbon Inventory
3B3 - Grassland	3B3a	Grassland remaining Grassland	NWL Carbon Inventory
3B3 - Grassland	3B3bi-3B3bv	Land converted to Grassland	NWL Carbon Inventory
3B4 - Wetland	3B4a	Wetland remaining Wetland	NWL Carbon Inventory
3B4 - Wetland	3B4b	Land converted to Wetland	NWL Carbon Inventory
3B5 – Developed Land	3B5a	Developed land remaining Developed land	NWL Carbon Inventory
3B5 – Developed Land	3B5bi-3B5bv	Land converted to Developed land	NWL Carbon Inventory
3B6 – Other Land	3B6a	Other Land remaining Other Land	NWL Carbon Inventory
3B6 – Other Land	3B6bi-3B6bv	Land converted to Other Land	NWL Carbon Inventory
3C - Aggregate Sources and Non-CO_2 Emissions Sources on Land	3C1a	Biomass Burning in Forest Land	NWL Carbon Inventory
3C - Aggregate Sources and Non-CO_2 Emissions Sources on Land	3C1b	Biomass Burning in Cropland	AB 32 GHG Inventory
3C - Aggregate Sources and Non-CO_2 Emissions Sources on Land	3C1c	Biomass Burning in Grassland	NWL Carbon Inventory
3C - Aggregate Sources and Non-CO_2 Emissions Sources on Land	3C1d	Biomass Burning in All Other Land	NWL Carbon Inventory
3C - Aggregate Sources and Non-CO_2 Emissions Sources on Land	3C2	Liming	AB 32 GHG Inventory
3C - Aggregate Sources and Non-CO_2 Emissions Sources on Land	3C3	Urea Application	AB 32 GHG Inventory
3C - Aggregate Sources and Non-CO_2 Emissions Sources on Land	3C4	Direct N_2O Emissions from Managed Soils (Fertilizer)	AB 32 GHG Inventory
3C - Aggregate Sources and Non-CO_2 Emissions Sources on Land	3C5	Indirect N_2O Emissions from Managed Soils (Fertilizer)	AB 32 GHG Inventory
3C - Aggregate Sources and Non-CO_2 Emissions Sources on Land	3C6	Indirect N_2O Emissions from Manure Management	AB 32 GHG Inventory
3C - Aggregate Sources and Non-CO_2 Emissions Sources on Land	3C7	Rice Cultivations	AB 32 GHG Inventory

Regional Assessment

Nine regions delineated by California's Fifth Climate Change Assessment were used to explore regional patterns in carbon stocks and stock change for each land type in the 2025 NWL Carbon Inventory (Appendix Figure 1). These regions spanned in size from 2.7 to 26.7 million acres (Appendix Table 8) and were established via a public process led by the Governor's Office of Land Use and Climate Innovation to capture and represent the climatic, ecological, and sociopolitical variation that exists across California.

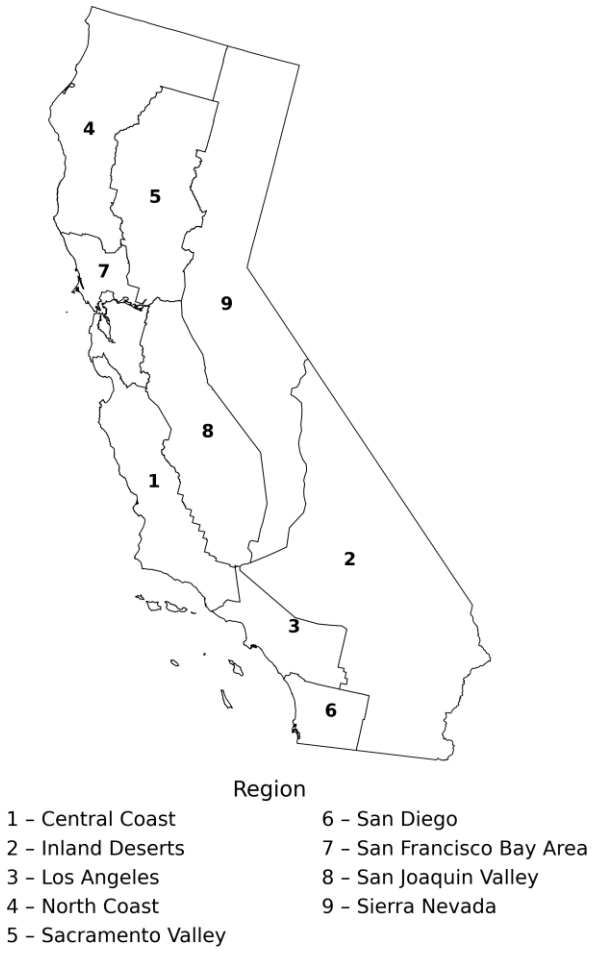

Appendix Figure 1 – Nine regions used to explore regional patterns by land type. Regions were adopted from the California Fifth Climate Change Assessment framework and reflect unique climatic, ecological, and sociopolitical conditions across the state. The San Francisco Bay Area (7) region spans above and below the Bay, although the number 7 is only displayed above it.

Appendix Table 8 – Land area extent within the nine regions across California. Area does not include open water.

Region	Area (Million Acres)
San Diego	2.7
Sierra Nevada	21.0
San Joaquin Valley	10.8
San Francisco Bay Area	4.1
Sacramento Valley	9.6
Los Angeles	4.5
North Coast	12.1
Inland Deserts	26.7
Central Coast	8.2

Using these regions, standardized assessments were performed across all land types and carbon pools. Regional maps of total carbon, biomass carbon, and soil carbon were produced, as well as tables summarizing land area (million acres), carbon stocks (million metric tons; MMT), and carbon densities (metric tons [MT] C/acre) by land type and region. In addition, net change in land area, biomass carbon stocks, and soil carbon stocks were calculated and plotted by land type and region for the reporting periods 2001-2013 and 2014-2022. Net change was calculated by subtracting values at the beginning of each reporting period (2001 and 2014) from the values at the end of each reporting period (2014 and 2022). Due to data limitations, the change assessment for biomass carbon stocks could not be conducted for developed lands across either period or for croplands in 2001-2013.

Biomass Carbon Methodological Details

Biomass carbon estimates were quantified for each land type using IPCC Tier 3 methodologies that varied in scope and approach (Appendix Table 9). Each land type specific methodology is described in more detail in the sections below.

Following quantification, statewide land cover maps with a unique classification for each 30 m pixel (see the Mapping section above) were used to create and assign biomass carbon values, producing spatially complete biomass carbon stock maps for 2012, 2018, and 2022. Due to data limitations, biomass carbon stock estimates outside of 2012, 2018, and 2022 were missing for developed lands. Similarly, croplands had missing estimates for 2001, 2003-06, 2008, 2010-11, 2013, 2015, and 2017.

Once the biomass carbon maps were produced, carbon stocks (MMT), carbon densities (MT C/acre), as well as annual and cumulative change were determined by comparing estimates over time. When values for developed land or cropland were missing in scatterplots, they were estimated using simple linear interpolation or extrapolation based on surrounding years. In addition to summarizing biomass carbon stocks by land type over time, net carbon stock change with land conversion was also evaluated by summing the annualized biomass carbon stock gains and losses associated with each transition under an equilibrium-based

framework. This approach accounted for carbon gains and losses over each transition period (2001-2013 and 2014-2022), ensuring the cumulative net change reflected the integrated effect of land cover dynamics over time.

Appendix Table 9 - IPCC Tier and methods summary for estimating biomass carbon by land type.

Reporting Category	Tier	Method Summary	Scope
Forest land	3	LANDFIRE-C modeling	Aboveground biomass, belowground biomass, dead wood, understory, litter
Shrubland	3	LANDFIRE-C modeling	Aboveground biomass, belowground biomass, dead wood, litter
Grassland	3	Rangeland Analysis Platform	Aboveground biomass, belowground biomass
Cropland	3	Allometry and orchard mapping	Aboveground biomass, belowground biomass
Developed land	3	Allometry and LANDFIRE-C modeling	Urban: aboveground & belowground biomass of standing live trees. WUI/R&E: same as forest land, shrubland, grassland
Other land	3	LANDFIRE-C modeling	Aboveground biomass, belowground biomass, dead wood, litter

Forest Land

2025 Methods

Methodological Updates

The 2025 NWL Carbon Inventory update for forests builds on the 2018 NWL Carbon Inventory by incorporating new LANDFIRE products for 2016, 2020, and 2022, as well as annual disturbance data for 2001–2022. LANDFIRE-C modeling was updated to use the 2016 LANDFIRE remapped base map and incorporated hindcasting to maintain continuity throughout the entire inventory period. Carbon stocks were annualized across the full inventory period, attributing changes to the exact disturbance year using annual LANDFIRE disturbance data. LANDFIRE-C was no longer used to quantify carbon in grasslands but

continued to track deadwood contributions from type-converting forest fires. Compared to 2018 methods, these updates enhanced spatial and temporal resolution, improved disturbance attribution, and created a continuous annual inventory for forests from 2001 to 2022.

Detailed Methods Description

Input Data Processing

LANDFIRE-C modeling from the 2018 NWL Carbon Inventory was updated to support new LANDFIRE products for 2016, 2020, and 2022 (Appendix Table 10). This included LANDFIRE Existing Vegetation Type (EVT), Existing Vegetation Cover (EVC), and Existing Vegetation Height (EVH) (LANDFIRE, 2022b,c,d). New data layers required crosswalks to properly interface with existing LANDFIRE-C architecture, and these approaches differed by land type. Crosswalk, in this context, refers to the translation of data from one format or categorical scheme to another, often by aggregating or disaggregated categories and reformatting text. Crosswalk structure refers to a collective system of many individual crosswalks. In forests, compatibility was achieved through the previous inventory method. New LANDFIRE EVT classes were crosswalked to existing classes in LANDFIRE-C using the existing crosswalk structure, spatial comparison of overlaps in undisturbed pixels, and expert opinion. EVC and EVH were reformatted to match the syntax used in the 2018 Carbon Inventory and existing LANDFIRE-C parameterization. This approach was necessary due to the absence of Forest Inventory Analysis (FIA) or comparable datasets to parameterize newly added EVT, EVC, and EVH classes for forest lands, limiting the updates possible within LANDFIRE-C.

In some cases, the land type indicated by LANDFIRE EVT did not align with the land type represented by EVC and EVH. For example, following high-severity wildfire, EVT may still classify an area as forest, while EVC and EVH reflect a transition to grassland. To maintain consistency with CARB's land type definitions and reflect current conditions, EVT was adjusted to correspond with EVC and EVH classifications. While this approach improves alignment and facilitates quantification, it introduces potential limitations in LANDFIRE-C modeling for post-wildfire ecosystems. Although major carbon pools such as deadwood are accounted for during this conversion, other biomass pools may differ from available EVT parameterizations under post-fire conditions, increasing uncertainty.

Appendix Table 10 - Data used to support the forest land methodological update.

Input Data	Source (Citation)	Purpose	Brief Description
LANDFIRE Existing Vegetation Type (EVT)	(LANDFIRE, 2022d)	LANDFIRE-C Input Dataset	Vegetation classes for the years 2001, 2010, 2012, 2014, 2016, 2020, and 2022
LANDFIRE Existing Vegetation Height (EVH)	(LANDFIRE, 2022c)	LANDFIRE-C Input Dataset	Vegetation height for the years 2001, 2010, 2012,

			2014, 2016, 2020, and 2022 (meters)
LANDFIRE Existing Vegetation Cover (EVC)	(LANDFIRE, 2022b)	LANDFIRE-C Input Dataset	Vegetation cover for the years 2001, 2010, 2012, 2014, 2016, 2020, and 2022 (percentage)
LANDFIRE Annual Disturbance	(LANDFIRE, 2022a)	LANDFIRE-C Input Dataset	Disturbance mapping for each year from 2001 to 2022.
CAL FIRE FRAP Historic Wildfire Perimeters	(CAL FIRE, 2025)	Disturbance Modifications for 2021	Wildfire Perimeters for the year 2021

Basemap Updates

LANDFIRE-C was updated to use LANDFIRE's 2016 basemap instead of the previous 2001 basemap. In the 2018 Carbon Inventory, LANDFIRE-C relied on LANDFIRE products produced for 2001, 2010, 2012, and 2014. LANDFIRE produces basemap-derived products, meaning conditions in later years (2010, 2012, and 2014) are contingent on the initial conditions set in 2001 and subsequent disturbance, growth factors, and other applied rules (Dewitz, 2025). In 2016, LANDFIRE completed a remap and updated to a 2016 basemap using modern data and methods (LANDFIRE, 2021). This new basemap only affects LANDFIRE products for 2016 onward; earlier LANDFIRE datasets were not retroactively updated. While the LANDFIRE remap provides multiple benefits to LANDFIRE-C modeling, it also introduced a break in continuity during the 2014–2016 inventory period using the previous method.

To mitigate the temporal discontinuity introduced by the 2016 remap, basemap updates were hindcasted from 2016 to 2001. During hindcasting, areas that experienced disturbance—as defined by LANDFIRE's annual disturbance data—retained the carbon quantification from 2001–2014 LANDFIRE-C outputs. Landscapes that did not experience disturbance between 2001 and 2016 relied on 2016 LANDFIRE outputs. All existing LANDFIRE-C model functionality was retained during this process, including accounting for deadwood following wildfire, regional growth factors, and land cover transitions. Following hindcasting from 2016 to 2001, LANDFIRE-C was run forward from 2016 to 2022 to create a continuous time series.

Annualization

Carbon stocks were updated to an annual timescale for the full inventory period of 2001 to 2022. Annualization relied on annual LANDFIRE disturbance data to reallocate carbon stock changes to the relevant disturbance year(s) (LANDFIRE, 2022a). For example, if a wildfire took place in 2008, this previously would have been accounted for in the next available LANDFIRE dataset year (2010). The updated annualization process reattributes these changes in carbon stock from 2010 to 2008 for all areas affected by that wildfire. If multiple disturbances took place between available dataset years, the carbon stock change was distributed evenly between the relevant years. Following annualization, growth of biomass

carbon stocks was also reattributed for affected pixels, allowing growth and recovery to follow annual intervals as well.

Given that LANDFIRE data releases occur at uneven intervals, the annualization scheme carries greater uncertainty during earlier inventory periods, particularly from 2001 to 2010. This limitation is most pronounced in areas experiencing frequent or repeated disturbances within these extended gaps. As annualization distributes carbon stock changes evenly across repeat disturbances, it does not capture the relative severity of disturbances. As a result, landscapes with multiple disturbances during a period may demonstrate simplified patterns that underestimate or overestimate relative effects but capture cumulative effect.

Disturbance Quantification

LANDFIRE-C disturbance data was updated to include annual disturbance from 2001 to 2022. Newly introduced disturbance codes were crosswalked to existing LANDFIRE-C disturbance codes (Battles et al., 2013). Annual disturbance data was used to create annual estimates of biomass carbon stock, as described above.

During the 2025 inventory update, LANDFIRE-C was no longer used to quantify carbon stock in grasslands but continued to attribute deadwood to grasslands following type-converting forest fires. Type-converting forest fires include any wildfire that resulted in the conversion of a forest land cover to another land cover and is most common in high-severity wildfire footprints. Deadwood from these wildfires was added to biomass carbon estimates for grasslands. This contributed to the significant increase in biomass carbon observed in grasslands during later inventory periods.

LANDFIRE-C was updated to allow retention and decomposition of deadwood following type-converting wildfire. This was implemented by converting 80% of aboveground live (AGL) biomass to deadwood post fire with a linear decay period of 20 years. Conversion factors were determined by averaging FOFEM simulations using ranges of overstory mortality from MTBS data and from field observations of combustion rates (Stenzel et al., 2019). A 20-year coefficient was used based on IPCC's default coefficient for transition between land classes (IPCC, 2006). Deadwood remains on site and decays with this pattern separately from deadwood produced through subsequent changes in EVT, EVC, and EVH.

Wildfire in the year 2021 was found to differ in LANDFIRE datasets when compared to other maps of wildfire. Multiple megafires generally considered to have occurred in 2021 were instead attributed to 2022 in LANDFIRE disturbance data (LANDFIRE, 2022a). This is likely related to how long these fires were active, particularly where suppression activities crossed a calendar year. To correct this, CAL FIRE FRAP fire perimeters (CAL FIRE, 2025) for 2021 were used to reattribute disturbance within the LANDFIRE product. Any wildfire disturbance that occurred in 2022 within LANDFIRE's map but occurred in 2021 within the CAL FIRE FRAP fire perimeters was reattributed from 2022 to 2021 in model inputs. This modification was then propagated through carbon stock and land cover processes.

Uncertainty Analysis

Uncertainty in the NWL Carbon Inventory forest estimates and the intercomparison forest carbon products was evaluated by comparing each product to CARB Offset Project sites within California for the year 2020. CARB Offset Project sites are operated as part of the Cap and Trade Program within CARB and are primarily located in high productivity forested areas in Northern California (*https://ww2.arb.ca.gov/our-work/programs/compliance-offset-program*). Each intercomparison product that contained raster data for the year 2020 was included. Aboveground standing biomass carbon for each Offset Project site was derived empirically based on field data and allometric equations. Aboveground live biomass carbon was averaged across the Offset Project sites. Aboveground live biomass carbon for the NWL Carbon Inventory and each intercomparison carbon product was computed by averaging the pixels corresponding to the CARB Offset Project site footprint.

The carbon values for the Offset Project sites were provided in aboveground standing biomass carbon, which contains both live and dead standing carbon. Dead standing carbon includes snags but not down wood. Due to the inclusion of standing dead, the Offset Project values may be biased upward. However, the total amount of standing dead carbon within the Offset Project sites was estimated to be less than 5% of total standing carbon.

QA/QC Activities

Due to the need for quantifying aboveground carbon for purposes beyond carbon inventories (e.g. research and offset programs), multiple governmental, university, and private research groups have developed carbon products over the past decade that may be leveraged to assess the quality of the NWL Carbon Inventory. These products range from global scale to national and regional scales, with some products developed primarily for forests whereas other products encompass all land cover types. The products generally differ in the data, methods, and sensors employed to derive carbon stock estimates, providing unique approaches for estimating carbon across the state that provide different strengths and weaknesses.

CARB leveraged the expertise and knowledge underlying these 'intercomparison' carbon products to inform California's understanding of carbon stocks. The results from NWL Carbon Inventory were compared to each of the intercomparison products with two emphases. First, the similarity in the total amount of carbon was assessed to evaluate whether the NWL Carbon Inventory was biased relative to the intercomparison products. Second, the temporal trajectories of each product were assessed to evaluate similarities in behavior between the products.

Forest Intercomparison Product Datasets

A total of eight independent carbon product datasets were incorporated into the forest intercomparison (Appendix Table 11). For participation in the comparison, CARB compiled a list of potential carbon product groups. Each of the groups were contacted with a request

to provide maps of aboveground live biomass or aboveground live biomass carbon, along with any other related variables that are available across the entire state of California. Aboveground live pools were specifically requested as this variable was the only common variable among all datasets.

Appendix Table 11 – List of intercomparison carbon products used to evaluate NWL Carbon Inventory. The years with available data and the key citations are also included.

Product	Years Available	Citation
CECS	2000-2023	NA
Ctrees	2000, 2015, 2020, 2021	NA
FIA_CA	2010-2021	Christensen et al. (2021)
LEMMA	2000-2021	Ohmann et al. (2002), Battles et al. (2018)
NFCMS	2000, 2010, 2020	Williams et al. (2012)
Planet	2013-2023	Anderson et al. (2025)
TreeMap	2016, 2020, 2022	Riley et al. (2022)
Yu et al.	2005, 2010, 2015-2017	Yu et al. (2022)

CECS: Above-ground biomass was provided by the Center for Ecosystems Climate Solutions (CECS) for the period from 2000 to 2023. No product details are available at this time.

CTrees: The CTrees' carbon product estimates above-ground biomass (AGB) by combining ground inventory data with remote sensing from aerial and satellite sources. The product can provide estimates for all woody vegetation types, including forests, woodlands, savanna, and wetlands. The product is available from 2000 to the present day at a 100 m spatial resolution. The methodology establishes above-ground biomass using a combination of satellite-based LIDAR measurements (ICESat and GEDI) calibrated with ground plots and airborne LIDAR. In addition, change detection is generated using machine learning with satellite radar and optical imagery. Uncertainty is assessed through error propagation models. Remote sensing datasets include Harmonized Landsat and Sentinel-2, ALOS PALSAR, GEDI, ICESAT-2, MODIS, and VIIRS. Further details can be found at the CTrees website: *https://ctrees.org/*.

FIA-CA: The FIA-CA product is based on estimates of Forest Inventory and Analysis (FIA) plots. FIA plots are surveyed on a decadal time scale, with about 10% of all plots being surveyed on an annual basis. Regional estimates of forest aboveground live biomass carbon are derived from regional FIA equations that consider bole, bark, branches and leaves. The FIA-CA biomass carbon estimates are not spatially distributed at a pixel scale. Consequently, FIA-CA carbon rasters were not produced for comparison with other intercomparison products or for validation. FIA-CA estimates were available annually from 2010 to 2021. Details about FIA-CA can be found in Christensen et al. (2017) and Christensen et al. (2021).

LEMMA: The Landscape Ecology Modeling, Mapping & Analysis (LEMMA) product combines change detection via LandTrendr and direct gradient analysis with nearest-

neighbor imputation for predictive forest mapping. The LandTrendr algorithm is used to remove noise from Landsat image time series and create maps that characterize major trends (e.g. growth, disturbance). The image time series is then matched with FIA plot data using a gradient nearest neighbor (GNN) algorithm to produce forest biomass maps. GNN incorporates an imputation methodology based on similar climate, topography, and spectral indices. Regional biomass expansion factors were used to estimate aboveground biomass from field data. LEMMA produces estimates of aboveground biomass at a 30 m spatial resolution and is available annually starting in 2000 for forested regions of Washington, Oregon, and California. Greater details about the methods underlying the LEMMA product can be found at Ohmann et al. (2002) and Battles et al. (2018).

NFCMS: The National Forest Carbon Monitoring System (NFCMS) combines an ecosystem carbon cycle model, FIA data, and satellite estimates of biomass and forest disturbances. NFCMS used FIA-based stand age and the Carnegie-Ames-Stanford Approach (CASA) forest carbon cycle model to calculate carbon stocks for combinations of forest-type, productivity level, local conditions, and disturbance. NFCMS is produced at a 30 m resolution and is available at a decadal timescale (e.g. 2000, 2010, 2020). Methodological changes to NFCMS occurred between the 2010 and 2020 versions, such that the product cannot be used to assess carbon change through time. The model, however, is still used for the intercomparison because the aboveground live carbon estimates from NFCMS provide a useful estimate of California biomass carbon for the years it is available. More information about NFCMS can be found at Williams et al. (2012).

Planet: Planet's Forest Carbon Diligence product estimates aboveground live biomass carbon based on machine-learning models that incorporate satellite observations and airborne and spaceborne LIDAR. The airborne LIDAR data was gathered from open-source datasets worldwide, while spaceborne LIDAR was obtained from GEDI and ICESat-2. Satellite imagery included Landsat and Sentinel-2. To generate biomass carbon, canopy height and canopy cover are first estimated from surface reflectance, wood density data and Synthetic Aperture Radar. Aboveground live biomass carbon is then generated based on canopy height, canopy cover, elevation, and location via light gradient-boosting machine (LightGBM) regression models. The Planet product is available globally at a 30 m resolution starting annually from 2013. Details on the Planet Forest Carbon Diligence product can be found at Anderson et al. (2025).

TreeMap: TreeMap combines machine learning, FIA plots, and LANDFIRE input data to generate estimates of aboveground live biomass carbon. The methodology imputes forest data from FIA to landscape maps based on a suite of LANDFIRE variables such as vegetation height, vegetation cover, and vegetation group, along with location, topography, and biophysical variables. A random forest machine learning algorithm is used for imputation. TreeMap also incorporates disturbance as a response variable. TreeMap has a resolution of 30 m and is available for forested areas of the contiguous United States. Further information on the TreeMap product can be found at Riley et al. (2022).

Yu et al. (2022): Yu et al. (2022) estimated aboveground biomass carbon at the CONUS-scale using a non-parametric remote sensing-based model. The model was based on a modified version of the Maximum Entropy Estimator (MaxEnt). Nine remote sensing-based datasets were used as inputs into the model. Four of the inputs were based on Landsat bands, two were based on L-band ALOS PALSAR polarizations, two were based on SRTM digital elevation model data, and the final input was based on tree-cover percentage derived from high-resolution NAIP and Landsat imagery. The model was calibrated and validated using more than 120,000 plots from the FIA program. Aboveground biomass carbon was generated for years 2005, 2010, 2015, 2016, and 2017 at 100 m resolution. Full details about the dataset can be found in Yu et al. (2021) and Yu et al. (2022).

Forest Intercomparison Methods

Once obtained, each intercomparison carbon raster was imported, reprojected to Conus Albers (EPGS - 5070), and resampled to a common 30m grid and California extent. Units were converted to metric tons of biomass carbon per acre (MT C/acre). Products provided as aboveground biomass were converted to aboveground biomass carbon assuming a 0.47 carbon fraction of biomass.

For direct comparison of forest biomass carbon between products, all rasters needed a common forest footprint. However, the forest extent of each carbon product differed, with some products having wall-to-wall California coverage across many land-cover types while others only encompassed forested regions using differing forest masks. For consistency across years and products, we defined the forest extent based on the LANDFIRE forest classification for the year 2001. For each product, all pixels with values within this footprint contributed to the aboveground live biomass carbon estimates for forested lands. Missing values were ignored.

The decision to use 2001 LANDFIRE forest footprint for all products and all years has some implications for the intercomparison. For the NWL Carbon Inventory, which is based on LANDFIRE-C, all pixels in 2001 should be expected to be forest. In subsequent years, land-cover change (e.g. forest to grass following fire) would likely decrease aboveground live biomass carbon within the footprint. Land-cover change to forest that occurs outside the footprint would have no impact. Thus, we may expect some decrease in carbon over time due to land-cover change. For the intercomparison products, missing pixels within the footprint do not contribute to the aboveground live biomass carbon totals. As such, products with a higher number of missing forest pixels may have carbon stocks that are biased downwards relative to products that provide fuller spatial coverage within the footprint.

Uncertainty in the NWL Carbon Inventory forest estimate and the intercomparison forest carbon products was evaluated by comparing each product to CARB Offset Project sites within California for the year 2020. CARB Offset Project sites are operated as part of the Cap-and-Invest Program within CARB and are primarily located in high productivity forested

areas in Northern California (*https://ww2.arb.ca.gov/our-work/programs/compliance-offset-program*). Each intercomparison product that contained raster data for the year 2020 was included. Aboveground standing biomass carbon for each Offset Project site was derived empirically based on field data and allometric equations. Aboveground live biomass carbon was averaged across the Offset Project sites. Aboveground live biomass carbon for the NWL Carbon Inventory and each intercomparison carbon product was computed by averaging the pixels corresponding to the CARB Offset Project site footprint.

2018 Methods

The 2018 NWL Carbon Inventory used LANDFIRE-C for biomass carbon estimation. LANDFIRE-C was developed for CARB in 2015 to assess carbon stocks and changes for all land categories in California with the exception of agricultural and urban areas (Battles et al., 2013, CARB 2018b). This method used California specific land-based data sets and satellite remote sensing data to estimate carbon contained in aboveground and belowground pools for both live and dead vegetation but excludes soil carbon. Data sources for the method included ground-based data from the Forest Inventory and Analysis (FIA) program of the USDA-Forest Service, remote sensing products from NASA's MODIS sensor, geospatial vegetation attributes and disturbance activity (fire, harvest etc.) data from the federal Landscape Fire and Resource Management Planning Tools Project (Landfire.gov). LANDFIRE-C calculates carbon stocks based on three LANDFIRE products—vegetation type (EVT), canopy cover (EVC), and height (EVH)—and established look-up tables. The look-up tables were created using the relationship between the LANDFIRE products and FIA data.

Shrubland

2025 Methods

Methodological Updates

The 2025 NWL Carbon Inventory update created shrublands as a new category. Within shrublands, LANDFIRE-C built on the 2018 NWL Carbon Inventory by recalibrating shrubland biomass quantification across the state, incorporating new LANDFIRE products for 2016, 2020, and 2022, and integrating annual disturbance data for 2001–2022.

Recalibration involved processing federal plot-level data into carbon densities using allometric equations. LANDFIRE-C modeling was updated to use the 2016 LANDFIRE remapped base map and incorporated hindcasting to maintain continuity throughout the entire inventory period. Carbon stocks were annualized across the full inventory period, attributing changes to the exact disturbance year using annual LANDFIRE disturbance data. Compared to 2018 methods, these updates enhanced spatial and temporal resolution, improved disturbance attribution, and created a continuous annual inventory for shrublands from 2001 to 2022.

Detailed Methods Description

Shrubland Disaggregation

Shrublands were quantified as a separate land cover class in the 2025 NWL Carbon Inventory. Previously, shrublands were quantified within forest lands for consistency with IPCC categories (IPCC, 2006). While this framework aligned with IPCC, it was not compatible with other inventories implemented under the same framework, such as the U.S. EPA's Greenhouse Gas Inventory (EPA, 2024). In the U.S. EPA Greenhouse Gas Inventory, shrublands are grouped into grasslands. This meant neither forest lands nor grasslands were directly comparable to federal programs until shrublands were disaggregated. In addition, other state efforts, such as the Nature-Based Solutions Climate Targets, set separate targets for forests and shrublands (CNRA, 2024). Thus, shrublands were quantified as a separate category for compatibility with other inventories and programs.

Input Data Processing

LANDFIRE-C modeling from the 2018 NWL Carbon Inventory was updated to support new LANDFIRE products for 2016, 2020, and 2022 (Appendix Table 12). This included LANDFIRE Existing Vegetation Type (EVT), Existing Vegetation Cover (EVC), and Existing Vegetation Height (EVH) (LANDFIRE, 2022b,c,d). New data layers required crosswalks to properly interface with existing LANDFIRE-C architecture, and these approaches differed by land type. Crosswalk, in this context, refers to the translation of data from one format or categorical scheme to another, often by aggregating or disaggregated categories and reformatting text. Please see the Recalibration section below for details on the approach used for shrublands.

In some cases, the land type indicated by LANDFIRE EVT did not align with the land type represented by EVC and EVH. For example, following high-severity wildfire, EVT may still classify an area as forest land, while EVC and EVH reflect a transition to shrubland. To maintain consistency with CARB's land type definitions and reflect current conditions, EVT was adjusted to correspond with EVC and EVH classifications. While this approach improves alignment and facilitates quantification, it introduces potential limitations in LANDFIRE-C modeling for post-wildfire ecosystems. Although major carbon pools such as deadwood are

accounted for during this conversion, other biomass pools may differ from available EVT parameterizations under post-fire conditions, increasing uncertainty.

Appendix Table 12 - Data used to support the shrubland methodological update.

Input Data	Source (Citation)	Purpose	Brief Description
LANDFIRE Existing Vegetation Type (EVT)	(LANDFIRE, 2022d)	LANDFIRE-C Input Dataset	Vegetation classes for the years 2001, 2010, 2012, 2014, 2016, 2020, and 2022
LANDFIRE Existing Vegetation Height (EVH)	(LANDFIRE, 2022c)	LANDFIRE-C Input Dataset	Vegetation height for the years 2001, 2010, 2012, 2014, 2016, 2020, and 2022 (meters)
LANDFIRE Existing Vegetation Cover (EVC)	(LANDFIRE, 2022b)	LANDFIRE-C Input Dataset	Vegetation cover for the years 2001, 2010, 2012, 2014, 2016, 2020, and 2022 (percentage)
LANDFIRE Annual Disturbance	(LANDFIRE, 2022a)	LANDFIRE-C Input Dataset	Disturbance mapping for each year from 2001 to 2022.
CAL FIRE FRAP Historic Wildfire Perimeters	(CAL FIRE, 2025)	Disturbance Modifications for 2021	Wildfire Perimeters for the year 2021
BLM Terrestrial Assessment, Inventory, and Monitoring (AIM) plot data	(BLM, 2025)	Input for plot-level carbon densities used to recalibrate LANDFIRE-C	Field Plot data collected through BLM AIM programs assessing the health, status, and trend in plots overlapping California's Shrublands and Other Lands
LANDFIRE-DB	(LANDFIRE, 2021)	Input for plot-level carbon densities used to recalibrate LANDFIRE-C	Field plot data synthesized by LANDFIRE from multiple programs.

Recalibration

In shrublands, LANDFIRE-C was recalibrated using field plot data. Using plot data, new EVT classes were parameterized where possible and crosswalked to previous classes where data was not available. Crosswalk, in this context, refers to the translation of data from one format or categorical scheme to another, often by aggregating or disaggregated categories and reformatting text. Crosswalk structure refers to a collective system of many individual crosswalks. Similarly, EVH crosswalks were updated to use modern formats. When crosswalking to earlier years with the previous EVH format, height was assumed to be the center of a provided range. In previous LANDFIRE-C versions, EVC was not included when quantifying shrublands (Gonzalez, 2015). Recalibration in the 2025 Carbon Inventory considered EVC where plot-level data were available. EVC inputs relied on modern formats for available years and were crosswalked to previous formats for earlier years, as with EVH.

Recalibration of LANDFIRE-C relied on 2,750 plot-level carbon densities and LANDFIRE-C inputs (EVT, EVC, and EVH) for shrublands. Plots were first separated into calibration and validation datasets, withholding 10% of all plots for validation. Calibration of AGL and total carbon relied on multiple linear regression of LANDFIRE-C EVC and EVH by EVT. Regressions were then used to create lookup keys for all potential canopy cover and canopy height combinations of each EVT. In processing a broad range of ecosystems, certain exceptions were made: (i) If fewer than three plots were available for calibrating an EVT class, parameters from the previous inventory were used instead of new parameters; (ii) If either EVC or EVH regressions resulted in a negative slope, the regression relied only on the other parameter; (iii) If both EVC and EVH resulted in a negative slope or if EVC and EVH did not show any variation across plots, carbon density was averaged and held static for all combinations of EVC and EVH.

Plot-level carbon data was synthesized from federal databases and converted to carbon densities using the Rangeland Vegetation Simulator (RVS). Plot-level data was collected from the BLM Assessment, Inventory, and Monitoring (AIM) and LANDFIRE-DB programs (LANDFIRE, 2021; BLM, 2025). From each dataset, parameters were reformatted and converted to match inputs required by the RVS plot module. These input data included shrub canopy cover (%), shrub canopy height (ft), grass/forb canopy cover (%), grass/forb canopy height (ft), dominant species, latitude, and longitude. The RVS model also sources inputs from LANDFIRE biophysical settings (BPS) and five years of precipitation and NDVI data for each plot (Reeves et al., 2016). As RVS is limited to one dominant species as input, carbon densities may be over- or underestimated where significant carbon pools are stored in subdominant species (such as sparse tree cover) or where allometries for a particular species were not available. In the event a species did not have an allometric equation, the species was crosswalked to a similar species with an allometry.

RVS produced outputs of aboveground live (AGL) carbon rather than total carbon. Total carbon includes AGL along with deadwood, belowground biomass, and litter. To reconstruct total carbon from RVS outputs, previous LANDFIRE-C parameterizations were converted into ratios of each pool with respect to AGL (Battles et al., 2013). When belowground carbon pool ratios were not available, an average ratio of 0.74 (root:shoot) was used based on published allometries for California shrub species (Kummerow et al., 1977; Miller & Ng, 1977).

Basemap Updates

LANDFIRE-C was updated to use LANDFIRE's 2016 basemap instead of the previous 2001 basemap. In the 2018 Carbon Inventory, LANDFIRE-C relied on LANDFIRE products produced for 2001, 2010, 2012, and 2014. LANDFIRE produces basemap-derived products, meaning conditions in later years (2010, 2012, and 2014) are contingent on the initial conditions set in 2001 and subsequent disturbance, growth factors, and other applied rules (Dewitz, 2025). In 2016, LANDFIRE completed a remap and updated to a 2016 basemap using modern data and methods (LANDFIRE, 2021). This new basemap only affects

LANDFIRE products for 2016 onward; earlier LANDFIRE datasets were not retroactively updated. While the LANDFIRE remap provides multiple benefits to LANDFIRE-C modeling, it also introduced a break in continuity during the 2014–2016 inventory period using the previous method.

To mitigate the temporal discontinuity introduced by the 2016 remap, basemap updates were hindcasted from 2016 to 2001. During hindcasting, areas that experienced disturbance—as defined by LANDFIRE's annual disturbance data—retained the carbon quantification from 2001–2014 LANDFIRE-C outputs. Landscapes that did not experience disturbance between 2001 and 2016 relied on 2016 LANDFIRE outputs. All existing LANDFIRE-C model functionality was retained during this process, including accounting for deadwood following wildfire, regional growth factors, and land cover transitions. Following hindcasting from 2016 to 2001, LANDFIRE-C was run forward from 2016 to 2022 to create a continuous time series.

Annualization

Carbon stocks were updated to an annual timescale for the full inventory period of 2001 to 2022. Annualization relied on annual LANDFIRE disturbance data to reallocate carbon stock changes to the relevant disturbance year(s) (LANDFIRE, 2022a). For example, if a wildfire took place in 2008, this previously would have been accounted for in the next available LANDFIRE dataset year (2010). The updated annualization process reattributes these changes in carbon stock from 2010 to 2008 for all areas affected by that wildfire. If multiple disturbances took place between available dataset years, the carbon stock change was distributed evenly between the relevant years. Following annualization, growth of biomass carbon stocks was also reattributed for affected pixels, allowing growth and recovery to follow annual intervals as well.

Given that LANDFIRE data releases occur at uneven intervals, the annualization scheme carries greater uncertainty during earlier inventory periods, particularly from 2001 to 2010. This limitation is most pronounced in areas experiencing frequent or repeated disturbances within these extended gaps. As annualization distributes carbon stock changes evenly across repeat disturbances, it does not capture the relative severity of disturbances. As a result, landscapes with multiple disturbances during a period may demonstrate simplified patterns that underestimate or overestimate relative effects but capture cumulative effect.

Disturbance Quantification

LANDFIRE-C disturbance data was updated to include annual disturbance from 2001 to 2022. Newly introduced disturbance codes were crosswalked to existing LANDFIRE-C disturbance codes (Battles et al., 2013). Annual disturbance data was used to create annual estimates of biomass carbon stock, as described above.

LANDFIRE-C was updated to allow retention and decomposition of deadwood following type-converting wildfire. This was implemented by converting 80% of aboveground live

(AGL) biomass to deadwood post fire with a linear decay period of 20 years. Conversion factors were determined by averaging FOFEM simulations similar to Forest Lands (Stenzel et al., 2019). A 20-year coefficient was used based on IPCC's default coefficient for transition between land classes (IPCC, 2006). Deadwood remains on site and decays with this pattern separately from deadwood produced through subsequent changes in EVT, EVC, and EVH.

Wildfire in the year 2021 was found to differ in LANDFIRE datasets when compared to other maps of wildfire. Multiple megafires generally considered to have occurred in 2021 were instead attributed to 2022 in LANDFIRE disturbance data (LANDFIRE, 2022a). This is likely related to how long these fires were active, particularly where suppression activities crossed a calendar year. To correct this, CAL FIRE FRAP fire perimeters (CAL FIRE, 2025) for 2021 were used to reattribute disturbance within the LANDFIRE product. Any wildfire disturbance that occurred in 2022 within LANDFIRE's map but occurred in 2021 within the CAL FIRE FRAP fire perimeters was reattributed from 2022 to 2021 in model inputs. This modification was then propagated through carbon stock and land cover processes.

Chaparral

Analysis of chaparral communities within the broader shrublands land type relied on CAL FIRE FRAP fveg and Carbon Inventory maps of forest lands. Chaparral and coastal sage scrub communities were delineated semantically from the fveg "WHRNAME" property (CAL FIRE, 2015). CAL FIRE FRAP fveg products from 2015 were used to align with LANDFIRE's 2016 basemap. Processing included removing pixels listed as chaparral in fveg but listed as forest at any point during the inventoried period, based on inventory land cover maps. This method removed the effects of type-converting forest fire on statewide chaparral carbon stocks, providing insight into areas which were already chaparral or transitioned into chaparral though other mechanisms. Biomass carbon stocks for chaparral would likely be higher and may have a larger, total carbon stock decline if chaparral in previously forested pixels was included. Future inventory updates would benefit from using temporally-explicit maps to disaggregate chaparral from shrublands.

Uncertainty Analysis

Uncertainty in the Shrublands NWL Carbon Inventory was evaluated by comparing shrubland total biomass carbon against total biomass carbon values generated from empirically based field site measurements. Field data included synthesized federal, state, and literature plots in California, scaled using allometric equations. Field data was divided into calibration and validation subcomponents. Only withheld validation plots were used for the uncertainty analysis. Total biomass carbon for the NWL Carbon Inventory was derived from the pixels corresponding to field plot footprints.

QA/QC Activities

Quality assurance and quality control procedures were applied to the shrubland workflow to ensure quantification and spatial integration were implemented correctly. First, estimates

were compared against intercomparison products that had spatial coverage encompassing shrublands - ranging from global scale to regional scale products. Second, randomly selected pixels within mapped shrublands were manually inspected to verify recalibration was applied correctly through time, including cases where land cover changed. Finally, summarized trends in carbon were visually examined to confirm that temporal patterns were consistent with expected system behavior and known land-use dynamics.

2018 Methods

The 2018 NWL Carbon Inventory used LANDFIRE-C for biomass carbon estimation. LANDFIRE-C was developed for CARB in 2015 to assess carbon stocks and changes for all land categories in California with the exception of agricultural and urban areas (Battles et al., 2013, CARB 2018b). This method used California specific land-based data sets and satellite remote sensing data to estimate carbon contained in aboveground and belowground pools for both live and dead vegetation but excluded soil carbon. Data sources for the method included ground-based data from the Forest Inventory and Analysis (FIA) program of the USDA-Forest Service, remote sensing products from NASA's MODIS sensor, geospatial vegetation attributes and disturbance activity (fire, harvest etc.) data from the federal Landscape Fire and Resource Management Planning Tools Project (Landfire.gov), and ancillary data on shrublands and grasslands. LANDFIRE-C calculates carbon stocks based on three LANDFIRE products—vegetation type (EVT), canopy cover (EVC), and height (EVH)—and established look-up tables. The look-up tables were created using the relationship between the LANDFIRE products and FIA data.

Grassland

2025 Methods

Methodological Updates

Grassland biomass stocks were estimated using an updated Tier 3 approach that incorporates recent advances in spatially explicit rangeland monitoring. Annual aboveground herbaceous biomass was derived from the Rangeland Analysis Platform (RAP), which provides annual remotely sensed estimates of herbaceous biomass based on satellite

data acquired at roughly 16-day intervals. Belowground biomass was calculated from aboveground biomass using ecosystem specific root-to-shoot ratios complied from published literature. Above- and belowground components were summed to obtain a total live biomass, which was converted to a carbon stock using a 0.45 carbon fraction. This produces spatially explicit, annually varying estimates of grassland biomass carbon stock.

The 2025 method replaces the earlier Tier 3 approach used in 2018, which relied on MODIS-derived annual NPP at 1-km resolution and applied a single root-to-shoot ratio to partition above- and belowground biomass. RAP based estimates provide an improvement in spatial resolution, temporal coverage, and the direct estimation of aboveground herbaceous production.

Detailed Methods Description

This analysis quantified live biomass carbon in areas classified as grassland or irrigated pasture, focusing on above- and below-ground herbaceous biomass. Only herbaceous vegetation (grasses and other non-woody plants) was included; woody shrubs and trees within grassland pixels were not included in the biomass estimate. The grassland portion of the inventory also accounted for legacy dead-wood biomass in areas that transitioned from forest to grassland (e.g., post-disturbance), which were classified as grassland but still contained standing or downed woody material. Dead-wood carbon was included for completeness but was quantified separately from the remote sensing derived herbaceous biomass estimates.

Herbaceous Biomass Estimation

Aboveground herbaceous biomass was estimated using the Rangeland Analysis Platform (RAP), a remote sensing–based product developed through USDA-NRCS, the Bureau of Land Management (BLM), and the University of Montana (Jones et al. 2021). RAP provides annual, spatially explicit estimates of herbaceous biomass at 30-m resolution across the western United States, derived from openly available Landsat surface reflectance, climate variables, and extensive field-plot data. RAP produces both 16-day biomass estimates and seasonal total biomass products; for this analysis, CARB used the seasonal total (peak-season) herbaceous biomass values. These annual RAP estimates form the foundation for calculating total herbaceous biomass and downstream carbon stock estimates in the grassland inventory.

Belowground biomass was estimated directly from aboveground herbaceous biomass using a generalized grass root-shoot allometric equation from Gao et al. (2024). CARB staff applied the published functional-type relationship for generalized grasses, which estimates root biomass from aboveground (leaf) biomass as:

$$BGB = 1.033965\ x\ (AGB)^{0.9654983}$$

Where BGB is belowground biomass and AGB is aboveground biomass. This equation integrates data from multiple grass species common in California and provides a single, empirically derived root–shoot relationship suitable for statewide application.

Total live biomass was then calculated by adding the estimated belowground biomass to the aboveground biomass for each pixel and year, and a carbon fraction of 0.45 was applied to convert total biomass to carbon, consistent with IPCC default values for herbaceous vegetation.

Uncertainty Analysis

To quantify uncertainty and evaluate the performance of RAP-based aboveground biomass estimates, CARB staff compared RAP values against independent empirical datasets (Appendix Table 13). These external datasets included: (1) field plot measurements compiled from 112 sites across (Appendix Table 14), and (2) forage production estimates from Liu et al. (2021), derived using a light-use-efficiency modeling approach for 2005–2017 and provided by the Yufang Jin Remote Sensing and Ecosystem Change Lab at UC Davis.

Appendix Table 13 - Data used to support the grassland methodological update.

Input Data	Source (Citation)	Purpose	Brief Description
Herbaceous biomass	Rangeland Analysis Product (RAP)	Aboveground biomass estimate	Units: Lbs/acre Extent: Statewide
Allometric relationships	Gao et al., 2024	Functional type specific allometric equations for leaf, stem and root biomass	Units: NA
Forage Production	Liu et al., 2021. Data provided by Yufang Jin Lab - Remote Sensing and Ecosystem Change	Compare and validate RAP model estimates	Units: Kg/ha Extent: Selected CA rangelands across the Coast Ranges and Sierra Nevada Foothills
Field Measurements	See Appendix Table 14	Compare and validate RAP model estimates	Units: kg/acre

For each dataset, RAP estimates at coincident field locations were extracted and evaluated using standard performance metrics, including mean bias error (MBE), mean absolute error (MAE), root-mean-square error (RMSE), mean absolute error (MAE), and coefficient of determination (R^2). These quantitative metrics provide a statistical basis for assessing RAP's accuracy in capturing the magnitude of observed herbaceous biomass across a range of environmental conditions and years (See Appendix Table 13 for a summary of datasets used to support the grassland methodological update).

Appendix Table 14 - Grassland field-plot datasets used in the analysis

Dataset	Project Name	Reference
1	Coastal Rangeland Dataset	Strohm, H., Foster, E., & Carey, C.J. (2025). *Bale Grazing Experiment* [Unpublished dataset]. TomKat Ranch.
2	Rangeland Carbon Management Project	Foster, E., Cook, A., Banuelos, A., Stricker, E., Paustian, K., Eash, L., & Carey, C. J. (2025). *Rangeland Carbon Management Project* [Unpublished dataset]. Point Blue Conservation Science.
3	Rangeland Management Series	Becchetti, T., George, M., McDougald, N., Dudley, D., Connor, M., Flavel, D., … & Markegard, G. (2016). *Rangeland Management Series: Annual Range Forage Production* (Publication 8018). University of California, Division of Agriculture and Natural Resources. Retrieved March 2025, from *https://escholarship.org/content/qt7kt9s61c/qt7kt9s61c.pdf*
4	Forage Production Summary Report	Larsen, R. E., Althouse, L., Brown, K., Horney, M., Striby, K. Humagain, K., Prendergast, M., & Shapero, M. 2024. Forage Production Summary Report: San Luis Obispo County, 2001–2022. San Luis Obispo, CA: University of California Cooperative Extension. Available at: https://ucanr.edu/sites/default/files/2024-05/397925.pdf

QA/QC Activities

QA/QC activities were conducted to verify the reliability of the grassland biomass estimates and to identify potential sources of inconsistency. As part of verification using independent external information, CARB staff compared multi-year time series of RAP biomass at shared field locations with both (1) direct field measurements and (2) the independently developed Liu et al. (2021) forage production dataset. These comparisons enabled staff to evaluate whether RAP captured interannual variability, relative differences among sites, and general productivity patterns over time. This step complements statistical uncertainty metrics by assessing temporal dynamics and identifying any systematic deviations or anomalies.

Additional QA/QC measures included screening RAP-derived biomass values for missing or anomalous values and examining the corresponding field plot data and Liu et al. (2021) estimates for outliers or inconsistencies. Staff reviewed multi-year values at each site to identify unusually high or low observations and applied a 95% filtering threshold to remove extreme outliers in the empirical datasets prior to comparison. When RAP values appeared anomalous, they were cross-checked against the filtered field and Liu datasets to determine whether they reflected real site conditions or potential data artifacts.

To assess whether grassland biomass showed increasing, decreasing, or non-significant trends over time, a Man-Kendall trend test was applied. The Man-Kendall trend is a non-parametric method widely used in ecological time-series analysis and evaluates whether a monotonic trend (consistently upward or downward) is present in a time series. This test was

applied separately to herbaceous biomass and to total biomass (herbaceous plus legacy dead wood from previously burned or converted forests) to distinguish whether observed trends in the inventory reflect changes in grassland herbaceous productivity or changes in the spatial extent and composition of grassland areas.

2018 Methods

In 2018, aboveground biomass carbon for grasslands was estimated using a Tier 3 method. MODIS annual NPP data (2000–2010) was determined at a 1 km spatial resolution using the MOD17A3 product, which was calibrated with field measurements by NASA. Above- and belowground biomass was estimated from the NPP values using a root-to-shoot ratio of 4.224. To quantify uncertainty in carbon stock changes, Monte Carlo methods were used as described in Gonzales et al. (2015).

Cropland

2025 Methods

Methodological Updates

Woody perennial biomass carbon was estimated using a spatially explicit Tier 3 approach, integrating ground-based data collection with remote sensing and statistical modeling techniques. Annual maps of perennial crop type and orchard age were combined with crop-specific allometric equations to estimate carbon stored in aboveground and belowground biomass.

For the 2014–2022 period, CARB updated its cropland biomass methodology in three primary ways. First, an averaged allometric relationship was added for "other orchard" categories lacking species-specific allometry, enabling quantification of a previously unaccounted biomass carbon pool. Second, orchard acreage and age inputs were derived from California Department of Water Resources (DWR) spatially explicit crop mapping products, replacing older, aggregated NASS statistics and simplified orchard age assumptions and thereby substantially improving spatial precision. Third, because early DWR crop maps (2014, 2016, 2018, 2019) did not report planting year, CARB developed machine-learning models to infer orchard age from multi-decadal Landsat surface reflectance and vegetation index time series. Separate models were trained for each crop-

map year using fields with stable crop types and known 2020 planting years as training labels, producing spatially complete orchard-age layers for 2014–2022 and enabling dynamic, field-level biomass carbon estimates across California croplands.

Detailed Methods Description

Cropland biomass consists of carbon stored in the aboveground (stems and branches) and belowground (coarse roots) of woody perennial crops. Woody perennial biomass carbon was estimated using a Tier 3 approach by combining maps of perennial crop type and orchard age with crop-specific allometric equations to estimate carbon stored. Carbon biomass stored in herbaceous annual crops was assumed to be ephemeral—grown and subsequently removed from the land within a year—and therefore considered negligible.

Orchard Allometry

Allometric equations are species-specific models that estimate tree biomass from measurable structural attributes such as diameter at breast height (DBH) and canopy height. Although satellite imagery can provide information on canopy structure, it typically must be coupled with allometric relationships to translate remotely sensed measurements into biomass estimates (Xu et al. 2018). CARB previously developed species-specific allometric equations that translate orchard type and age into carbon density per unit area for key perennial crops including almonds, walnuts, pistachios, and citrus (see the Cropland 2018 Methods section for more detail).

For this inventory update, these crop-specific equations were averaged to derive an allometric relationship for "other orchard" types lacking species-specific allometry (e.g., peaches, plums, cherries). This averaged equation carries higher uncertainty than the crop-specific equations, but it is assumed that biomass for other orchard types falls within this expanded uncertainty range. Incorporating this "other orchards" equation adds a biomass carbon pool that was not previously quantified.

Orchard allometry is composed of two sub-equations. The carbon-per-tree (CPT) function follows a power-law form:

$$CPT(age) = a \times age^{b}$$

where age is the orchard age in years and the fitted coefficients a and b are crop-specific. The trees per acre (TPA) function is logarithmic:

$$TPA(age) = a\, ln(age) + b$$

where age is the orchard age in years and the fitted coefficients a and b are crop-specific. The TPA function captures how tree density changes with stand age. For a given orchard type and age, the sub equations estimate carbon per tree and trees per acre and then multiplies them to produce carbon per acre allometry:

$$Carbon\ per\ acre = TPA(age) \times CPT(age)$$

Applying an area scaling (e.g., total acres) yields total carbon for each orchard type. Species-specific fitted coefficients for CPT and TPA functions, including the averaged allometric equation for other orchards, are provided in (Appendix Table 15). Age-dependent allometry was not available for grapes; therefore, a non–age-specific carbon density of 10.0 Mg C ha^{-1}, representing woody components only (cordons, trunk, and roots), was applied based on Morandé, et al. (2017).

Appendix Table 15 - Fitted coefficients a and b for each orchard type for the trees per acre (TPA) function and the carbon per tree function. "Others" refers to the fitted coefficients from the averaged allometry of almonds, walnuts, pistachios, and citrus, which is assumed to sufficiently represent other orchard species growing in California.

Orchard Type	TPA *a*	TPA *b*	CPT *a*	CPT *b*
Almonds	-15.45	125.72	12.98	1.39
Walnuts	-19.97	103.50	9.33	1.61
Pistachios	-24.70	184.98	1.29	1.88
Citrus	-34.71	223.83	2.44	1.37
Others	-27.23	170.80	5.71	1.57

Orchard Acreage and Age Data

Orchard acreage and age were derived from the spatially explicit DWR statewide crop mapping dataset (DWR, 2022). DWR crop mapping is produced annually from 2014–2023 (except 2015 and 2017) and delineates agricultural fields as polygons with attributes for crop type, irrigation method, and land use class. Beginning in 2020, the dataset also includes orchard planting year for major perennial crops (e.g., almonds, pistachios, walnuts, citrus, and other tree crops). Because orchard acreage and age are core inputs to the biomass allometric equations, these field-based layers provide more precise, spatially explicit, and time-varying estimates of acreage and age distributions used to calculate orchard biomass carbon. This time series enables dynamic, spatially explicit orchard age quantification for the 2014–2022 period.

Appendix Table 16 - Data used to support the cropland methodological update.

Input Data	Source (Citation)	Purpose	Brief Description
DWR crop mapping dataset	California Department of Water Resources (DWR)	Input data	Annual, field-level crop classification and age maps produced by DWR across

			California. Years included: 2012, 2014, 2016, 2018–2022.
Crop data layer	USDA Cropland Data Layer (CDL)	Input data	National, raster-based crop classification dataset provides consistent land use coverage where DWR data are unavailable.

Orchard Age Modeling Approach

Earlier DWR crop map products (2014, 2016, 2018, and 2019) did not include orchard planting year. To generate consistent orchard age estimates across these datasets, a machine learning–based approach was used to infer orchard establishment year from long-term satellite observations. Orchard development follows a characteristic temporal trajectory with low and spatially variable vegetation cover immediately after planting, followed by rapid canopy expansion, and ultimately a relatively stable mature phase. These stage transitions are detectable in satellite time series using vegetation indices, particularly the Normalized Difference Vegetation Index (NDVI), which captures changes in vegetation greenness and canopy density over time (Appendix Figure 2).

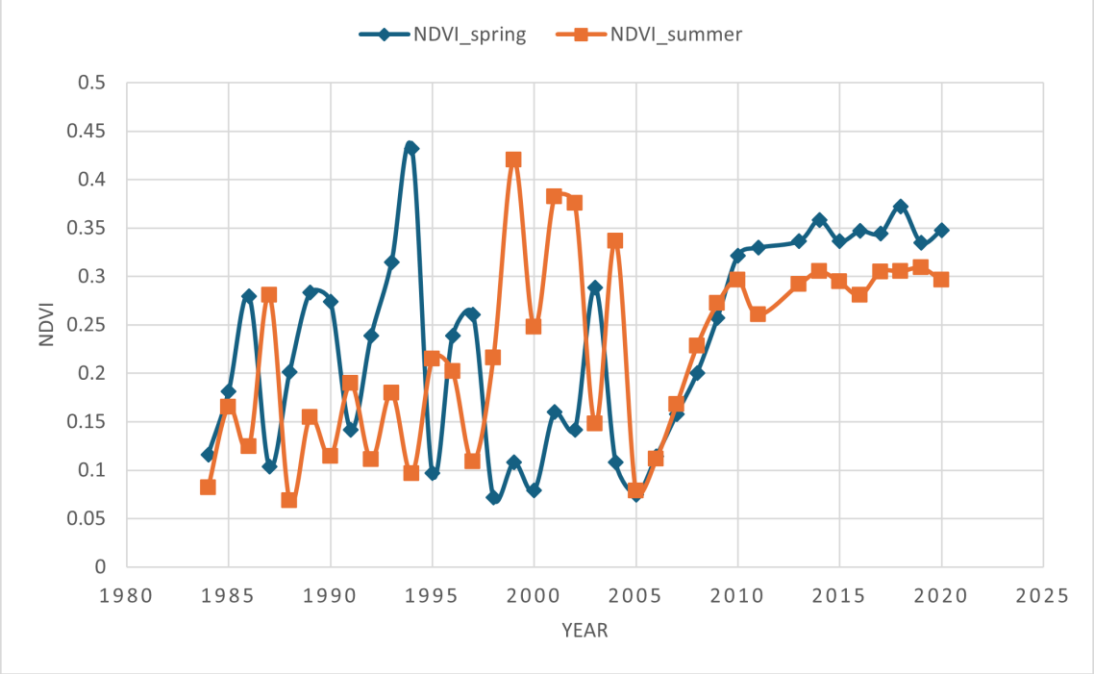

Appendix Figure 2 - Spring (April–June) and summer (July–September) NDVI time series for a representative orchard field from 1984 to 2020 derived from Landsat data. NDVI values are low and variable prior to orchard establishment, followed by a clear increase beginning around 2005, indicating orchard planting and early canopy development. After establishment, NDVI stabilizes at higher levels, reflecting mature orchard conditions, with seasonal differences between spring and summer capturing phenological variation.

Multi-decade NDVI time series capture the characteristic trajectory associated with orchard establishment and canopy development, enabling orchard planting signals to be detected and mapped. This approach was implemented as a supervised machine-learning framework that uses long-term vegetation patterns to estimate orchard planting year. The modeling framework relied on Landsat Collection 2 Level-2 surface reflectance products, which provide consistent, atmospherically corrected observations suitable for long-term trend analysis. Data were compiled from Landsat 5 (Thematic Mapper), Landsat 7 (Enhanced Thematic Mapper Plus), and Landsat 8 (Operational Land Imager), spanning 1984–2020 to leverage the full continuous Landsat archive for statewide mapping. For each year, seasonal composites were generated for (i) Spring (April–June) to capture early-season canopy development; and (ii) Summer (July–September) to capture peak canopy condition. For each orchard polygon, mean reflectance and NDVI were calculated for both seasons in each year, yielding two long-term NDVI trajectories per field (spring and summer) across multiple decades.

To model orchard age for the 2019 crop map, training data were drawn from orchard fields in the DWR 2020 crop map that met two quality criteria: (1) stable crop type, meaning the orchard crop label did not change between the target crop map year and 2020; and (2) spatial consistency, meaning orchard field boundaries overlapped by at least 95% between years. These filters help ensure the training set represents persistent orchards rather than areas affected by crop conversion or boundary edits. Planting year reported in the DWR 2020 dataset was used as the supervised target variable for model training.

Orchard establishment year was estimated using a convolutional neural network (CNN) based on the ResNet-50 architecture. CNNs are widely used in satellite and time-series pattern recognition because they can learn complex, nonlinear signatures from high-dimensional inputs. In this application, the network was trained to associate characteristic NDVI growth trajectories with the timing of orchard establishment. Training leveraged pretrained weights to improve efficiency, used a stratified split by planting year, and applied an 80%/20% training–validation partition. Regularization techniques, including weight decay and dropout, were applied during model training to reduce overfitting and improve generalization performance. After initial training, all network layers were fine-tuned, and performance was evaluated using custom accuracy metrics reflecting practical uncertainty (e.g., the fraction of predictions within ±1 year of the reference planting year). Independent accuracy assessment was conducted by withholding orchard samples from training and comparing predicted planting years to the reference data.

Model performance for the 2019 planting-year estimation achieved $R^2 = 0.62$, RMSE = 6.4 years, MAE = 2.5 years, and mean error ≈ 0.0 years, indicating no systematic bias. Approximately 85% of predicted planting years fell within ±3 years of the reference planting year. Separate models were trained for each crop map year requiring planting-year inference, and the resulting orchard-age layers were used as inputs to the biomass

epistemic allometric equations to enable consistent, spatially explicit orchard biomass and carbon estimates across California croplands.

For years prior to 2014, the woody perennial biomass carbon methodology followed the 2018 NWL Carbon Inventory approach, which relied on three components. First, species-specific allometric equations for major orchard types (almond, walnut, pistachio, citrus, and vineyards) were used to translate orchard type and age into biomass carbon per unit area. Second, statewide orchard acreage and orchard age distributions were estimated using available agricultural statistics and remote sensing. County-level orchard acreage was derived from USDA NASS Census of Agriculture reporting (e.g., 2002, 2007, 2012), so biomass carbon was calculated for those census years where consistent acreage inputs were available. Orchard age prior to 2014 was estimated using a pixel-based classification approach leveraging Landsat time series and the NASS Cropland Data Layer (CDL) to detect establishment and disturbance history (USDA, 2010). Due to computational constraints, the orchard age distribution was derived from a single reference year and then assumed to be static for 2001–2013. Third, uncertainty was quantified using Monte Carlo analysis to capture uncertainty associated with tree measurements (e.g., height, DBH, stand density) and variability in allometric relationships.

Uncertainty Analysis

Uncertainty in cropland biomass carbon was quantified for (i) total woody perennial biomass carbon and (ii) biomass carbon by orchard category using a Monte Carlo framework. Multiple sources of uncertainty were incorporated (Appendix Table 17). For allometry, sources of uncertainty included field-based measurements of tree height, diameter at breast height (DBH), and trees per acre. Uncertainty in the carbon fraction of biomass and the statistical uncertainty of the fitted allometric equations were also included. Additional sources captured uncertainty in the relationship between tree age and DBH and spatial uncertainty in orchard area estimates by crop type.

Appendix Table 17 - List of uncertainties incorporated in Monte Carlo simulations to quantify variability in orchard biomass carbon stocks.

Uncertainty source	Description
Carbon fraction	Uncertainty in the fraction of dry biomass converted to carbon
Allometry	Uncertainty in allometric equations used to estimate biomass from tree measurements
DBH sampling	Sampling variability in diameter-at-breast-height measurements
Height sampling	Sampling variability in tree height measurements
Trees per acre (TPA)	Uncertainty in orchard tree density estimates
Orchard area	Uncertainty in orchard area estimates derived from datasets
Grape biomass components	Uncertainty in grape-specific cane, woody, and root biomass components

For each orchard category and year, the carbon stock estimate was perturbed using a multiplicative error model, where total uncertainty was represented by the combined effect of normally distributed error terms. The simulated carbon stock was computed as:

$$\left(1 + \sum_{i} X_i\right) \times \hat{C}$$

where $\hat{C}$ is the baseline carbon estimate and $X_i \sim N(0, SE_i)$, where X_i is the random error for each simulation draw i sampled from a normal distribution with mean zero and standard deviation equal to the reported standard error (SE) for each uncertainty source. Additional details are provided in the 2018 Technical Support Document for the NWL Inventory (CARB, 2018b).

Each orchard category–year combination was simulated using 1,000 random draws generated with NumPy's default random number generator and a fixed seed (42) to ensure reproducibility. All standard error (SE) terms were treated as epistemic uncertainty in parameter estimates and propagated through the multiplicative error model. For each simulated distribution, the mean, sample standard deviation, and two-sided 95% confidence interval were computed as mean ± 1.96 × SD. Results were summarized in tables by year and visualized using bar plots with associated 95% confidence intervals. All analyses were conducted in Python using NumPy, pandas, and Matplotlib.

QA/QC Activities

For DWR crop mapping data, QA/QC checks were performed to confirm that mapped cropland extent and crop-specific acreage totals exhibited reasonable spatial patterns and year-to-year trends consistent with expected agricultural dynamics in California. Crop type and land-use class assignments were verified after reclassification of DWR and CDL datasets to confirm that each pixel was correctly mapped to the appropriate biomass allometric equation group (e.g., annual crops, perennial orchards). Allometric coefficients applied in the cropland biomass workflow were reviewed using field plot data. Intermediate biomass estimates were summarized by crop class and year and compared against previous CARB inventory to identify outliers or anomalous values. Final cropland biomass rasters were screened for invalid or missing values and reviewed to ensure continuity across years and consistency with total cropland extent.

2018 Methods

In the 2018 NWL Carbon Inventory, carbon stocks in cropland orchard biomass were estimated using an IPCC Tier 3 method that integrated ground-based data collection with remote sensing and statistical modeling techniques. A key component of CARB's effort was producing species-specific allometric equations which translate orchard type and age to carbon density per area for key orchard species. Developing these allometric equations

involved three steps. First, CARB used high-resolution WorldView satellite imagery alongside Google Street View to gather tree measurements, specifically diameter at breast height (DBH), a critical metric for biomass calculations. This data was paired with USDA allometric equations to estimate tree biomass based on DBH values, though these equations traditionally focus on DBH rather than tree age. Second, recognizing this limitation, CARB collaborated with the Wolfskill Experimental Orchards at UC Davis, where a variety of nut and fruit tree species with known ages allowed CARB staff to establish age-specific tree biomass measurements (CARB, 2018a). Allometric equations were thus quantified at the tree-level according to the relationship between carbon and tree age. Third, carbon had to be scaled from the tree-level to the orchard field-level, in an estimate of carbon per area. Age-dependent orchard tree density is a critical metric that scales estimates of carbon from the tree-level to the orchard field-level. CARB used high spatial resolution imagery in Google Earth Pro to measure tree density across a range of orchard types and ages. For each orchard age, CARB calculated the average number of trees per hectare, providing a reliable metric to scale biomass estimates from individual trees to larger orchard areas. These three steps produced species-specific allometric equations of carbon per area for key orchard types of almonds, walnuts, pistachios, vineyards, and citrus. The equations, based on both age and tree species, enable more precise biomass calculations, reflecting the unique growth, orchard density, and carbon accumulation patterns of each species.

A second key component of CARB's effort was to develop an estimate of the acreage of each orchard type and the ages of each orchard in croplands statewide. These orchard type and orchard age acreage estimates are necessary to derive a biomass carbon estimate for croplands statewide using the species-specific allometric equations. The National Agricultural Statistics Service (NASS) census was used to derive the county level acreage of each orchard type. Second, CARB developed a method to classify orchard age, using a pixel-based approach that leverages Landsat time series and the NASS Cropland Data Layer (CDL) data. This orchard age classification captures orchard planting and disturbance history, which aids in determining the age of each orchard pixel. This approach was computationally intensive, so CARB was limited to producing an estimate of the distribution of orchard age based on a single year's data; the distribution of orchard age was subsequently assumed to be static over time. Subsequent annual updates to estimates of biomass carbon in croplands maintained this static age distribution assumption and only factored changes in acreage derived from NASS census data (CARB, 2018b). These data inputs of orchard acreage and orchard age were coupled with the species- and age-specific allometric equations produced by CARB to produce an estimate of carbon for the key orchard species of almonds, walnuts, pistachios, oranges, and vineyards at the county level.

The final component of CARB's approach to estimating carbon stocks in cropland orchard biomass was to produce an uncertainty estimate. Uncertainty was quantified using a Monte

Carlo analysis, addressing potential errors from measurements of tree height, DBH, density, and allometric variability. This approach allowed CARB to systematically assess and quantify uncertainties, resulting in robust, spatially refined carbon stock estimates for California's perennial croplands.

Developed Land

2025 Methods

Methodological Updates

Developed lands were separated into three subgroups with unique biomass calculation methods: urban, wildland urban interface (WUI), or roads and energy infrastructure (R&E). Woody biomass carbon within urban areas of the state was quantified using a Tier 3 approach that used a CARB-developed sample dataset to create regionally stratified statistical relationships between tree density, canopy cover, and woody biomass carbon. The statistical relationships were then applied to maps of tree location and canopy cover within census-delineated urban areas to estimate above- and below-ground woody biomass carbon.

The 2025 NWL Carbon Inventory updated the 2018 inventory methods by including two high resolution canopy cover datasets (0.6 m resolution of canopy cover in 2018 and 2022, produced by USFS) for the quantification of urban biomass carbon. This is an improvement from the rough sample-based approximation of canopy cover implemented in the 2018 inventory. High resolution mapping of canopy cover improves precision in quantifying changes in tree coverage in the urban area. The 2025 methods also incorporated a new AI tree detection dataset which provides a map of tree density, adding another explanatory variable to implement in biomass carbon model calibration. Additionally, the number of field-based tree measurements in the statewide urban forest inventory increased dramatically since the 2018 inventory, increasing the sample data used to calibrate the biomass carbon models. The i-Tree Eco software suite was used to calculate carbon using the statewide urban forest inventory data. This latest software incorporates new science and allometric equations developed since the i-Tree Streets software used in the 2018 inventory. The addition of these datasets enabled new, ecoregion-specific biomass carbon predictive models to be calibrated.

Biomass carbon within WUI areas, identified as areas adjacent to urban areas, was quantified by taking the average biomass values of surrounding forest land, shrubland, and grassland. Biomass carbon within roads and energy infrastructure areas, identified as primary and secondary roads and energy-related infrastructure in 2022, was quantified by overlaying these features on top of biomass estimates from other land types. These methods are new additions to the 2025 NWL Inventory as the 2018 inventory did not identify areas or quantify carbon within WUI or roads and energy infrastructure areas.

Detailed Methods Description

Urban areas are specific regions delineated by the U.S. Census Bureau according to housing unit and population density. The Census Bureau updates its urban area map every 10 years. The NWL Carbon Inventory used the 2010 census-delineated urban area map for 2001-2019 and the merged 2010 and 2020 census-delineated urban area maps for 2020-2022 (U.S. Census Bureau, 2021 & 2023a) (Appendix Table 18). WUI areas are regions outside or bordering urban areas in which there is some amount of impervious surface present, as mapped by the National Land Cover Database (NLCD) impervious surface product integrated into LANDFIRE-C Landcover mapping. R&E areas were mapped by U.S. Census Bureau Topologically Integrated Geographic Encoding and Referencing system (TIGER) lines and data from the Office of Energy Infrastructure Safety, some of which is confidential data (U.S. Census Bureau, 2023b; Office of Energy Infrastructure Safety, 2025). Roads and energy infrastructure data from 2022 were used for 2001-2022.

Urban Biomass Quantification

Biomass carbon in urban areas includes carbon stored in woody tree species (above- and below-ground) and was quantified with a combination of three datasets: remotely-sensed tree canopy data and tree detection data, and field-based tree inventory data (Appendix Table 18). Tree canopy data for California's urban areas is derived from NAIP imagery and produced by USFS (EarthDefine, 2012; USFS, 2025). Tree canopy data for 2012, 2018, and 2022 was used. Since tree canopy data was critical to urban biomass quantification, estimates of urban biomass were produced only for 2012, 2018, and 2022 due to data availability. Tree detection data maps the locations of urban trees and is produced by researchers at Cal Poly from remotely sensed imagery and an AI algorithm. The tree detection points were created by applying deep learning tree detection methods to NAIP multispectral data across California's urban areas. Individual trees were predicted using a convolutional neural network-based regression model trained on manual annotations (Ventura et al., 2024a,b). Tree detection data from 2020 was used. The statewide urban forest inventory is the repository for the field-based tree inventory data, and it consists of tree location, species, and diameter at breast height (Urban Forest Ecosystem Institute, 2025). Inventory measurements for individual trees can be directly converted to biomass carbon stock using the US Forest Service software i-Tree Eco, which stores urban species-specific allometric equations (i-Tree, 2024). The statewide urban forest tree inventory consists of over 8 million trees. Although the inventory is extensive, only a portion of the

total trees in the urban environment are catalogued. To quantify biomass carbon in the entire urban environment, it's necessary to scale the carbon derived from tree inventory data to remotely sensed metrics that cover the entire census-delineated urban area of California, like remotely sensed tree canopy and tree detection data.

Appendix Table 18 - Data used to support the developed land methodological update.

Input Data	Source (Citation)	Purpose	Brief Description
Census-delineated urban area map	U.S. Census Bureau, 2021, 2023a.	Urban area delineation	Urban area boundaries based on census results. Years: 2010, 2020
Climate zones	McPherson et al., 2010	Regional delineation for urban areas	Six zones based on climate and ecoregions.
Energy infrastructure map	Office of Energy Infrastructure Safety, 2025	Energy infrastructure delineation	Confidential layer of above- and below-ground energy infrastructure. Years: 2022
NAIP 4-band imagery	U.S. Forest Service, 2025	Tree canopy cover estimation	Aerial imagery. Years: every 2 years Resolution: 60cm
NLCD Percent impervious	LANDFIRE, 2022b	Impervious surface identification for WUI areas	Land cover map. Years: annual Resolution: 30m
Topologically Integrated Geographic Encoding and Referencing system (TIGER) lines (roads)	U.S. Census Bureau, 2023b	Roads delineation	Road layer. Years: 2022
Tree canopy cover	EarthDefine, 2012	Tree canopy cover variable for urban areas	Tree canopy cover map. Years: 2012, 2018, 2022 Resolution: 1m
Tree detection maps	Ventura et al., 2024a,b	Tree density variable for urban areas	AI detected tree map. Years: 2020
Urban forest inventory	Urban Forest Ecosystem Institute, 2025	Individual tree data for biomass carbon estimation in urban areas	Database of urban forest inventory data. Years: varied Resolution: varied, uneven plots
Urban tree allometric equations	i-Tree, 2024	Biomass carbon estimation in urban areas	From i-Tree Eco software suite

Therefore, a critical step was to establish a statistical relationship between tree carbon, tree canopy, and tree density. To calibrate this statistical relationship, a sample dataset was created by applying a 60m X 60 m square grid to a map of urban area. To qualify as a valid sample cell, an individual grid cell must have enough data coverage from the tree inventory, tree canopy, and tree detection datasets to relate its total woody biomass carbon with its tree density and percent canopy cover (Appendix Figure 3). Since the entire urban area had tree canopy and tree density (the latter derived from tree detection data) quantified, the tree inventory data (i.e. the field-based catalogue of tree species and diameter at breast

height) was the limiting dataset. Only grid cells in which all existing trees were catalogued in the tree inventory data were considered suitable samples.

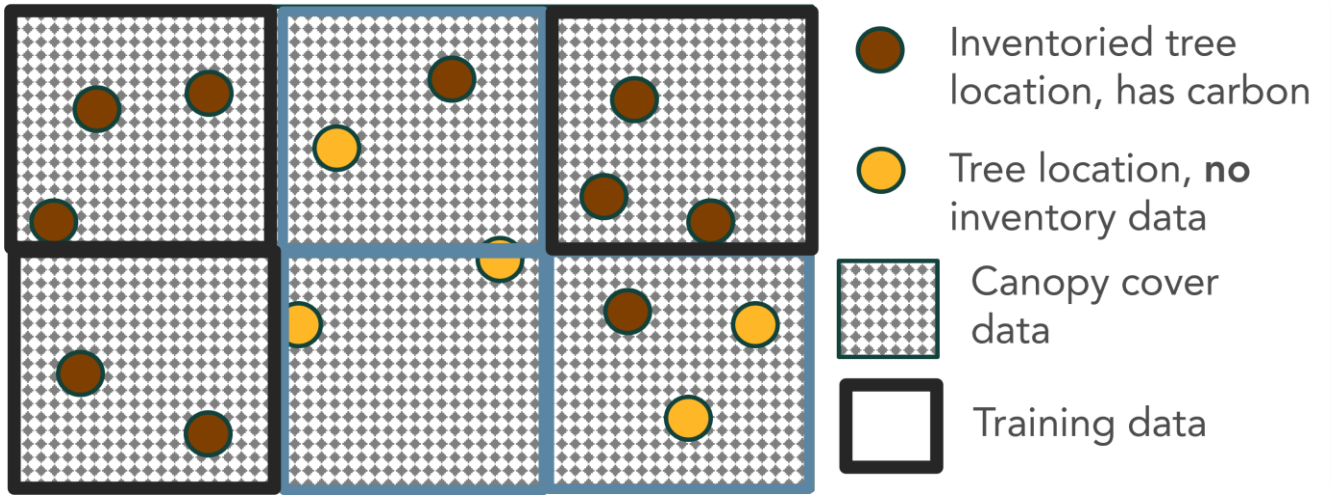

Appendix Figure 3 - A schematic demonstrating how valid sample cells (i.e. 'training data'), bordered in black, were 60m X 60 m grid cells with full coverage of canopy cover data and with every identified tree location documented in the urban forest tree inventory, enabling a total biomass carbon estimate for the entire grid cell.

Once the 60m X 60m sample grid cells were identified, woody biomass carbon was related to tree canopy and tree density at the grid cell-level. An estimate of woody biomass carbon for each grid cell was calculated using the US Forest Service software i-Tree Eco. I-Tree Eco ingests tree species and diameter at breast height and uses urban species-specific allometry to provide an estimate of above- and below-ground tree carbon stock. The carbon stock estimates for all trees within a sample grid cell was summed to produce its estimate of woody biomass carbon. Tree canopy percent cover and tree density were derived for each grid cell from the tree canopy data and the tree detection data, respectfully. Multiple statistical relationships relating percent tree canopy or a combination of percent tree canopy and tree density as explanatory variables predicting woody biomass carbon as the response variable were evaluated, both aggregated across all urban areas and disaggregated by the six climate zones (Appendix Figure 4). The climate zones were based on aggregated Sunset Climate Zones and ecoregion boundaries that have been commonly used to assess urban forest characteristics (McPherson et al., 2010). To be consistent with previous work and to better capture distinct climatic and ecological regions across the state, a unique model for each climate zone was selected to estimate urban biomass carbon.

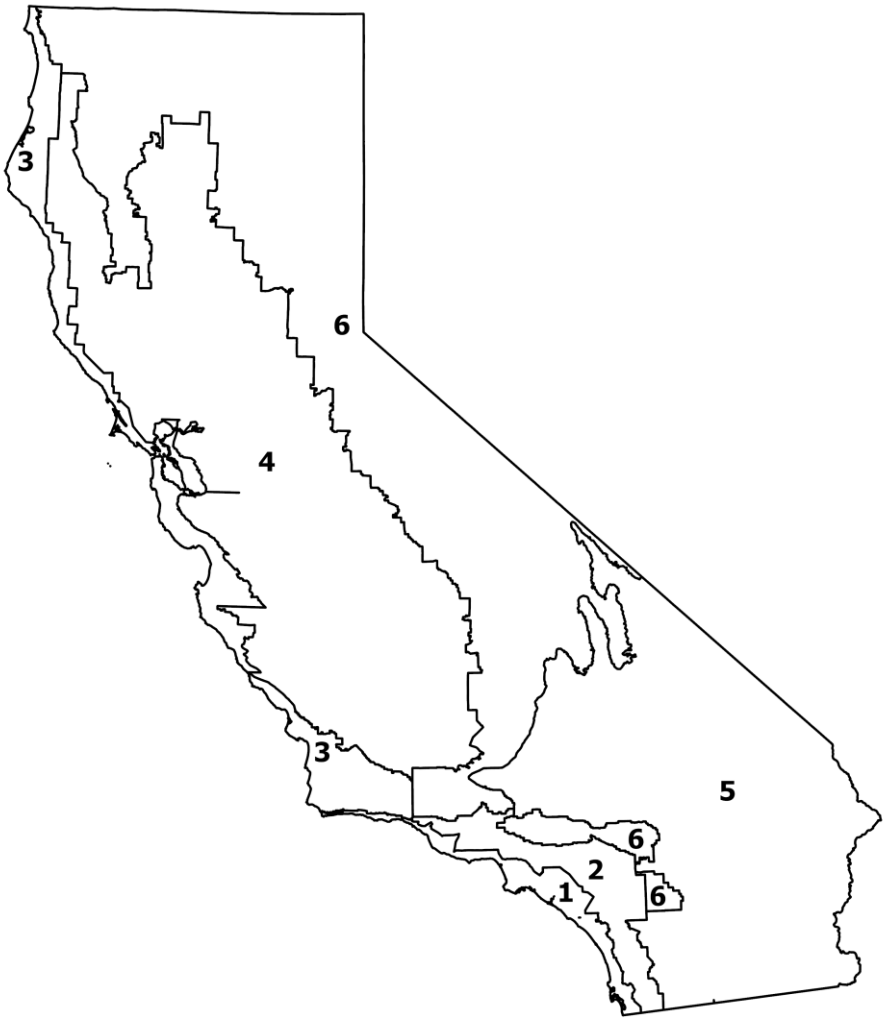

Climate Zone
1 - Southern California Coast CZ
2 - Inland Empire CZ
3 - Northern California Coast CZ
4 - Inland Valleys CZ
5 - Southwest Desert CZ
6 - Interior West CZ

Appendix Figure 4 - Six climate zones used to assess developed lands urban biomass carbon. Climate zones were adopted from McPherson (2010) and reflect distinct climatic and ecological boundaries across the state.

The models fit with data from 2022 was used to predict carbon in years 2018 and 2022. To predict carbon for 2012, a separate model based on 2012 canopy cover was fit due to differences observed in the 2012 canopy cover data (Thorne et al., 2023). Once the linear models were defined, a carbon estimate for every 60m X 60m grid cell within the urban area boundaries was predicted using either the 2022 model (for 2018 and 2022 biomass carbon) or the 2012 model (for 2012 biomass carbon) for the appropriate climate zone (Appendix Table 19). Each year's predicted biomass carbon map used its respective canopy cover data (i.e. 2012, 2018, and 2022 canopy cover) and the AI-detected tree data (quantified for year 2020 only) for tree density as the two explanatory input variables. The only exception was the 2012 model for zone 6 which used tree canopy data as its only explanatory input variable.

The 2012, 2018, and 2022 estimates were extrapolated/interpolated for the remaining inventory period years between 2001-2022. These extrapolated/interpolated values are solely intended to complete the statewide inventory of all land cover types and are best viewed at the broader statewide context along with biomass estimates of other land cover types.

Wildland Urban Interface Quantification

WUI features were identified by applying an alternative classification scheme after the Land Cover Classification Hierarchy processes described earlier in this document which was conducted for each year of the inventory period 2001-2022. Remaining pixels that contained the "developed" identifier tag within the LANDFIRE-C attributes, indicating some amount of impervious surface, were considered WUI areas, except for croplands and wetlands identified through this process which were assigned back to the Cropland and Wetland cover types. At present, the wildland urban interface pixels are not intended to be a comprehensive map of all WUI area in the state of California and may differ from other WUI mapping products and definitions. Instead, these regions are designated as WUI because they meet the specific criteria of shrub/forest/grass cover (excluding cropland and wetland) with some amount of impervious surface present as mapped by NLCD and LANDFIRE-C.

Biomass carbon was estimated per pixel by averaging the immediately surrounding pixels (up to 8 pixels in a 3x3 window). The biomass estimates of these surrounding pixels followed its respective land cover type biomass carbon methodologies. This was done iteratively for each year of the inventory period, starting with the WUI pixels immediately adjacent to other classified land types with biomass carbon estimates, to first populate biomass carbon of pixels along edges, and then fill in the WUI areas in a step-wise manner. For details, refer to the specific land type methodological details. A limitation of this approach is that biomass carbon estimates are not based on site-specific data but are instead based on the adjacent areas that may or may not be representative. Biomass differences and changes over time within the WUI areas may not be captured.

Roads and Energy Infrastructure

Road features considered in the inventory include primary (e.g. multi-lane highways, freeways, etc.) and secondary roads (e.g. moderate to high traffic urban streets). Tertiary roads (e.g. low traffic, narrower roads) and many roads in rural areas, both paved and unpaved, are not included in the inventory because of resolution limitations. The primary and secondary roads matched well with roads identified in LANDFIRE-C. The smallest unit mapped was 30m X 30m pixels, and pixels could not be partially attributed to narrow roads. Energy infrastructure features considered in the inventory include substations and any energy distribution infrastructure including transformers and above and belowground power lines. These road features and energy infrastructure features were combined, and biomass and soil carbon falling within these feature boundaries was subsequently attributed to R&E. The R&E features from 2022 were applied to biomass and soil carbon maps for all land types and for all years to produce biomass carbon estimates for each year of the inventory period. Only the 2022 footprint was used, therefore a major limitation is that changes to the road and energy infrastructure footprint over time are not accounted for. For details of the energy infrastructures biomass estimates, refer to the specific land type methodological details. Soil carbon estimates followed the methodology described below in this document.

Uncertainty Analysis

Performance metrics were calculated for the urban biomass linear models for each climate zone. Appendix Table 19 summarizes the intercept, coefficients, r^2, mean total carbon, and root mean square error (RMSE) of the final linear models, both 2022 and 2012. While model r^2 values ranged from 0.19–0.32, indicating substantial unexplained variation at the grid cell-level, these models provide the best available climate zone-level predictions for 2022 carbon. The 2012, 2018, and 2022 results should be interpreted as predictive estimates rather than precise mechanistic relationships. There are several limitations in the 2025 methodology that could be improved upon in the future. Only tree density and tree canopy cover are used as explanatory variables due to data availability. Adding an explanatory variable such as species or functional plant type would likely strengthen the predictive capacity of these models. Such an improvement could only be implemented if there were improved mapping of urban features like species distribution. Further, street trees are overrepresented in the urban forest inventory compared to trees in private yards, which can often be different species. Non-tree vegetation such as shrubs and grass are also not included in the urban forest inventory, which can store substantial carbon. Since the 2012 and 2022 predicted models were calibrated with urban forest inventory data, this bias towards street trees affects the accuracy of the final biomass carbon estimates for the urban area. Adding samples of private yard trees and non-tree vegetation to the inventory, in addition to expanding the urban forest inventory in general to sample more areas, would help reduce this bias in future carbon quantification work.

A limitation to the temporal resolution of urban biomass carbon estimates was the availability of urban tree canopy cover maps, which restricted biomass carbon estimates to 2012, 2018, and 2022. Annual high-resolution tree canopy cover maps would allow annual estimates of biomass carbon. Two other key datasets could be improved temporally to improve the Inventory's ability to track urban biomass carbon change over time. (1) The urban forest inventory could track date of measurements for each tree. This metadata would help allocate urban forest inventory calibration data to its most appropriate time period. (2) The AI-tree detection data could be reproduced for multiple years of tree cover, capturing tree removal and tree planting across years, which are important drivers of change to urban biomass carbon.

Appendix Table 19 - Intercept, coefficients, model r^2, mean observed total carbon, model root mean square error (RMSE), and number of sample grid cells n of both the 2022 and 2012 linear models used to predict woody biomass carbon. The 2022 model was used to predict urban area woody biomass for 2018 and 2022 and the 2012 model was used for predictions in 2012. Note: for the 2012 model for zone 6, only 2012 percent canopy was used as an explanatory variable.

Climate zone	2022/ 2012 Intercept (MT C)	2022/ 2012 percent canopy coefficient (MT C)	2022/ 2012 Tree density (trees/3600 m^2) coefficient (MT C)	2022/ 2012 model r^2	2022/ 2012 mean observed total carbon (MT C)	2022/ 2012 model RMSE (MT C)	2022/ 2012 Sample cell n
1: Southern California coast	-0.201/ -0.245	0.13/ 0.09	0.30/ 0.37	0.28/ 0.25	2.52/ 2.54	3.34/ 3.47	25379/ 24807
2: Inland Empire	-0.241/ -0.212	0.16/ 0.13	0.24/ 0.34	0.30/ 0.30	2.65/ 2.68	3.41/ 3.52	25246/ 24460
3: Northern California Coast	-0.005/ -0.041	0.08/ 0.07	0.28/ 0.31	0.26/ 0.23	2.09/ 2.12	2.89/ 3.05	8047/ 7798
4: Inland Valleys	0.067/ -0.063	0.089/ 0.091	0.15/ 0.20	0.27/ 0.28	2.26/ 2.32	2.70/ 2.74	17323/ 16351
5: Southwest Desert	-0.089/ -0.013	0.22/ 0.11	0.079/ 0.25	0.30/ 0.20	1.52/ 1.59	2.27/ 2.60	1803/ 1679
6: Interior West	-1.064/ 1.224	0.085/ 0.15	0.42/ NA	0.32/ 0.19	2.79/ 3.13	6.42/ 5.08	106/ 90

To estimate uncertainty in the sum total amount of urban tree biomass carbon predicted by climate zone and by total urban area, error was propagated based on the per-climate zone linear regression models developed for 2012 and 2018/2022. For each climate zone, the root mean squared error (RMSE) was extracted from the corresponding linear model used to predict carbon, which quantifies the deviation between observed and predicted carbon at the 60 m × 60 m grid scale. The number of grid cells (n) that had a predicted value of

biomass carbon within each climate zone was determined based on the number of 60 m x 60 m grid cells that fit within the footprint for each urban area: For 2012 and 2018, only grid cells falling within the 2010 census- delineated urban footprint of California had biomass carbon predictions. For 2022, grid cells falling within the joined footprint of 2010 and 2020 census-delineated urban areas had biomass carbon predictions.

The 95% confidence interval (CI) of the aggregated carbon per climate zone was approximated as:

$$CI_{95} = 1.96 \times RMSE \times \sqrt{n}$$

where the 95% confidence interval CI_{95} is calculated as 1.96 multiplied by the root mean square error (RMSE) of the biomass carbon predictive model, multiplied by the square root of n , the total number of grid cells in which biomass carbon was predicted using the model. This approach assumes independence of grid-cell predictions and treats the RMSE as representative of per-cell prediction uncertainty. The same approach was applied to all climate zones, and total urban carbon uncertainty was computed as the square root of the sum of squared per-zone uncertainties. Values are reported in Appendix Table 20 in metric tons of carbon (MT C).

A limitation to this uncertainty approach is that it does not capture spatial autocorrelation or a full probabilistic uncertainty distribution and most likely underestimates true uncertainty of the sum. If the uncertainty of each model input was known (e.g. uncertainty of AI tree-detection data, uncertainty of canopy cover data, uncertainty of urban forest inventory diameter at breast height measurements, and uncertainty of i-Tree allometric equations), a Monte Carlo approach towards quantifying uncertainty could give a more robust estimate of the expected error of the urban carbon quantification approach.

Roads were assigned zero biomass carbon and therefore did not have associated uncertainty. No additional uncertainty analysis was conducted for WUI or energy infrastructure estimates derived from the other land type biomass carbon values beyond those described in their respective land type methodologies.

Appendix Table 20 - The root mean square error (RMSE), total number of grid cells predicted (n), and 95% confidence interval for 2012, 2018, and 2022 modeled predictions of urban biomass carbon aggregated by zone and total.

Zone	2012 RMSE (MT C)	2012 n	2012 95% CI (MT C)	2018 RMSE (MT C)	2018 n	2018 95% CI (MT C)	2022 RMSE (MT C)	2022 n	2022 95% CI (MT C)
1	3.47	1132520	7243.46	3.34	1132520	6962.07	3.34	1207728	7189.52
2	3.53	1560389	8635.76	3.41	1560389	8355.69	3.41	1661676	8622.62

3	3.05	614588	4688.32	2.89	614588	4433.37	2.89	695595	4716.51
4	2.74	2096297	7780.66	2.71	2096297	7676.75	2.71	2353019	8133.25
5	2.60	441338	3383.01	2.27	441338	2956.13	2.27	487057	3105.48
6	5.08	106354	3245.65	6.42	106354	4103.32	6.42	150496	4881.14
Total	NaN	5951486	15216.51	NaN	5951486	14914.81	NaN	6555571	15745.0

QA/QC Activities

No additional QA/QC activities beyond those performed by the stewards of the input data were conducted for the urban biomass estimates. WUI and R&E biomass carbon estimates relied on the methodologies of the other land types; therefore, refer to the other land type methodologies for QA/QC activities.

2018 Methods

The 2018 NWL Carbon Inventory quantified urban tree biomass using baseline carbon values derived from forest inventory data, allometric equations, and tree cover (CARB, 2018a,b). The baseline carbon value was regionally stratified and calculated according to methodology outlined by Bjorkman et al. (2015). Changes from the baseline carbon value were inferred from changes in tree canopy cover, which were estimated using a manual point-density assessment of aerial imagery. The methodology is classified as IPCC tier 3, because it relied on extensive, localized data. However, the method relied on measured changes in canopy cover to drive changes in carbon, rather than modeling changes in tree height as a driver, as implemented in other tier 3 approaches.

Other Land

2025 Methods

Methodological Updates

The 2025 NWL Carbon Inventory update for other lands built on the 2018 NWL Carbon Inventory by recalibrating biomass quantification across the state, incorporating new LANDFIRE products for 2016, 2020, and 2022, and integrating annual disturbance data for 2001–2022. Recalibration involved processing federal plot-level data into carbon densities using allometric equations. LANDFIRE-C modeling was updated to use the 2016 LANDFIRE remapped base map and incorporated hindcasting to maintain continuity throughout the entire inventory period. Carbon stocks were annualized across the full inventory period, attributing changes to the exact disturbance year using annual LANDFIRE disturbance data. Compared to 2018 methods, these updates enhanced spatial and temporal resolution, improved disturbance attribution, and created a continuous annual inventory for other lands from 2001 to 2022.

Detailed Methods Description

Input Data Processing

LANDFIRE-C modeling from the 2018 NWL Carbon Inventory was updated to support new LANDFIRE products for 2016, 2020, and 2022 (Appendix Table 21). This included LANDFIRE Existing Vegetation Type (EVT), Existing Vegetation Cover (EVC), and Existing Vegetation Height (EVH) (LANDFIRE, 2022b,c,d). New data layers required crosswalks to properly interface with existing LANDFIRE-C architecture, and these approaches differed by land type. Crosswalk, in this context, refers to the translation of data from one format or categorical scheme to another, often by aggregating or disaggregated categories and reformatting text. Crosswalk structure refers to a collective system of many individual crosswalks. Please see the Recalibration section for details on the approach for other lands.

In some cases, the land type indicated by LANDFIRE EVT did not align with the land type represented by EVC and EVH. For example, following high-severity wildfire, EVT may still classify an area as forest land, while EVC and EVH reflect a transition to other land. To

maintain consistency with CARB's land type definitions and reflect current conditions, EVT was adjusted to correspond with EVC and EVH classifications. While this approach improves alignment and facilitates quantification, it introduces potential limitations in LANDFIRE-C modeling for post-wildfire ecosystems. Although major carbon pools such as deadwood are accounted for during this conversion, other biomass pools may differ from available EVT parameterizations under post-fire conditions, increasing uncertainty.

Appendix Table 21 - Data used to support the other land methodological update.

Input Data	Source (Citation)	Purpose	Brief Description
LANDFIRE Existing Vegetation Type (EVT)	(LANDFIRE, 2022d)	LANDFIRE-C Input Dataset	Vegetation classes for the years 2001, 2010, 2012, 2014, 2016, 2020, and 2022
LANDFIRE Existing Vegetation Height (EVH)	(LANDFIRE, 2022c)	LANDFIRE-C Input Dataset	Vegetation height for the years 2001, 2010, 2012, 2014, 2016, 2020, and 2022 (meters)
LANDFIRE Existing Vegetation Cover (EVC)	(LANDFIRE, 2022b)	LANDFIRE-C Input Dataset	Vegetation cover for the years 2001, 2010, 2012, 2014, 2016, 2020, and 2022 (percentage)
LANDFIRE Annual Disturbance	(LANDFIRE, 2022a)	LANDFIRE-C Input Dataset	Disturbance mapping for each year from 2001 to 2022.
CAL FIRE FRAP Historic Wildfire Perimeters	(CAL FIRE, 2025)	Disturbance Modifications for 2021	Wildfire Perimeters for the year 2021
BLM Terrestrial Assessment, Inventory, and Monitoring (AIM) plot data	(BLM, 2025)	Input for plot-level carbon densities used to recalibrate LANDFIRE-C	Field Plot data collected through BLM AIM programs assessing the health, status, and trend in plots overlapping California's Shrublands and Other Lands
LANDFIRE-DB	(LANDFIRE, 2021)	Input for plot-level carbon densities used to recalibrate LANDFIRE-C	Field plot data synthesized by LANDFIRE from multiple programs.

Recalibration

In other lands, LANDFIRE-C was recalibrated using field plot data. Using plot data, new EVT classes were parameterized where possible and crosswalked to previous classes where data was not available. Many EVT classes within the other lands category do not have numeric EVC or EVH representations and have one EVC and one EVH per EVT. In these cases, all EVC and EVH combinations with that EVT were assumed synonymous. If a numeric EVH was present, EVH crosswalks were updated to use modern formats. When crosswalking to earlier years with the previous EVH format, height was assumed to be the center of a provided

range. EVC inputs relied on modern formats for available years and were crosswalked to previous formats for earlier years, as with EVH.

Recalibration of LANDFIRE-C relied on 359 plot-level carbon densities and LANDFIRE-C inputs (EVT, EVC, and EVH) for other lands. Plots were first separated into calibration and validation datasets, withholding 10% of all plots for validation. Calibration of AGL and total carbon relied on multiple linear regression of LANDFIRE-C EVC and EVH by EVT. Regressions were then used to create lookup keys for all potential canopy cover and canopy height combinations of each EVT. In processing a broad range of ecosystems, certain exceptions were made: (i) If fewer than three plots were available for calibrating an EVT class, parameters from the previous inventory were used instead of new parameters; (ii) If either EVC or EVH regressions resulted in a negative slope, the regression relied only on the other parameter; (iii) If both EVC and EVH resulted in a negative slope or if EVC and EVH did not show any variation across plots, carbon density was averaged and held static for all combinations of EVC and EVH.

Plot-level carbon data was synthesized from federal databases and converted to carbon densities using the Rangeland Vegetation Simulator (RVS). Plot-level data was collected from the BLM Assessment, Inventory, and Monitoring (AIM) and LANDFIRE-DB programs (LANDFIRE, 2021; BLM, 2025). From each dataset, parameters were reformatted and converted to match inputs required by the RVS plot module. These input data included shrub canopy cover (%), shrub canopy height (ft), grass/forb canopy cover (%), grass/forb canopy height (ft), dominant species, latitude, and longitude. The RVS model also sources inputs from LANDFIRE biophysical settings (BPS) and five years of precipitation and NDVI data for each plot (Reeves et al., 2016). As RVS is limited to one dominant species as input, carbon densities may be over- or underestimated where significant carbon pools are stored in subdominant species (such as sparse tree cover) or where allometries for a particular species were not available. In the event a species did not have an allometric equation, the species was crosswalked to a similar species with an allometry.

RVS produced outputs of aboveground live (AGL) carbon rather than total carbon. Total carbon includes AGL along with deadwood, belowground biomass, and litter. To reconstruct total carbon from RVS outputs, previous LANDFIRE-C parameterizations were converted into ratios of each pool with respect to AGL (Battles et al., 2013). When belowground carbon pool ratios were not available, an average ratio of 0.74 (root:shoot) was used based on published allometries for California shrub species (Kummerow et al., 1977; Miller & Ng, 1977).

Basemap Updates

LANDFIRE-C was updated to use LANDFIRE's 2016 basemap instead of the previous 2001 basemap. In the 2018 Carbon Inventory, LANDFIRE-C relied on LANDFIRE products produced for 2001, 2010, 2012, and 2014. LANDFIRE produces basemap-derived products, meaning conditions in later years (2010, 2012, and 2014) are contingent on the initial

conditions set in 2001 and subsequent disturbance, growth factors, and other applied rules (Dewitz, 2025). In 2016, LANDFIRE completed a remap and updated to a 2016 basemap using modern data and methods (LANDFIRE, 2021). This new basemap only affects LANDFIRE products for 2016 onward; earlier LANDFIRE datasets were not retroactively updated. While the LANDFIRE remap provides multiple benefits to LANDFIRE-C modeling, it also introduced a break in continuity during the 2014–2016 inventory period using the previous method.

To mitigate the temporal discontinuity introduced by the 2016 remap, basemap updates were hindcasted from 2016 to 2001. During hindcasting, areas that experienced disturbance—as defined by LANDFIRE's annual disturbance data—retained the carbon quantification from 2001–2014 LANDFIRE-C outputs. Landscapes that did not experience disturbance between 2001 and 2016 relied on 2016 LANDFIRE outputs. All existing LANDFIRE-C model functionality was retained during this process, including accounting for deadwood following wildfire, regional growth factors, and land cover transitions. Following hindcasting from 2016 to 2001, LANDFIRE-C was run forward from 2016 to 2022 to create a continuous time series.

Annualization

Carbon stocks were updated to an annual timescale for the full inventory period of 2001 to 2022. Annualization relied on annual LANDFIRE disturbance data to reallocate carbon stock changes to the relevant disturbance year(s) (LANDFIRE, 2022). For example, if a wildfire took place in 2008, this previously would have been accounted for in the next available LANDFIRE dataset year (2010). The updated annualization process reattributes these changes in carbon stock from 2010 to 2008 for all areas affected by that wildfire. If multiple disturbances took place between available dataset years, the carbon stock change was distributed evenly between the relevant years. Following annualization, growth of biomass carbon stocks was also reattributed for affected pixels, allowing growth and recovery to follow annual intervals as well.

Given that LANDFIRE data releases occur at uneven intervals, the annualization scheme carries greater uncertainty during earlier inventory periods, particularly from 2001 to 2010. This limitation is most pronounced in areas experiencing frequent or repeated disturbances within these extended gaps. As annualization distributes carbon stock changes evenly across repeat disturbances, it does not capture the relative severity of disturbances. As a result, landscapes with multiple disturbances during a period may demonstrate simplified patterns that underestimate or overestimate relative effects but capture cumulative effect.

Disturbance Quantification

LANDFIRE-C disturbance data was updated to include annual disturbance from 2001 to 2022. Newly introduced disturbance codes were crosswalked to existing LANDFIRE-C

disturbance codes (Battles et al., 2013). Annual disturbance data was used to create annual estimates of biomass carbon stock, as described above.

LANDFIRE-C was updated to allow retention and decomposition of deadwood following type-converting wildfire. This was implemented by converting 80% of aboveground live (AGL) biomass to deadwood post fire with a linear decay period of 20 years. Conversion factors were determined by averaging FOFEM simulations similar to Forest Lands (Stenzel et al., 2019). A 20-year coefficient was used based on IPCC's default coefficient for transition between land classes (IPCC, 2006). Deadwood remains on site and decays with this pattern separately from deadwood produced through subsequent changes in EVT, EVC, and EVH.

Wildfire in the year 2021 was found to differ in LANDFIRE datasets when compared to other maps of wildfire. Multiple megafires generally considered to have occurred in 2021 were instead attributed to 2022 in LANDFIRE disturbance data (LANDFIRE, 2022a). This is likely related to how long these fires were active, particularly where suppression activities crossed a calendar year. To correct this, CAL FIRE FRAP fire perimeters (CAL FIRE, 2025) for 2021 were used to reattribute disturbance within the LANDFIRE product. Any wildfire disturbance that occurred in 2022 within LANDFIRE's map but occurred in 2021 within the CAL FIRE FRAP fire perimeters was reattributed from 2022 to 2021 in model inputs. This modification was then propagated through carbon stock and land cover processes.

Uncertainty Analysis

Uncertainty in the other lands NWL Carbon Inventory was evaluated by comparing other lands total biomass carbon against total biomass carbon values generated from empirically based field site measurements. Field data included synthesized federal, state, and literature plots in California, scaled using allometric equations. Field data was divided into calibration and validation subcomponents. Only withheld validation plots were used for the uncertainty analysis. Total biomass carbon for the NWL Carbon Inventory was derived from the pixels corresponding to field plot footprints.

QA/QC Activities

Quality assurance and quality control procedures were applied to the other land workflow to ensure quantification and spatial integration were implemented correctly. First, estimates were compared against intercomparison products that had spatial coverage encompassing other lands—ranging from global scale to regional scale products. Second, randomly selected pixels within mapped other lands were manually inspected to verify recalibration was applied correctly through time, including cases where land cover changed. Finally, summarized trends in carbon were visually examined to confirm that temporal patterns were consistent with expected system behavior and known land-use dynamics.

2018 Methods

The 2018 NWL Carbon Inventory used LANDFIRE-C, an IPCC Tier 3 model based on Forest Inventory Analysis (FIA) data and literature derived values, to quantify carbon stocks in other lands (Battles et al. 2013; USFS, 2012). LANDFIRE-C has undergone iterative revisions to improve model functioning and to incorporate additional allometric data for sparsely vegetated ecosystems (Gonzalez et al. 2015; Saah et al. 2016). As the FIA program does not sample within sparsely vegetated ecosystems, literature derived values of biomass were used for other lands and some shrubland communities. Allometric equations for other lands included all available studies with LANDFIRE-compatible metadata, including at least plot location, date of sampling, canopy height, and canopy cover/density.

Wetland

2025 Methods

Methodological Updates

Biomass carbon stock quantification in wetlands was newly introduced in the 2025 NWL Carbon Inventory update. The process relied on the LANDFIRE-C method, even in cases where LANDFIRE classified CARB-mapped wetlands as non-wetland land types. Wetland biomass carbon was not estimated using a separate method or independent recalibration; instead, it was entirely dependent on LANDFIRE-C methods for other land types and the existing LANDFIRE-C wetland calibration (Gonzalez et al. 2015). While this approach accounts for major live and dead biomass carbon pools—such as those in montane meadows and riparian zones—it is not specifically tailored to the unique vegetation found in wetlands. Consequently, biomass carbon stock estimates for wetlands are less certain, particularly where vegetation differs significantly from that modeled by LANDFIRE's existing vegetation type, height, or cover products (LANDFIRE, 2022b, c, d). For additional details, please see the Land Cover Classification and Mapping and Forest Land Biomass Carbon sections.

Detailed Methods Description

For detailed methods description of wetlands biomass carbon, please see the Forest Land Biomass Carbon section.

QA/QC Activities

For QA/QC steps undertaken for wetlands biomass carbon, please see the Forest Land Biomass Carbon section.

2018 Methods

The 2018 NWL Carbon Inventory did not report wetland biomass carbon (CARB, 2018a). Initial carbon densities for wetlands were established by LANDFIRE-C based on an annual average of net primary productivity (NPP) from MODIS satellite data (Gonzalez et al. 2015); however, wetland mapping limitations necessitated quantifying wetlands separately from LANDFIRE-C quantified land types. This separate analysis did not quantify wetland biomass carbon.

Soil Carbon Methodological Details

Soil carbon estimates were quantified following a unified soil framework. In this framework, mineral soils were estimated using a single IPCC Tier 3 methodology and organic soils were estimated using a combination of Tier 1 and Tier 2 methodologies (Appendix Table 22). Detailed methods are described in the sections below.

Following quantification, mineral and organic soil carbon maps were combined to produce spatially complete soil carbon stock maps for the entire inventory period (2001-2022).

Once the soil carbon maps were produced, carbon stocks (MMT), carbon densities (MT C/acre), as well as annual and cumulative change were determined by comparing estimates over time. In addition to summarizing soil carbon stocks by land type over time, net carbon stock change with land conversion was also evaluated by summing the annualized soil carbon stock gains and losses associated with each transition under an equilibrium-based framework. This approach accounted for carbon gains and losses over each transition period (2001-2013 and 2014-2022), ensuring the cumulative net change reflected the integrated effect of land cover dynamics over time.

Appendix Table 22 - IPCC Tier and methods summary for estimating soil organic carbon by land type.

Reporting Category	Tier	Method Summary	Scope
Mineral Soils			
Forest land	3	Digital soil mapping	Soil organic carbon to 30 cm
Grassland	3	Digital soil mapping	Soil organic carbon to 30 cm
Cropland	3	Digital soil mapping	Soil organic carbon to 30 cm
Developed land	3	Digital soil mapping	Soil organic carbon to 30 cm
Other land	3	Digital soil mapping	Soil organic carbon to 30 cm
Wetland	3	Digital soil mapping	Soil organic carbon to 30 cm
Organic Soils			
Forest land	1	Stock change factor	Soil organic carbon to 30 cm
Grassland	1	Stock change factor	Soil organic carbon to 30 cm
Cropland	2	Stock change factor	Soil organic carbon to 30 cm
Developed land	1	Stock change factor	Soil organic carbon to 30 cm
Other land	1	Stock change factor	Soil organic carbon to 30 cm
Wetland	2	Stock change factor	Soil organic carbon to 30 cm

Mineral Soils

2025 Methods

Methodological Updates

Relative to the 2018 NWL Carbon Inventory, which estimated soil organic carbon (hereafter 'soil carbon') of mineral soils using a primarily Tier 2 approach, the current inventory incorporated several key methodological enhancements. In 2018, soil carbon stocks for mineral soils were derived from a global soil map and Tier 2 stock change factors. The exception was croplands remaining croplands, where carbon stocks and stock changes were estimated via the process-based Denitrification Decomposition (DNDC) model. In contrast, the present inventory estimated mineral soil carbon stocks using a Tier 3 digital soil mapping approach (McBratney et al. 2003; Ugbaje et al. 2024), in which a machine-learning model was trained and validated on thousands of soil samples from California and applied to generate annual, spatially explicit maps over time.

Detailed Methods Description

Most of the state's land area sits on soil that is categorized as mineral (Appendix Figure 5). Mineral soils have organic carbon[1] levels below 12% and usually occur under moderate to well drained conditions (IPCC, 2006). Organic carbon of mineral soils was estimated from 0-30 cm depth using a digital soil mapping (DSM) approach (Appendix Figure 6). While inorganic carbon[1] is also present in soils in California's more arid environments, assessing changes in soil inorganic carbon stocks remained beyond the scope of the NWL Carbon Inventory for this update.

Appendix Figure 5 - Map of mineral and organic soil extent. Organic soils are defined as histosols based on USDA soil classification and as coastal wetlands based on the California Aquatic Resources Inventory (CARI). Map is scaled to 1 km^2 resolution to aid with visualization.

[1] Soil organic carbon refers to the carbon component of organic matter present in the soil, which is derived from decaying plant material, root deposits, and other organisms. Soil inorganic carbon refers to carbon present in mineral forms (e.g., carbonates) that originates from rocks and geochemical processes in the soil.

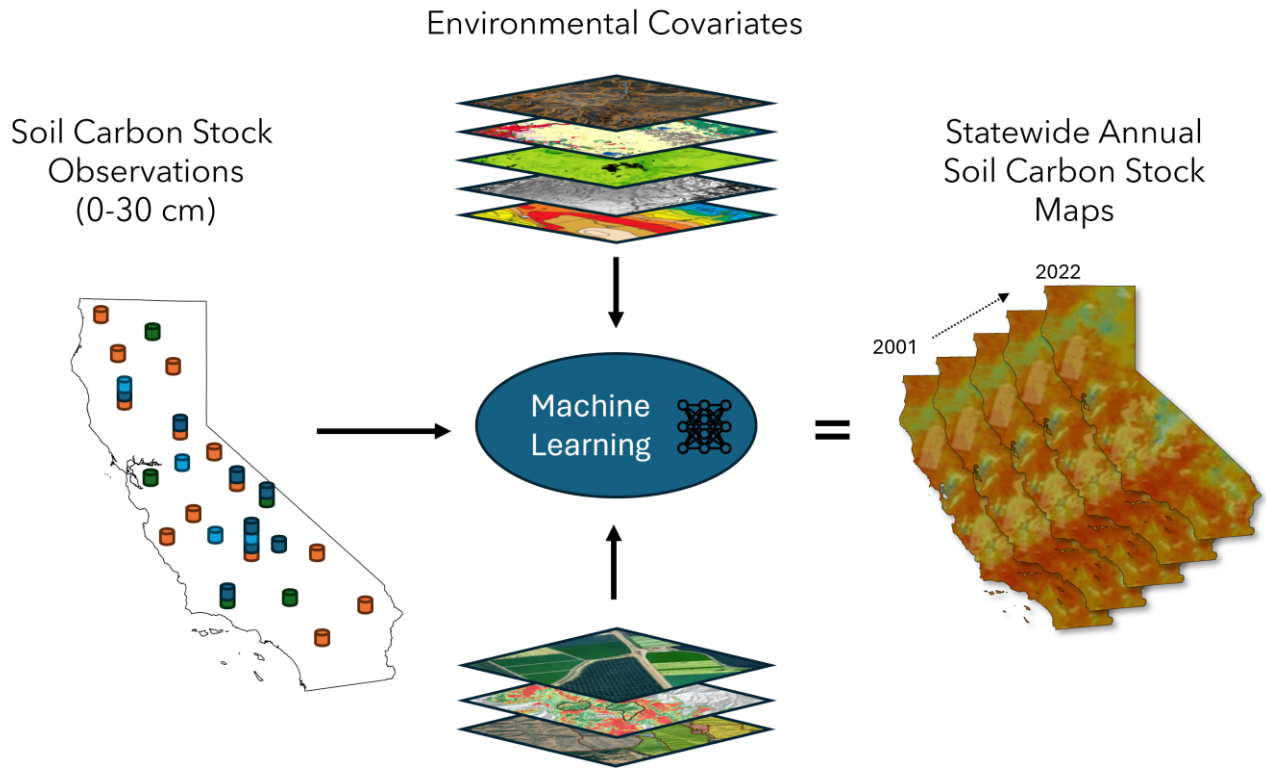

Appendix Figure 6 – Digital soil mapping framework. The lefthand side represents training data from empirical soil samples collected statewide. Point locations are hypothetical (not actual) and different colors denote different sampling years. Note that some locations have repeat measurements (stacked cylinders) whereas others have only a single time point (a lone cylinder). In this framework, the soil sample data were harmonized and related to environmental covariates in a machine learning model (middle) that was used to generate annual wall-to-wall soil carbon maps for 2001-2022 (right).

Soil Sample Data

A total of 2,908 soil carbon stock observations were compiled from multiple soil databases and project-specific field campaigns for the years 2001-2024. This included both published and unpublished datasets derived from national soil surveys, regional programs, and targeted studies (Appendix Table 23). The majority of data contained single timepoint observations. Only a dozen projects contributed time series information with repeat observations generally collected less than five years apart.

Appendix Table 23 – Data used to generate the harmonized soil carbon stock dataset for digital soil mapping (DSM) purposes.

Dataset	Project Name	Reference
1	Rapid Carbon Assessment Program	Soil Survey Staff and Loecke, T. 2016. Rapid Carbon Assessment: Methodology, Sampling, and Summary. Wills, S. (ed.). U.S. Department of Agriculture, Natural Resources Conservation Service.
2	National Cooperative Soil Survey	National Cooperative Soil Survey. NCSS Soil Characterization Database (Lab Data Mart). Available online. Accessed March 2025.
3	National Ecological Observatory Network	NEON (National Ecological Observatory Network). Soil physical and chemical properties, periodic (DP1.10086.001), RELEASE-2025. DOI: 10.48443/8w7d-dk04. Dataset accessed from https://data.neonscience.org/data-products/DP1.10086.001/RELEASE-2025.
4	Healthy Soils Program	California Department of Food and Agriculture. 2017-2020. Healthy Soils Demonstration Projects: Unpublished datasets.
5	Delta Soil Carbon Dataset	Anthony, T. L., & Silver, W. L. (2020). Mineralogical associations with soil carbon in managed wetland soils. *Global Change Biology*, *26*(11), 6555–6567. Anthony, Tyler (2021). *Quantification and Controls on Soil Carbon and Greenhouse Gas Fluxes From Managed Peatland Ecosystems*. [Doctoral Dissertation, University of California Berkeley]. ProQuest Dissertations & Theses.
6	The Coastal Carbon Library	Holmquist, J. R., Klinges, D., Lonneman, M., Wolfe, J., Boyd, B., Eagle, M., ... & Megonigal, J. P. (2024). The Coastal Carbon Library and Atlas: Open source soil data and tools supporting blue carbon research and policy. Global Change Biology, 30(1), e17098.
7	Dryland Nitrogen Deposition Study	Püspök, J. F., Zhao, S., Calma, A. D., Vourlitis, G. L., Allison, S. D., Aronson, E. L., ... & Homyak, P. M. 2023. Effects of experimental nitrogen deposition on soil organic carbon storage in Southern California drylands. Global Change Biology, 29(6), 1660-1679.
8	Soil Carbon Accrual Project	Daley, C., Oikawa, P., Lasalle, T., Clement, R., Matiasek, S., Smith, L., Boyd, E., Brimlow, J., Liles, G., Knowles, J., Mitchell, R. 2025. Soil Carbon Accrual Project: Unpublished dataset. Chico State Center for Regenerative Agriculture and Resilient Systems.
9	Coastal Rangeland Dataset	Strohm, H., Foster, E., Carey, C.J. 2025. Bale Grazing Experiment: Unpublished dataset. TomKat Ranch.
10	Rangeland Carbon Management Project	Foster, E., Cook, A., Banuelos, A., Stricker, E., Paustian, K., Eash, L., Carey, C.J. 2025. Rangeland Carbon Management Project: Unpublished dataset. Point Blue Conservation Science.

11	Sierra Meadow Soil Carbon Monitoring, Sierra Meadows Partnership Meadow Restoration for Greenhouse Gas Reduction Study, Sierra Meadow Research and Restoration Partnership	Reed, C. C., Merrill, A. G., Drew, W. M. et al. (2021). Montane meadows: A soil carbon sink or source? Ecosystems, 24, 1125-1141. Reed, C. C., Berhe, A. A., Moreland, K. C., Wilcox, J., Sullivan, B. (2022). Restoring function: Positive responses of carbon and nitrogen to 20 years of hydrologic restoration in montane meadows. Ecological Applications, 32(7), 1-17. Truckee River Watershed Council. 2022. Sardine and Lacey Meadow Soil Carbon: Unpublished dataset. American Rivers. 2023. Calf and Wilson Meadows Soil Carbon: Unpublished dataset. South Yuba River Citizens League. 2022. Freeman Meadows Soil Carbon: Unpublished dataset.
12	Soil Health Assessment for Vineyard Management Project	North Coast Soil Hub. 2025. Soil health assessment for climate-beneficial vineyard management practices within the North Coast Area Project: Unpublished dataset.
13	Kings River Experimental Watershed Study	Johnson, D. W., Hunsaker, C. T., Glass, D. W., Rau, B. M., & Roath, B. A. 2011. Carbon and nutrient contents in soils from the Kings River Experimental Watersheds, Sierra Nevada Mountains, California. Geoderma, 160(3-4), 490-502.
14	Death Valley Soil Dataset	Treonis, A. M., Sutton, K. A., Unangst, S. K., Wren, J. E., Dragan, E. S., & McQueen, J. P. (2019). Soil organic matter determines the distribution and abundance of nematodes on alluvial fans in Death Valley, California. Ecosphere, 10(4), e02659.
15	Loma Ridge Soil Dataset	Fiore, N. 2025. Soil carbon from Loma Ridge Global Change Experiment: Unpublished dataset.
16	Abandoned Agriculture Study	Weverka, J. 2025. Legacy effects of tillage on soil carbon: Unpublished dataset.
17	The Century Experiment	Raffeld, A., Jackson, R., Sanford, G., Rath, D., Tautges, N. 2024. The importance of accounting method and sampling depth to estimate changes in soil carbon stocks. Published dataset. DOI: 10.5061/dryad.p2ngf1w06
18	Suburban Soil Study	Suratt, A. (2024). Suratt_Data from Southern California Soils Study_Generated 2022. Figshare. Published dataset. DOI: 10.6084/m9.figshare.25429579.v1
19	Residential Yard Study	Trammell, T. 2018. American Residential Macrosystems - Soil Carbon and Nitrogen from seven North American Cities, 2008-2015 ver 1. Environmental Data Initiative. DOI: 10.6073/pasta/a8feb9c66e6a3cb6a7e628076fbc51ad
20	Lawn Turfgrass Study	Selhorst, A., & Lal, R. (2013). Net Carbon Sequestration Potential and Emissions in Home Lawn Turfgrasses of the United States. Environmental Management, 51(1), 198–208.
21	Urban Habitat Project	Vourlitis, G. L., van der Veen, E. L., Cangahuala, S., Jaeger, G., Jensen, C., Fissore, C., ... & Meyer III, W. M. (2022). Examining decomposition and nitrogen mineralization in five common

		urban habitat types across southern California to inform sustainable landscaping. Urban Science, 6(3), 61.
22	Garden of Eden Experiment	McFarlane, K. J., Schoenholtz, S. H., Powers, R. F., & Perakis, S. S. (2010). Soil organic matter stability in intensively managed ponderosa pine stands in California. Soil Science Society of America Journal, 74(3), 979-992.
23	Blodgett Forest Project	Riley, W, Tao, J, & Pegoraro, E (2024): Experimental Soil Warming Impacts Soil Moisture and Plant Water Stress and Thereby Ecosystem Carbon Dynamics (Blodgett, CA). Belowground Biogeochemistry Scientific Focus Area, ESS-DIVE repository. Dataset. DOI:10.15485/2480291. Soong, J, Pries, C, Castanha, C, Porras, R, ... & Riley, W. (2022). Soil C stock and CO2 production data for Soong et al. 2021: Effects of five years of soil warming at Blodgett Forest, CA. ESS-DIVE. DOI:10.15485/1896308.
24	Teakettle Experiment	Minocha, R, Long, S, & North, M. P. 2020. Data on the effects of silvicultural thinning and prescribed fire on soil chemistry and foliar physiology of three coniferous species at the Teakettle Experimental Forest, California, USA. Fort Collins, CO: Forest Service Research Data Archive. DOI: 10.2737/RDS-2020-0074.
25	Redwood Study	Clark, B. C. (2021). Characteristics and management implications of mollic soils in forest versus grassland settings in central California. Master's thesis, California Polytechnic State University.
26	Dryland Elevation Gradient Project	Chatterjee, A., & Jenerette, G. D. (2015). Variation in soil organic matter accumulation and metabolic activity along an elevation gradient in the Santa Rosa Mountains of Southern California, USA. Journal of Arid Land, 7(6), 814-819. Chatterjee, A., & Jenerette, G. D. (2011). Spatial variability of soil metabolic rate along a dryland elevation gradient. Landscape Ecology, 26(8), 1111-1123.
27	California Annual Grassland Validation Dataset	Mayer, A & Silver, W (2022). DayCent simulations for California annual grasslands: Monthly data outputs [Dataset]. Dryad. DOI: 10.6078/D1DD85
28	Sage Scrub and Grassland Study	Wallace Meyer, & Caspi, T. (2018). Carbon and nitrogen storage in the topsoils of Inceptisols and Mollisols under native sage scrub and non-native grasslands in southern California. Knowledge Network for Biocomplexity. DOI:10.5063/F1000081.
29	Desert Soil Carbon Study	Mills, J., Lammers, L., & Amundson, R. (2020). Carbon balance with renewable energy: Effects of solar installations on desert soil carbon cycle (CEC-500-2020-075). California Energy Commission, Energy Research and Development Division.
30	Salt Marsh Dataset	Curtis, J.A., Thorne, K.M., Freeman C.M., Buffington, K.J., & Drexler, J.Z., 2022, Salt marsh monitoring during water years 2013 to 2019, Humboldt Bay, CA – water levels, surface deposition, elevation change, and soil carbon storage: U.S. Geological Survey data release, DOI: 10.5066/P9QLAL7B

All soil observations were standardized prior to modeling to ensure consistency in soil depth, units, spatial reference, and temporal attribution. Datasets were processed through one of two harmonization pathways depending on whether they directly reported carbon stock estimates or provided underlying measurements (e.g., carbon concentrations and bulk density) that could be used to derive soil carbon stocks.

For datasets where soil carbon was presented as a concentration, values were standardized to percent units. A small amount of loss-on-ignition data were included, and values were converted from soil organic matter to soil carbon using a standard conversion factor of 0.58. Samples with incomplete depth coverage (e.g., 0-15 cm) were estimated to 30 cm using an ecosystem-specific exponential decay function with decay constants calibrated from observed depth profiles within the compiled dataset:

$$C_x = C_0 * e^{-kz}$$

where C_0 is soil carbon at the surface, z is the midpoint depth, and k is an ecosystem-specific decay constant (Appendix Table 24).

Appendix Table 24 - Decay constants used to estimate soil carbon to 30 cm depth, where necessary.

Land Cover Category	Decay Constant
Cropland	0.0248
Other Land	0.0304
Grassland	0.0310
Wetland	0.0350
Shrubland	0.0362
Forest	0.0530
Developed Land	0.0630

Where bulk density measurements were missing or incomplete for the full 0-30 cm depth, location-specific bulk density values from gNATSGO were used instead. Soil carbon stocks were then calculated to 30 cm depth using depth-weighted averages of soil carbon concentration, bulk density, and rock fragment content (which was also derived from gNATSGO) in the following equation:

$$Soil\ carbon\ stock\ \left(\frac{Metric\ Ton}{Hectare}\right) = Bulk\ density\left(\frac{g}{cm^3}\right) * Soil\ carbon\ (\%) * Soil\ Depth\ (cm) * (1 - rocks)$$

Datasets that directly reported soil carbon stocks were processed through a much simpler parallel harmonization pathway. Here, reported carbon stocks were standardized to 30 cm depth using the function:

$$Soil\ carbon_{0-30cm} = Soil\ carbon_{ref} * \frac{1 - e^{-k*30}}{1 - e^{-k*z_{ref}}}$$

Where $Soil\ carbon_{ref}$ is the reported carbon stock over depth Z_{ref}, Z_{ref} is the lower boundary of the reported depth interval in centimeters, and k is the ecosystem-specific decay constant (Appendix Table 24).

To represent soil carbon stocks beneath sealed surfaces[2] in developed lands, a synthetic dataset was generated by augmenting each observation in the harmonized soil dataset with a corresponding sealed-surface estimate. This approach preserved all original spatial, temporal, and ancillary attributes to support the assumption that synthetic values will similarly correlate with climate and other spatial gradients. Carbon loss with sealing was modeled as a proportional reduction based on empirical comparisons of sealed and unsealed conditions (Raciti et al. 2012; Wang et al. 2020; O'Riordan et al. 2021; Pereira et al. 2021). The proportional reduction was represented as a normally distributed precent change with a mean loss of 43.2% and a standard deviation of 23.2%. For each observation, a single random draw from this distribution was applied to the original 0-30 cm soil carbon stock estimate to predict the corresponding sealed surface value. Any resulting values that were less than or equal to zero were identified and re-assigned new percent change values, with this process repeated iteratively until all synthetic values were positive. Following this, a generalized additive model was used to relate sealed surface soil carbon with their spatial coordinates and then predict sealed surface carbon for a separate list of 28 known sealed locations for digital soil mapping purposes.

Covariate Data

Soil carbon stocks were modeled as a function of both static and time-varying environmental covariates (Appendix Table 25). This combination reflects both long-term soil-forming factors and dynamic land surface processes that influence soil carbon storage and variability.

Static covariates represent slowly varying or time-invariant controls on soil carbon and include variables related to terrain, soil type, and climate. Static variables used in this analysis included topographic metrics derived from 30 m digital elevation models (elevation, slope, and aspect); soil properties derived from gNATSGO, including available water holding capacity, soil texture fractions (sand and clay), soil pH, and soil order; climate variables derived from PRISM and gridMET, including mean annual precipitation (MAP), mean annual temperature (MAT), annual precipitation and minimum and maximum annual temperature; seasonal median Landsat land surface temperature composites; and categorical soil classification information represented by soil order. All static covariates were spatially aligned to a common 250 m grid and normalized prior to model training to ensure numerical stability and comparability across variables.

[2] Sealed surfaces are areas where the soil is covered by impervious materials such as asphalt, concrete, or buildings that physically isolate the soil from the atmosphere, rain, and plant inputs.

Time-varying covariates were derived primarily from satellite remote sensing products. Landsat imagery was summarized into seasonal composites representing spring and summer conditions, capturing phenological and productivity-related signals relevant to soil carbon dynamics. For each year, seasonal image chips were extracted and used as spatial inputs to the model.

In addition, moderate-resolution satellite time series data (e.g., MODIS surface reflectance and vegetation indices) were used to characterize intra-annual land surface dynamics. For each year, a fixed-length sequence of observations spanning the current year and the preceding year was selected to ensure temporal consistency across samples. These time series covariates capture seasonal variability and short-term lagged effects in vegetation productivity and climate–vegetation interactions that influence soil carbon patterns.

Explicit, spatially resolved land management data were not available consistently across California or through time and therefore were not included as direct model covariates. Consequently, management influences on soil carbon were captured only indirectly through the inclusion of vegetation cover, surface reflectance, or other environmental covariates that themselves were responsive to management interventions.

Appendix Table 25 - Data used to support the mineral soil methodological update.

Input Data	Source (Citation)	Purpose	Brief Description
Field-based soil measurements	Various	Digital Soil Mapping training and validation	Empirical measurements of carbon stocks to 30 cm
Elevation	USGS Digital Elevation Model	Digital Soil Mapping covariate layer	Ground surface elevation
Slope	USGS Digital Elevation Model	Digital Soil Mapping covariate layer	Rate of elevation change calculated from the DEM
Aspect	USGS Digital Elevation Model	Digital Soil Mapping covariate layer	Direction of slope orientation derived from the DEM
Soil pH	gNATSGO	Digital Soil Mapping covariate layer	A measure of soil acidity/alkalinity
Soil clay content	gNATSGO	Digital Soil Mapping covariate layer	Units: %.
Soil sand content	gNATSGO	Digital Soil Mapping covariate layer	Units: %.
Soil order	gNATSGO	Digital Soil Mapping covariate layer	USDA Soil Taxonomy classification
Available water holding capacity	gNATSGO	Digital Soil Mapping covariate layer	Volume of water that soil can store and make available to plants,
Bulk density	gNATSGO	Soil carbon stock calculations	Mass of soil per volume
Rock content	gNATSGO	Soil carbon stock calculations	Volume of rocks per volume
Mean annual temperature	PRISM	Digital Soil Mapping covariate layer	PRISM 30-year normals of annual temperature

Mean annual precipitation	PRISM	Digital Soil Mapping covariate layer	PRISM 30-year normals of annual precipitation
Landsat image (Landsat 5, 7, and 8)	USGS Landsat Program	Digital Soil Mapping covariate layer	Surface reflectance image subsets ("chips") derived from Landsat 5 TM, Landsat 7 ETM+, and Landsat 8 OLI imagery; provide consistent, 30-m multispectral observations for characterizing vegetation, land cover, and long-term surface conditions.
MODIS 8-day surface reflectance	NASA MODIS	Digital Soil Mapping covariate layer	8-day composite surface reflectance time series; used to capture seasonal and interannual dynamics in vegetation, phenology, and land surface conditions.
Annual climate variables (Tmin, Tmax, precipitation)	gridMET	Digital Soil Mapping covariate layer	Annual summaries derived from daily gridMET minimum temperature, maximum temperature, and precipitation; used to represent interannual climate variability

Unique Spatial Identifier

A Unique Spatial Identifier (UID) was used to link target variables, predictor variables, and model outputs across datasets and time steps. One UID was assigned to each modeling unit and corresponded to a fixed spatial grid cell within a regularly spaced grid at 250 m resolution. The UID was created by dividing California into uniform grid cells of equal size and assigning a unique identification number to each cell. All datasets used in the DSM framework were indexed to the UID. This included:

- Soil organic carbon measurements
- Static environmental covariates
- Seasonal remote sensing composites
- Satellite-derived time series covariates
- Model predictions

Soil observations were spatially joined to the grid and assigned the UID of the grid cell in which they occurred. Covariates and model outputs were generated for each UID and, where applicable, for each year.

Digital Soil Mapping Model Architecture

Soil carbon predictions were generated using a multi-input deep learning model designed to integrate static environmental variables, seasonal spatial imagery, and satellite time series data. The model architecture consisted of three primary components.

First, a convolutional neural network was applied to seasonal image composites (spring and summer) to extract spatial features associated with vegetation condition and land surface characteristics. Second, a temporal neural network summarized satellite-derived time series data, capturing intra-annual dynamics and interannual variability relevant to soil carbon. Third, a multilayer perceptron processed static covariates representing long-term soil, climate, and terrain controls.

Latent features produced by these three components were concatenated and passed through fully connected layers to generate a single soil carbon stock prediction for each spatial unit and year. Conceptually, the model can be expressed as:

$$\hat{C}_{i,t} = f_{\text{DSM}}\left(X_{\text{static},i},\ X_{\text{seasonal},i,t},\ X_{\text{ts},i,t}\right)$$

where $\hat{C}_{i,t}$is the predicted soil carbon stock at location $i$and year t, and f_{DSM} represents the trained deep learning model, $X_{\text{static},i}$ represents time-invariant covariates at location i, such as soil properties, topography, and long-term climate normals. $X_{\text{seasonal},i,t}$ denotes seasonal remote sensing features at location $i$and year t, derived from multi-spectral image chips that capture intra-annual vegetation and surface conditions. $X_{\text{ts},i,t}$ represents MODIS 8-day surface reflectance time-series inputs at location $i$and year t, used to characterize seasonal dynamics and interannual variability.

Model training used a mean squared error loss function and was optimized using stochastic gradient-based methods. Regularization strategies, including dropout, weight decay, and early stopping based on validation performance, were applied to reduce overfitting. The DSM model employed a five-fold ensemble approach, in which the dataset was partitioned into five subsets. For each fold, 80% of the data was used for model training and the remaining 20% was reserved for validation. The model was trained and evaluated across all five folds (see the Uncertainty Analysis section for details), and the mean prediction from the five model runs was used to produce the soil carbon maps for all subsequent analysis and reporting.

Spatial and Temporal Analyses

The DSM model described above was trained using point-based soil observations and applied to a statewide 250 m grid to generate spatially continuous soil carbon estimates.

Temporal analysis was conducted by explicitly incorporating year-specific covariates into the modeling framework, enabling estimation of annual soil carbon stocks over the analysis period (2001–2024). Temporal variation in soil carbon estimates arose from interannual

variability in climate and vegetation dynamics as captured by remote sensing time series and annual climate metrics. The model did not simulate soil carbon turnover mechanistically; rather, temporal patterns were learned empirically from relationships between covariates and observed soil carbon stocks. Because model training relied largely on single timepoint soil observations whose locations varied by year, modeled interannual differences may reflect a combination of true temporal change as well as spatial variability among sampling locations over time.

Soil Depth Correction

Annual maps of soil carbon produced by the mean of the five model runs were adjusted post-hoc to account for spatial variation in soil depth. This was necessary because the soil observations used to train the model were standardized to a common reference depth (0-30 cm) using a process that did not take into account actual soil depth at the point locations; therefore, this standardization might have introduced overestimation in locations with shallower soils. To address this, a map of bedrock depth from gNATSGO was used to constrain modeled soil carbon stocks to the actual depth of soil present at each location. Specifically, an exponential depth-correction function was applied to each year's carbon map, reducing modeled stocks where soil depth was less than 30 cm using the following equations:

$$\text{For d} < 30\text{ cm: } frac(d) = \frac{1-\exp(-kd)}{1-\exp(-k*30)}$$

$$\text{For d} \geq 30\text{ cm: } frac(d) = 1$$

Where d is the soil depth in centimeters and k is an exponential decay constant of 0.03 cm^{-1}. The depth-adjusted soil carbon was then calculated as:

$$Soil\ carbon_{adjusted} = Soil\ carbon * frac(d)$$

The depth-adjusted mineral soil carbon maps were used for final reporting purposes for the inventory years 2001-2022.

Uncertainty Analysis

To quantify uncertainty in the DSM model, a 5-fold cross-validation scheme was applied, where the soil carbon model was trained five separate times, each time withholding a distinct 20% subset of soil measurements. Predictions were generated only for these held-out samples to avoid information leakage and ensure an unbiased evaluation. This approach provided a robust assessment of model performance by ensuring that every observation was used once for testing and four times for training.

Once all folds were completed, predictions from all held-out subsets were combined into a single dataset representing model performance across the full observational record. This combined dataset reflected both the spatial heterogeneity of California soils and the

inherent modeling uncertainty—and formed the basis for evaluating uncertainty associated with the statewide soil carbon estimates.

QA/QC Activities

Quality assurance/quality control activities were performed throughout the process of generating soil carbon estimates for mineral soils. For example, soil carbon and bulk density data for carbon stock calculations were screened for implausible values. In addition, independent hand calculations were used to verify that scripted carbon stock computations executed correctly across a range of data structures and conditional logic, including cases with measured versus inferred inputs and partial versus complete depth information. These checks ensured that unit conversions, depth adjustments, and conditional logic behaved as intended when generating the harmonized soil carbon dataset.

In addition, the harmonized soil carbon dataset was visually explored using boxplots and other graphs of soil carbon concentrations and stocks by ecosystem type and other factors. This exercise was used to identify and check outliers or suspicious/unexpected patterns based on expert judgement and published literature. For the synthetic sealed-surface soil carbon dataset, quality control included automated screening to prevent physically implausible (<0) values.

When running the model, quality control focused on raster and data consistency. Specifically, inputs were checked for matching coordinate reference systems, grid alignment, resolution, and extent prior to all pixel-wise operations.

Once soil carbon maps were generated, they were visually assessed for spatial and temporal patterns, using expert judgment to iteratively evaluate general trends and refine the model inputs and final products as necessary. In addition, reported estimates were repeatedly cross-checked for internal consistency across multiple summaries, spatial aggregations, and reporting breakdowns (e.g., statewide versus regional totals) to ensure that values were consistent across all reporting sections.

Finally, quality assurance was provided through internal and external review by individuals not directly responsible for generating the estimates. Methods, assumptions, and preliminary outputs were reviewed prior to and during implementation. Final results were also evaluated in some cases through comparison with independent estimates.

2018 Methods

With the exception of croplands remaining croplands, carbon stocks for mineral soils across all land types and conversion scenarios were estimated in the 2018 NWL Carbon Inventory using an IPCC Tier 2 approach (CARB, 2018a). Briefly, initial soil carbon values were estimated based on SoilGrids (2017) and stock change factors were applied to different land conversion scenarios following standard IPCC equations (CARB, 2018b). This resulted in annualized and total estimates for carbon stock change over the inventory period (2001-

2010). Changes in soil carbon stocks for croplands remaining croplands were estimated using the Denitrification Decomposition (DNDC) model (Li et al. 1992). Results for mineral and drained organic soils were combined for final estimates, and extrapolated from 2001-2010 through 2014.

Organic Soils

2025 Methods

Methodological Updates

In the 2018 NWL Carbon Inventory, organic soils were limited to the Delta Ecoregion and treated as purely emissive using global IPCC Tier 1 stock change factors, resulting in aspatial estimates of carbon loss. The 2025 NWL Carbon Inventory retained the use of stock change factors but embedded them within a spatially explicit framework by leveraging California-wide carbon maps produced through digital soil mapping as a baseline (described above for mineral soils). This allowed organic soil carbon dynamics to be represented with realistic spatial variation and with updated Tier 2 stock change factors in some cases. In addition, the mapped extent of organic soils was expanded beyond the Delta to include histosols and coastal wetlands statewide.

Detailed Methods Description

Organic soils contain high amounts of organic matter, storing more than 12% organic carbon by weight, and are developed under poorly drained conditions that limit decomposition. In California, organic soils are found in the Delta ecoregion, where they have mostly been drained for land use purposes (Deverel et al. 2020). However, organic soils are also found in coastal wetlands outside of the Delta, such as in coastal salt marsh ecosystems.

For the 2025 NWL Carbon Inventory, organic soils were treated separately from mineral soils to account for foundational differences in carbon dynamics (IPCC, 2006) that were not captured in the harmonized soil carbon database. To begin, a statewide mask was created to define the spatial boundary of organic soils based on their maximum observed spatial extent during the inventory period. Here, organic soils were defined as Histosols based on USDA soil classification and as coastal wetlands based on the California Aquatic Resources Inventory (CARI; Appendix Table 26).

Appendix Table 26 - Data used to support the organic soil methodological update.

Input Data	Source (Citation)	Purpose	Brief Description
Soil order	gNATSGO	Creating organic soil mask	Used to delineate histosol soils
Wetland extent	California Aquatic Resources Inventory (CARI)	Creating organic soil mask	Used to delineate coastal wetlands
Land cover classification map	Various (see mapping section)	Assigning land cover to each organic soil pixel	Includes IPCC land cover categories and subdivisions from Appendix Table 28
Stock Change Factors	Various	Estimating annual gains or loss in soil carbon by land type	In MT C/Ha/Yr

After masking the organic soil extent, cumulative carbon change was estimated for each pixel and year based on land type specific Tier 1 and Tier 2 stock change factors. For pixels containing land types with positive stock change factors in 2022, cumulative stock change was initialized at zero in 2001 and accrued forward in time (Appendix Table 27). For pixels containing land types with negative stock change factors in 2022, cumulative stock change was initialized at zero in 2022 and accrued backward in time using the inverse of the stock change value. Pixels that transitioned between land types with positive or negative stock change factors during the inventory period retained their original processing pathway, but gained or lost carbon annually according to the appropriate land type specific stock change factors (Appendix Table 27).

Appendix Table 27 – Illustrative examples of pixel-wise cumulative soil carbon stock change calculations for different land cover scenarios based on the Tier 1 and Tier 2 stock change factors.

Land Cover	Stock Change Factor (MT C/Ha/Yr)	Cumulative Stock Change (MT C/Ha)	Trend
Brackish Salt Marsh (2001-2022)	1.08	2001: 1.08 2002: 2.16 2003: 3.24 … 2020: 21.60 2021: 22.68 2022: 23.76	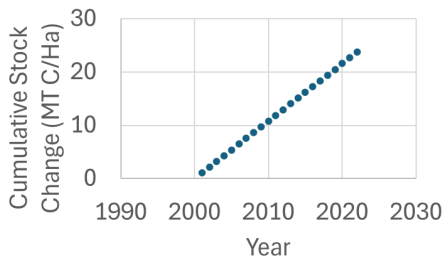

Rice Cropland (2001-2022)	-3.63	2022: 3.63 2021: 7.26 2020: 10.89 … 2003: 72.60 2002: 76.23 2001: 79.86	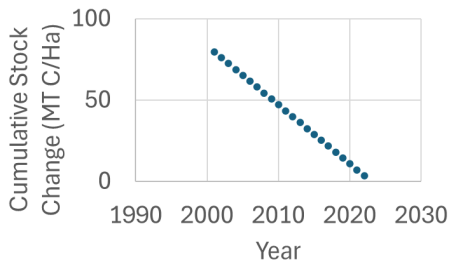
Freshwater Organic Wetland (2001-2020) to Developed Land (2021 to 2022)	0.74 & -10.00	2022: 10.00 2021: 20.00 2020: 19.26 … 2003: 6.68 2002: 5.94 2001: 5.20	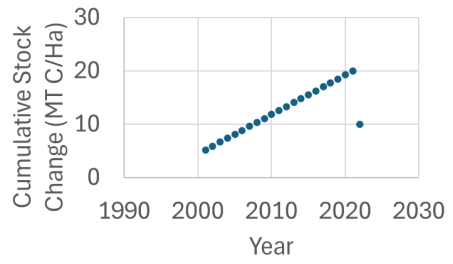

Once cumulative carbon stock change trajectories for each organic soil pixel were constructed, they were applied to the DSM-derived soil carbon stock map for 2022 using the following equation:

$$Soil\ carbon_t = Soil\ carbon_{2022} + C_t$$

Where $Soil\ carbon_t$ is soil carbon stock in year t, $Soil\ carbon_{2022}$ is the DSM-derived baseline stock for 2022, and C_t is the cumulative stock change for year t.

This approach leveraged the spatial patterns and baseline stock values of organic soils derived from the DSM model while ensuring that carbon stock values remained above zero and the year-to-year dynamics reflected standardized, system-specific estimates of carbon accumulation and loss. Upon completion, the resulting organic soil carbon maps for 2001-2022 were merged back with the mineral soil carbon maps to produce final estimates for reporting and analysis purposes.

Stock Change Factors

For wetlands, stock change factors were sourced from previously published estimates or were calculated as the net ecosystem carbon balance of CO_2 and CH_4 emissions (Appendix Table 28) (see the GHG Flux Methodological Details section for more information on the derivation of CO_2 and CH_4 emissions). Lateral flux of carbon in tidal systems was assumed to be 41% of the net ecosystem carbon exchange, based on measurements in Suisun Marsh

(Bogard et al., 2020). As this methodology does not quantify lateral flux in non-tidal systems, carbon stock change may be over or underestimated when those systems experience significant sediment deposition, erosion, dissolved carbon, or other lateral movements of carbon. In addition, tidal systems experience a range of lateral fluxes, which are likely to change with changing climate and sea levels. Tier 3 modeling approaches can resolve some of these limitations and should be explored for future inventory updates (OPC, 2024). For other land types, stock change factors were sourced from previously published estimates (Appendix Table 28).

Appendix Table 28 - Carbon stock change factors in metric tons (MT) of carbon per hectare (Ha) per year (Yr). Values are provided for IPCC land cover categories and, where appropriate, for land cover subdivisions. Negative values denote annual losses in soil carbon and positive values denote annual gains in soil carbon. The tier and citation for each carbon stock change factor is also provided.

IPCC Land Cover Category	Subdivision	Carbon Stock Change Factor (MT C/Ha/Yr)	Tier & Citation
Forest Land	N/A	-0.68	Tier 1; 2018 NWL Carbon Inventory
Shrubland	N/A	-0.68	Tier 1; 2018 NWL Carbon Inventory
Grassland	N/A	-2.50	Tier 1; 2018 NWL Carbon Inventory
Other Land	N/A	-2.50	Tier 1; 2018 NWL Carbon Inventory
Developed Land	N/A	-10.00	Tier 1; 2018 NWL Carbon Inventory
Cropland	Rice	-3.63	Tier 2; 2022 Scoping Plan
Cropland	All Other Cropland	-5.30	Tier 2; 2022 Scoping Plan
Wetland	Seasonal Organic Wetland	-2.42	Tier 2; 2022 Scoping Plan
Wetland	Rewetted Organic Wetland	3.41	Tier 2; 2022 Scoping Plan
Wetland	Managed Brackish Wetland	-2.24	Tier 2; 2022 Scoping Plan
Wetland	Freshwater Organic Wetland	0.74	Tier 2; 2022 Scoping Plan; Arias-Ortiz et al. 2024; Bogard et al., 2019
Wetland	Brackish Salt Marsh	1.08	Tier 2; Shahan et al., 2022; Bogard et al., 2019; Bergamaschi & Windham-Myers, 2018; Arias-Ortiz et al., 2024
Wetland	Saline Salt Marsh	1.09	Tier 2; Shahan et al., 2022; Bogard et al., 2019; Bergamaschi & Windham-Myers, 2018; Arias-Ortiz et al., 2024

QA/QC Activities

Quality assurance and quality control procedures were applied to the organic soil workflow to ensure that stock-change factors and spatial integration were implemented correctly.

First, randomly selected pixels within mapped organic soils were manually inspected to verify that Tier 1 and Tier 2 stock-change factors were applied correctly through time, including cases where land cover changed. Second, summarized trends in organic soil carbon stocks and stock change were visually examined to confirm that temporal patterns were consistent with expected system behavior and known land-use dynamics. Finally, mineral soil carbon values were compared before and after merging with the organic soil layers to ensure that mineral soil carbon estimates were preserved exactly and that the stitching process did not alter mineral soil carbon stocks.

2018 Methods

For the 2018 NWL Carbon Inventory, drained organic soils, which were constrained to land types in the Delta Ecoregion, were assumed to be purely emissive. Losses in carbon over time were determined using global "emission" factors from IPCC using a Tier 1 standard IPCC equation. Results for drained organic soils were combined with those of mineral soils for final estimates, and extrapolated from 2001-2010 through 2014.

GHG Flux Methodological Details

Wetland greenhouse gas (GHG) flux estimates were quantified using an emissions factor approach, based on a combination of IPCC Tier 1 and Tier 2 factors (Appendix Table 29). Detailed methods are described in the sections to follow.

Following quantification, wetland GHG maps were combined to produce complete GHG flux maps for the entire inventory period (2001-2022).

Once wetland GHG maps were produced, net CO_2e flux was quantified over space and time. Annual GHG fluxes (MT CO_2e/yr) were summarized by wetland type (incorporating salinity, management, IPCC category, and soil type), then aggregated to produce regional and statewide totals. This approach accounted for GHG flux over each transition period (2001-2013 and 2014-2022). All analyses included the subset of mapped wetlands that could be quantified under the IPCC framework.

Appendix Table 29 - IPCC Tier and methods summary for estimating GHG fluxes in wetlands.

Reporting Category	Tier	Method Summary	Scope
Wetland	Tier 2/Tier 1	Emission Factor	CO_2 and CH_4

Wetland

2025 Methods

Methodological Updates

Relative to the 2018 NWL Carbon Inventory, which relied on Tier 1 IPCC factors and IPCC categories, the 2025 NWL Carbon Inventory primarily used Tier 2 emission factors (derived from California data) and expanded wetland categories to incorporate salinity classes. In 2018, wetland GHGs were quantified through a standalone analysis and mapping did not allow interaction with other land types. In contrast, the present inventory includes wetlands as a land type which can convert to or from other land types. Additionally, restoration and management were tracked in the Delta, quantifying GHGs for various subsidence reversal projects on an annual time scale.

Detailed Methods Description

Emissions Factors

Quantification of greenhouse gas emissions from wetlands relied on a mixed Tier 2 and Tier 1 emissions factor approach. Emissions factors were developed for various wetlands categories across the state. These categories disaggregated wetlands based on geographic location, major drivers of methane emissions (such as temperature and salinity), management status, and overarching IPCC categorization (IPCC, 2014). Emissions factors were synthesized from existing emissions factors, eddy covariance and multi-site chamber data, and Tier 1 IPCC emissions factors. Eddy covariance is a direct measurement method for landscape-scale fluxes of trace gases (such as greenhouse gases). Chamber measurements rely on enclosures to measure trace gas flux from a smaller portion of the landscape, thus only chamber studies measuring multiple sites were included. Data and emissions factors from within California were preferred, but measurements of wetlands in the United States were also included when appropriate.

Wetlands emission factors account for the greenhouse gas contribution of both CO_2 and CH_4. Existing CARB emissions factors for CO_2 and CH_4 in rewetted organic wetlands, seasonal organic wetlands, and managed brackish wetlands were sourced from the 2022

Scoping Plan, Appendix I (CARB, 2022). Default IPCC emissions factors for CH_4 were used for managed freshwater mineral wetlands. All other emissions factors were generated from the literature (Appendix Table 30). Both eddy covariance and multi-chamber studies with complete annual budgets were considered for emissions factor development. Where multiple eddy covariance or multi-chamber measurements were available, data were averaged, weighted by the number of years available for each site. Emissions factors for CO_2 and CH_4 were converted to CO_2e factors using a CH_4 global warming potential of 28.

Two categories of wetlands were not quantified for greenhouse gas emissions—unmanaged freshwater mineral wetlands and vernal pools (Appendix Figure 7). Both wetland types are part of the IPCC Inland Wetland Mineral Soils category. IPCC does not provide default guidance nor emissions factors for unmanaged inland wetland mineral soils, requiring state- or county-specific data and approaches to include them in the inventory. Insufficient data was found to quantify these wetland categories within the 2025 NWL Carbon Inventory update.

Appendix Table 30 – Emissions factors for wetlands. Emissions factors are net exchanges of CO_2 and/or CH_4 and are presented as CO_2 equivalent (CO_2e). Conversion of CH_4 to CO_2e assumes a global warming potential of 28. Negative values denote a net uptake (net movement from the atmosphere to the surface), while positive values denote a net source (net movement from the surface to the atmosphere). Ranges represent the minimum and maximum annual estimate from synthesized literature or existing emissions factors.

Wetland Category	GHG Emissions Factor (MT CO2e/ha/yr) [GWP-28]	Range (MT CO2e/ha/yr) [GWP-28]	CO2 GHG Emissions Factor (MT CO2e/ha/yr)	CH4 GHG Emissions Factor (MT CO2e/ha/yr) [GWP-28]	Citations
Rewetted Organic Wetlands	3.31	1 to 5.6	-14.21	17.53	Please See 2022 Scoping Plan Appendix I
Seasonal Organic Wetlands	8.87	4.2 to 13.6	8.87	0.00	Please See 2022 Scoping Plan Appendix I
Freshwater Organic Wetlands	7.22	-12.4 to 55.7	-8.15	15.37	Please See 2022 Scoping Plan Appendix I for CO_2 emissions factors. CH_4 emissions factors were synthesized by Arias-Ortiz et al., 2024.
Brackish Salt Marshes	-8.36	-14.9 to 3.1	-9.81	1.45	Brackish and Saline Wetland CO_2 emissions factors derived from Shahan et al., 2022; Bogard et al., 2019; Bergamaschi & Windham-Myers, 2018. CH_4 emissions factors synthesized from Arias-Ortiz et al., 2024.
Managed Brackish Wetlands	8.61	4.9 to 12.8	8.15	0.46	Please See 2022 Scoping Plan Appendix I

Saline Salt Marshes	-9.49	-14.3 to 0.3	-9.81	0.32	Brackish and Saline Wetland CO_2 emissions factors derived from Shahan et al., 2022; Bogard et al., 2019; Bergamaschi & Windham-Myers, 2018. CH_4 emissions factors synthesized from Arias-Ortiz et al., 2024 and Shahan et al., 2022.
Montane Meadows	-0.04	-31.1 to 21.7	-0.37	0.33	Reed et al., 2021 and Oliphant et al., 2024
Managed Freshwater Mineral Wetlands	10.87	-31.7 to 28.7	-5.39	16.25	CO_2 emissions factors were synthesized from Rocha & Goulden, 2010 and Point Blue Conservation Science, 2023. CH_4 emissions factors relied on IPCC Tier 1 factors for managed inland wetlands mineral soils

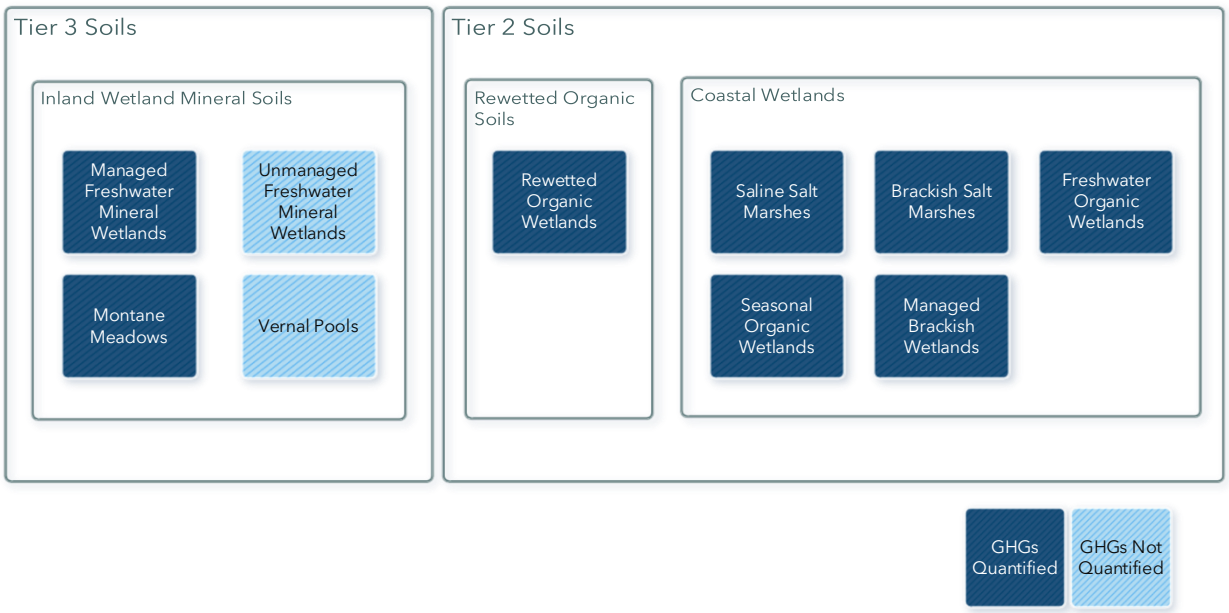

Appendix Figure 7 – Conceptual figure of wetlands quantification approach. Nested boxes, from the outside in, represent quantification differences based on organic (Tier 2 Soils) or mineral (Tier 3 Soils) assignments, IPCC wetland categories, and CARB wetland categories. Dark blue boxes denote CARB categories where greenhouse gases (GHGs) were quantified, while light blue boxes denote CARB categories where GHGs were not quantified. For more information on organic and mineral soils division, please see the Soil Carbon Methodological Details section. "Tier 2 Soils" denotes the major methodological tier, but includes some tier 1 IPCC emissions factors.

Wetland Mapping

Mapping of wetland categories relied on the California Aquatic Resources Inventory (CARI) (SFEI, 2024). and maps of subsidence reversal projects in the Delta. As with the 2018 inventory, CARI was crosswalked into IPCC relevant categories of Inland Wetland Mineral Soils and Coastal Wetlands based on "major_class" and "wetland_type" properties. Crosswalk, in this context, refers to the translation of data from one format or categorical scheme to another by aggregating or disaggregated categories and reformatting text. Updated from the 2018 inventory, IPCC rewetted organic soils were identified using maps of rewetting activities in the Delta (Appendix Table 31). Inland wetland mineral soils were further disaggregated into managed freshwater mineral wetlands, unmanaged freshwater mineral wetlands, and vernal pools using "wetland_type" and "anthropogenic_modifier" properties. Additionally, Montane meadows were extracted from other mineral wetlands by setting unmanaged freshwater mineral wetlands in the Sierra and Klamath ecoregions to a separate category (Appendix Table 31). This approach was taken in the absence of a suitable montane meadows maps but is likely an overestimate of current montane meadows extent. Coastal wetlands were further disaggregated into saline salt marshes, brackish salt marshes, managed brackish wetlands, and freshwater organic wetlands using the "Salinity_modifer" and "Anthropogenic_modifer" properties of CARI. Seasonal organic wetlands were further identified as any freshwater wetland on histosol soils—other than rewetted organic wetlands—in the Delta ecoregion (Appendix Table 31). The mapping strategy for Wetland GHGs is consistent with all other quantified carbon pools and the overarching land cover mapping. Please see the Land Cover Classification and Mapping section for more details on how wetland mapping interacted with other land types.

Maps of CARI wetlands were held constant through the inventory period, but were allowed to interact with maps from other lands types. This approach introduces several limitations. Primarily, a static map of wetlands through the inventory period provided limited capacity to monitor change. Annual mapping of wetlands across the state poses significant scientific challenge and is an active area of research (OPC, 2025). Wetland mapping with explicit detection of change would have significant benefits for future carbon inventory updates. In addition, the rasterization approach used to convert CARI into a land type map compatible with other land types may modify the extent of wetland throughout the state. Particularly for wetlands that are smaller than 30 m^2 or have complex geometries, rasterization likely overestimates total area when converted to a 30 m^2 resolution raster.

Restoration and Management Tracking

The 2025 NWL Carbon Inventory update integrated wetland restoration where sufficient emissions factors and mapping were available, which limited this approach to the Delta. The 2018 inventory relied on aggregated datasets, such as the San Fransico Estuary Institute's Habitat Project Tracker (Project Tracker) (SFEI, 2024). Project tracker was reviewed for implementation in the 2025 inventory, however spatial artifacts created incompatibility with the updated land cover mapping approach for wetlands. In addition, many wetland

categories do not currently have emissions factors for restoration and other management effects. While some of this data is under development—particularly for coastal wetlands—there was not sufficient data to determine emissions factors for restored coastal wetlands or other management effects as part of this update. Instead, the Delta Conservancy and Delta Independent Science Board provided data on current and in progress subsidence reversal projects in the Delta. Mapping of restoration and management in the Delta was achieved by combining these project maps with the CARI base maps and rewetted soils emissions factors. Management data was temporally specific, thus acreage of rewetted organic wetlands increased over time and showed GHG variation on annual time scales.

Appendix Table 31 - Data used to support the wetland GHG methodological update.

Input Data	Source (Citation)	Purpose	Brief Description
California Aquatic Resources Inventory	(San Francisco Estuary Institute, 2024)	Used to create maps of wetlands across California	Shapefiles of wetlands across the state, including multiple properties used to disaggregate wetland categories. This is a single, aggregated map depending on data collected in various years.
Subsidence Reversal Projects	Data provided by the Delta Conservancy and Delta Independent Science Board	Used to generate rewetted organic wetland map assignments.	Shapefiles of current and in-progress subsidence reversal projects in the Delta.
US EPA Ecoregions (Levels 3 and 4)	(EPA, 2025)	Level 3 and Level 4 products were used to identify montane meadows and the Delta ecoregion	Shapefiles of ecoregions where ecosystems are generally similar. This product is provided at various levels, which correspond to the relative area of each polygon and the scale of ecosystem aggregation.

Uncertainty Analysis

From all synthesized data and existing emissions factors, the range of annual greenhouse gas budgets for each wetlands category was recorded. This range of annual emissions or sequestration is reported in Appendix Table 30. For literature reviews or existing emissions factors which reported a single, averaged value and an error term, efforts were first made to contact the authors for raw, annual values. If raw data was unavailable, the average annual value, plus or minus the standard error, was considered for range values. Ranges were determined for both CO_2 and CH_4, then converted to a single range in terms of CO_2e.

QA/QC Activities

Quality assurance and quality control procedures were applied to the wetland workflow to ensure emission factors and spatial integration were implemented correctly. First, emissions data were checked to ensure correct aggregation from lower reporting levels to higher reporting levels. Second, randomly selected pixels within mapped wetlands were manually inspected to verify emissions factors were applied correctly through time, including cases where land cover changed or rewetting had occurred. Finally, summarized trends in GHG emissions were visually examined to confirm that temporal patterns were consistent with expected system behavior and known land-use dynamics.

2018 Methods

The 2018 NWL Carbon Inventory employed an IPCC Tier 1 approach to quantify CO_2 and CH_4 emissions from three key wetland types: inland wetland mineral soils, rewetted organic soils, and tidal marshes. Emissions calculations incorporated land cover data from the California Aquatic Resources Inventory (CARI) (SFEI, 2024) and IPCC emission factors to determine statewide emissions. The effects of restoration on wetlands were accounted for by mapping rewetted organic soils using EcoAtlas's Habitat Project Tracker (SFEI, 2024).

Harvested Wood Products Methodological Details

Harvested wood product carbon estimates were developed using a Tier 3 methodology (Appendix Table 32). Detailed methods are described in the sections to follow.

Appendix Table 32 - IPCC Tier and methods summary for estimating harvested wood products.

Reporting Category	Tier	Method Summary	Scope
Harvested Wood Products	3	IPCC Stock-Change approach	Products in-use (PIU); solid waste disposal sites (SWDS); GHG emissions

Harvested Wood Products

2025 Methods

Methodological Updates

Harvested wood product (HWP) carbon estimates were derived using a Tier 3 approach with California-specific modelling parameters and data associated with production, trade, utilization, and disposal. The Harvested Wood Products Carbon Model (HWP-C vR) was used to estimate how domestically-produced carbon moves into, within, and out of California's HWP pool over time—including carbon stored in products in use (PIU) and in solid-waste disposal sites (SWDS), along with associated carbon emissions. Exports were deducted from the reported estimates, and imported products were excluded from the totals. However, supplemental information on exports and imports was provided as an informational item in Appendix C.

The 2025 inventory represented the first inclusion of a statewide HWP carbon pool in the NWL Carbon Inventory. Key methodological considerations for 2025 included:

- Consistency with IPCC Tier 3 Stock-Change approach for carbon stock accounting that reported domestic harvest, excluded exports from reported stocks, and included imports as an informational item.
- Implementation of the Harvested Wood Products Carbon model (HWP-C vR) to estimate annual stocks, stock change, and emissions from PIU and SWDS pools, using California-specific parameters and data where available.
- Updated model inputs and internal accounting schemes to explicitly track domestic production, imports, and exports through the model workflow, including new ownership categories for Imports and Exports and post-processing logic to remove exports from California end-use array prior to PIU/SWDS fate calculations.
- Established a calibration and validation framework using independent datasets and alternative models (e.g., domestic production datasets; economic input/output (I/O) and Computable General Equilibrium (CGE) modeling via Regional Economic Modeling, Inc. (REMI); disposal and recycling data via CalRecycle; synchronizing boundaries with AB32 GHG inventory).

- Implemented QA/QC and uncertainty characterization, including mass-balance checks and Monte Carlo uncertainty analysis for key inputs and parameters, to support reproducibility and transparent reporting.

Detailed Methods Description

This section describes the Tier 3 Stock-Change accounting framework and the implementation of HWP-C vR used to estimate annual HWP carbon stocks, stock change, and atmospheric releases for California. The HWP pool included carbon contained in wood and paper products that were both produced and consumed statewide within California boundaries (IPCC, 2006). Additional results for HWPs imported into California were calculated and included as an informational item in Appendix C: Supporting Results.

Boundary Establishment

For the 2025 NWL Carbon Inventory Update, the carbon stock accounting and reporting approach followed a Tier 3 Stock-Change Approach, using methods outlined under IPCC Guidelines for National Greenhouse Gas Inventories (Appendix Figure 8). This method relied on tracking statewide input and output flows using a mixture of detailed jurisdictional harvest, utilization, trade, and discard data alongside process-based product allocation and decay assumptions. A brief description of this method from IPCC is described below:

> *"Use detailed country data beginning with a number of decades in the past and estimate each year, up to the present time, including (i) additions to pools of HWP in use, (ii) discards from use, (iii) additions to pools of HWP in SWDS, and (iv) decay from SWDS. Estimates for SWDS may use survey estimates of the amount of HWP placed in SWDS each year, rather than the amount of HWP going out of use and the portion going to SWDS. This method is also based on flux data and lifetime analysis just as for Tier 1 and Tier 2 methods, but the rate at which products are discarded from use may differ from the first-order decay assumption used in Tiers 1 and 2."*

Carbon stock accounting for the HWP pool in the NWL Carbon Inventory included lumber, paper and pulp, durable timber products such as furniture and building materials, as well as decomposable wood in landfills and throughout California's NWLs outside of the original harvest site. It did not include compost, woody mulches, and other woody biomass converted for energy production in processing facilities and power plants. It also did not include forest and perennial crop woody residues used for advanced biofuels like hydrogen, biomethane, and sustainable aviation fuel (IPCC, 2006). While some of these utilization pathways may be incorporated in future inventory efforts, including work associated with SB 905, they were treated as short-lived for this inventory and therefore assumed to be 100% emissive under the HWP carbon accounting framework. However, carbon contained in soil amendments (e.g. compost and mulch) was accounted for within the NWL ecosystem carbon portion of this inventory, categorized under land management to each relevant landscape type. Given its durability (i.e. resistance to degradation) and

diverse utilization pathways, biochar was included in the HWP category and reported within the miscellaneous "Other" end-use bin.

The inventory tracked carbon in HWPs consumed within California by routing annual inflows of harvested material through a mass-balance production and use framework and then simulating transfers into two long-term stock pools: products in use (PIU) and solid waste disposal sites (SWDS; landfills and dumps), with associated emissions quantified for each pool using the HWP-C vR model (Stockman et al. 2014; Groom & Tase 2022). To avoid double counting with CARB's AB 32 GHG Inventory, CO_2e emissions from combustion and SWDS decomposition were only included here as informational items. These emissions (e.g., CO_2, CH_4, N_2O) were instead reported in the GHG inventory (CARB, 2025) while the corresponding carbon stock change was reported in the 2025 NWL Carbon Inventory.

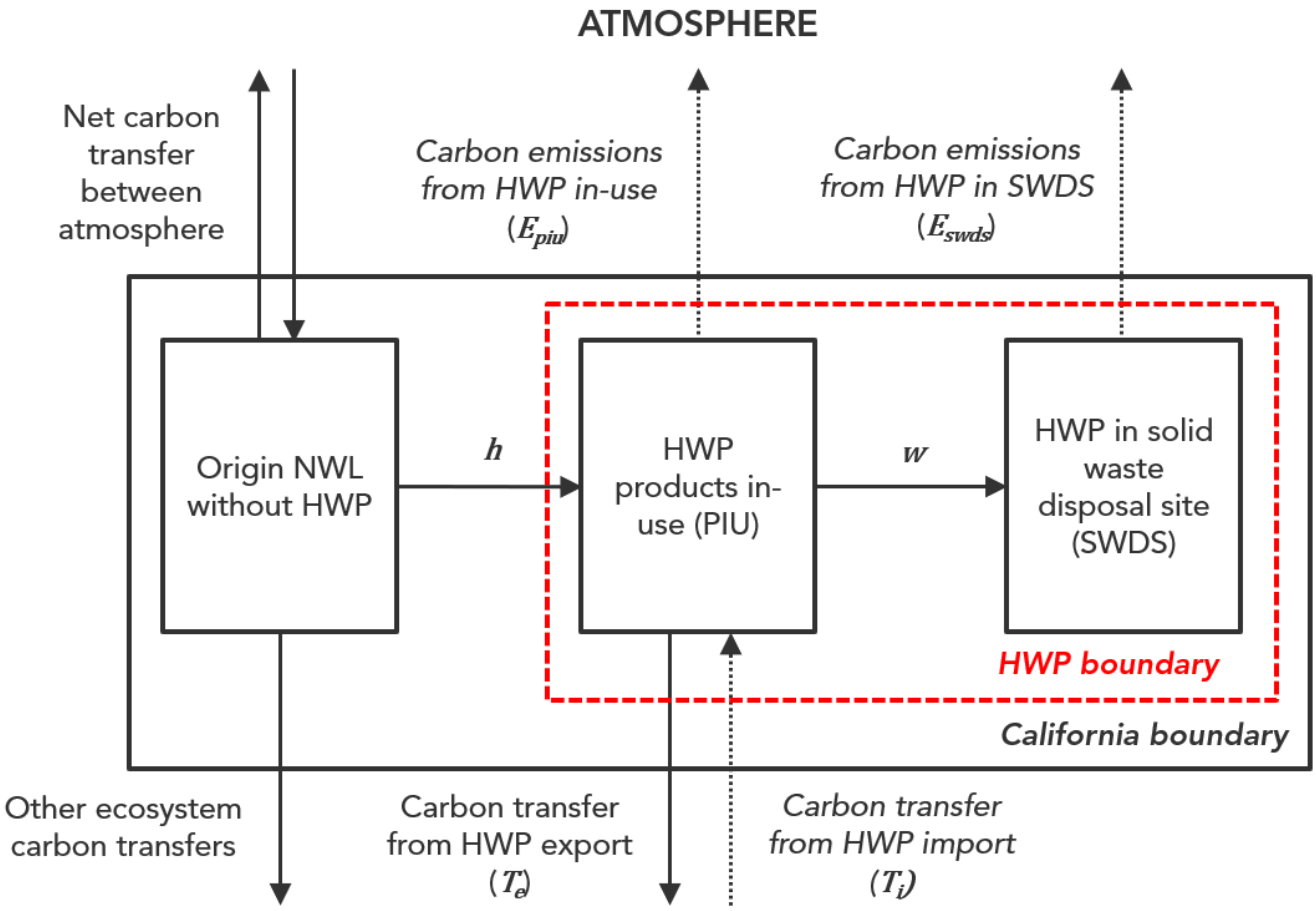

Appendix Figure 8 – System boundary of the HWP Stock-Change approach (adapted from IPCC Guidelines for National GHG Inventories, 2006). Carbon enters the HWP boundary through domestic harvest (H) and imports (T_i), and leaves through exports (T_e) and emissions from products in use (E_{piu}) and solid waste disposal sites (E_{swds}). Dotted arrow lines denote flows that are tracked for informational context but excluded from official NWL inventory reporting.

Spatial and Temporal Extent

The Harvested Wood Products (HWP) component of the NWL Carbon Inventory was statewide in extent, representing carbon stocks and stock change for HWPs within California's borders. In contrast to the biomass and soil components of the inventory, which were spatially explicit and supported mapping and regional stratification, the HWP accounting was aspatial and did not generate wall-to-wall gridded outputs. As a result, the HWP section did not support sub-regional assessments and was not intended to detect localized differences in wood product use, disposal, recycling, or waste management practices.

Estimates were produced annually for the NWL reporting period beginning in 2001 through 2022, the most recent year with finalized inputs. CARB used 2014 as the reference year for statewide carbon stock targets and associated comparisons. However, HWP inventories must also account for historical time series because current HWP stocks reflect accumulated inflows and retirements over many decades, not just the official reporting window. Accordingly, the underlying HWP time series extended back to 1904, when California domestic harvest data began. While the HWP-C vR model run spanned 1904–2022, the availability of key disaggregation variables differed by component dataset. Specifically, ownership-class harvest attribution began in 1952, import inflow estimation began in 1965, and export outflow estimation began in 2001 due to availability of the respective datasets for each component. Prior to these start years, the historical series could represent overall domestic harvest contributions to the statewide HWP pool, but it could not resolve ownership or trade components at the same level of detail. This staged temporal coverage was carried through transparently in the reporting (e.g., ownership and trade series were only shown beginning in their respective start years).

Extending the time series to 1904 improved the internal consistency of carbon stocks during the official reporting period because it better captured legacy inflows that still contributed to modern stocks. However, earlier decades necessarily relied on more limited and aggregated historical data, and the interpretability of disaggregated drivers was constrained to periods where the underlying datasets existed. As a result, trend interpretation for the official period (2001–2022) was most robust, while earlier-period patterns were best used to establish historical context and stock legacy rather than to infer detailed drivers.

Harvested Wood Products Modeling Framework

The influence of land management on harvested wood product (HWP) carbon stocks was represented in HWP-C vR through changes in (i) domestic harvest volumes and species mix, (ii) portfolio of products manufactured and used, (iii) utilization pathways (e.g., long-lived vs. short-lived uses), (iv) retirement and disposal practices, and (v) trade (imports and exports). Model inputs were converted to carbon using product-appropriate unit conversions (e.g., bone dry tons (BDT), thousand cubic feet (MCF), thousand square feet (MSF), thousand

board feet (MBF)) and carbon content assumptions (e.g., density and carbon fraction), and all flows were tracked to ensure conservation of mass across processing, end-use, and disposal pathways (Fonseca, 2005; Skog, 2008; Doraisami et al. 2022).

The inventory included the wood and paper product categories represented in HWP-C vR, organized as (i) primary products (e.g., softwood and hardwood lumber; structural and non-structural panels; veneer/plywood and engineered wood products; pulp; paper and paperboard) and (ii) end-use categories used for reporting and policy interpretation. End-use categories were harmonized with an economic reporting structure (e.g., NAICS-aligned groupings) and included housing and construction, residential repair and remodeling, furniture, paper products, packaging and shipping, manufacturing, and other industrial products, with a residual miscellaneous "other" bin as needed. Domestic harvest flows entered the HWP-C vR workflow as harvest inputs and were allocated through the model's ratio framework from Timber Product Ratios (TPR) to primary products, Primary Product Ratios (PPR) to intermediate products where relevant, and End-Use Ratios (EUR) to end-use categories using California-specific data where available and regional or national defaults where needed (e.g., mill surveys, Timber Product Output (TPO) distributions, industry statistics, and related classification crosswalks) (Scott et al. 2024). These ratio structures were applied in sequence to translate harvest inputs into product- and end-use-specific inflows while preserving mass balance. Imported materials that entered the inventory boundary as primary products were also allocated to end uses using the EUR framework.

Short-lived uses (e.g., fuelwood, process energy, bioenergy) were included within the flow accounting but were treated as immediate oxidation for stock reporting. Consequently, only the fraction of inflows routed to PIU and SWDS contributed to reported HWP stocks (IPCC, 2006). Transfers from PIU to the SWDS pool, and the periodicity of emissions, were simulated using product-specific retirement (discard) functions, SWDS allocation fractions (including diversion and recycling), and SWDS decay and emission generation parameters within HWP-C vR (Stockman et al. 2014). The SWDS disposal and emissions dynamics were calibrated and validated, where feasible, using California waste management datasets, including CalRecycle's Solid Waste Information System (SWIS) facility reporting and CARB and CalRecycle landfill methane information used in the AB 32 GHG Inventory. Recycling and diversion assumptions were evaluated against available California program data (e.g., CalRecycle SB 1383 reporting) and through internal mass-balance checks to ensure consistency across pathways. Additionally, HWP trade was incorporated into certain analyses to reflect California consumption. Exports were tracked and excluded from in-state stocks and stock change prior to PIU and SWDS fate calculations, ensuring that reported HWP stocks represented carbon retained in products used and disposed within California. Imports were tracked as additional inflows to in-state product use and were reported as an informational item, though they were not included in the official NWL reported values.

Domestic Harvest Data

Annual domestic harvest inputs were compiled as roundwood-equivalent volumes and converted to thousand board feet (MBF) for model inputs. Roundwood MBF data was first converted to thousand cubic feet (MCF) before entering the HWP-C vR model framework:

$$MCF_t = \frac{MBF_t}{\left(\frac{BF}{CF}\right)_t}$$

where $\frac{BF}{CF}$ was the year-specific board-feet-per-cubic-foot factor. This factor varies throughout time t due to changes in i) log rules and scaling conventions; ii) the diameter and length mix of harvested logs; and iii) milling technology, all of which affect BF recovery per CF unit. Once harvest was converted to MCF, it was routed through the model ratio structures (TPR →PPR→EUR) and then converted to carbon stocks using the model's CCF-to-metric tons of carbon conversion factors, with primary-product-specific multipliers:

$$MTC_{y,o,e} = \sum_p [H_{y,o}^{CCF} \cdot TPR_{y,o,p} \cdot PPR_{y,p} \cdot EUR_{y,p,e} \cdot k_p]$$

where a given primary product p from an ownership class o and year y was assigned to a specific end-use category e (e.g., housing & construction, repair & remodeling, furniture, packaging, paper, etc.). Land class ownership attribution was assigned to state, federal, private and tribal lands, derived from the best-available identifiers in California administrative reporting when present. The statewide harvest time series was built from California administrative harvest statistics and mill survey results reported in U.S. Forest Service Timber Product Output (TPO) publications (Appendix Table 33). TPO product categories and ownership classes were then matched to corresponding harvest tax reporting records from the California Department of Tax and Fee Administration (CDTFA).

Appendix Table 33 – Data used to support the HWP methodological update.

Input Data	Source (Citation)	Purpose	Brief Description
United States Forest Service (USFS) Timber Product Output (TPO) reports	Bureau of Business and Economic Research (BBER), University of Montana	Domestic production, including species mix and land-ownership class distribution	Units: million board feet (MMBF) Years: 1904-2022
Timber Yield Tax reports	California Department of Trade and Fee Administration (CDTFA)	Domestic production, including species mix and land-ownership class distribution	Units: million board feet (MMBF) Years: 2018-2022
Annual Survey of Manufacturers (ASM)	United States Census Bureau (USCB)	Domestic manufacturing activity for NAICS wood and paper industries	Units: value (nominal $) Years: 2000-2021, except Economic Census years (e.g. 2002, 2007, 2012, 2017)

Commodity Flow Survey (CFS)	United States Census Bureau (USCB); United States Bureau of Transportation Statistics (BTS)	National trade (import/export) origin-destination freight flows by industry	Units: value (nominal $); million metric tons (MMT) Years: 1993-2022 (every 5 years)
United States International Trade Commission (US-ITC) DataWeb reports	United States Census Bureau (USCB)	International trade (import/export) origin-destination freight flows by industry and country	Units: value (nominal $); million metric tons (MMT) Years: 1989-2022
Regional Economic Models, Inc (REMI) modeling outputs	REMI	National and international trade modeling of activity by industry	Units: value (nominal $) Years: 1965-2022
Western Lumber Statistics reports	Western Wood Products Association (WWPA)	Domestic production and secondary market reporting and analytics	Units: value (nominal $); million board feet (MMBF) Years: 2017, 2022
American Panel Association (APA) reports	American Panel Association (APA)	Domestic production and secondary market reporting and analytics	Units: value (nominal $); Million square feet (MMSF) Years: 2017, 2022
Solid Waste Information System (SWIS)	California Department of Resources Recycling and Recovery (CalRecycle)	Solid waste disposal facility inventory, permitting, and inspection records	Units: million metric tons (MMT) Years: 1989-2022
Recycling and Disposal Reporting System (RDRS)	California Department of Resources Recycling and Recovery (CalRecycle)	Solid waste disposal and diversion reporting system	Units: million metric tons (MMT) Years: 2019-2022

Trade Data

Imported and exported HWPs were derived from Regional Economic Modeling, Inc (REMI) modeling outputs, which quantified interstate and international trade flows between California and other regions based on economic activity, input–output linkages, and commodity-specific trade elasticities (Treyz et al. 1991). In short, REMI import and export values were generated endogenously by combining regional demand by industry commodity with market-share equations that allocated each region's demand across competing supplier regions. The domestic market shares that drove these flows followed a gravity-style specification. For industry (i), region (k), and year (t), REMI represents output (O) as demand captured across all markets:

$$O_{i,t}^{k} = \sum_{l=1}^{m} s_{i,t}^{k,l} DD_{i,t}^{l} + EXRWD_{i,t}^{k}$$

where $DD_{i,t}^{l}$ was domestic demand in market region l, $s_{i,t}^{k,l}$ was region k's share of region l's market (with $s_{i,t}^{k,l}$ also referred to as the regional purchase coefficient, RPC), and $EXRWD_{i,t}^{k}$ represented exports from region k to the rest of the world.

REMI provided estimates of wood and paper product flows by North American Industry Classification System (NAICS) sector, which were converted to physical quantities using producer price indices (PPI), sectoral value–to–volume ratios, and commodity-specific conversion factors (e.g., MBF, BDT, or metric tons per dollar of output). These modeled

flows were both calibrated and validated against multiple independent datasets including U.S. Census Bureau Foreign Trade Statistics, U.S. International Trade Commission (USITC) DataWeb, Timber Product Output (TPO) data, and relevant industry sources such as Western Wood Products Associate (WWPA) and American Forest & Paper Association (AF&PA) to ensure consistency with observed domestic production, import, and export volumes by product class and year (Appendix Table 19).

Where direct data was available from trade records, they were used to benchmark and adjust REMI estimates at the commodity level. Economic datasets were converted from nominal dollars ($) to MTC through annual PPI that were calibrated against available years for Annual Survey of Manufactures (ASM), Commodity Flow Survey (CFS), and other industry datasets using:

$$MTC_t^i = \frac{E_t \cdot PPI_t}{E_\theta \cdot (PPI_\theta \cdot MTC_\theta)}$$

where for a given industry (i) and year (t), economic activity (E) was normalized to a reference year (θ) with known E and MTC, using the relative change in the PPI to scale between years.

Imports represented HWPs entering California for use or consumption and were included as inflows to the in-state HWP pool. Exports represented both HWPs produced in California and imported materials that were converted but left the state for use elsewhere and were excluded from reported in-state stocks. Because imported and exported HWPs were already in the form of primary or end-use products, they bypassed the domestic TPR and PPR steps and were mapped directly to the relevant primary or end-use categories in the HWP-C vR model. Export flows were subtracted after the End-Use Ratio (EUR) allocation and before PIU or SWDS fate calculations to avoid double counting in the mass-balance framework.

GHG Emissions

The NWL Carbon Inventory reported carbon stock change for SWDS, fuel, and energy pathways and therefore aligned with the AB 32 GHG Emissions Inventory boundary, which reported in-state emissions from these sectors. Multiple reconciliation steps were applied to align the SWDS boundary, including constraining HWP-C vR modeled CO_2e emissions to the reported AB 32 sector totals. Parameters informed by the AB 32 inventory were also used to calibrate HWP-C vR and to propagate the resulting adjustments through modeled HWP carbon stock outputs, ensuring NWL estimates remained consistent with the GHG inventory boundary. This reconciliation did not produce a 1:1 match across all stock and emissions components between inventories, and official values should be sourced from the appropriate inventory.

For informational purposes, supporting results in Appendix C also disaggregated total CO_2e into its constituent CO_2 and CH_4 components. This speciation was implemented by applying material-specific emission factors for decomposition and combustion, derived

from published literature to the modeled carbon stock flows routed through SWDS and fuel and energy pathways. These estimates were provided to support interpretation and quality checks (e.g., contributions of CO_2 vs. CH_4 relative to literature values), were applied post-hoc to HWP-C vR outputs, and did not affect the NWL reported carbon stock values.

Uncertainty Analysis

Uncertainty in statewide HWP carbon stock change was characterized using a Monte Carlo (MC) framework embedded into the HWP-C vR model (Groom & Tase 2022). The MC simulation was run for 2,000 iterations (HWP-C vR default), and convergence was assessed by examining stabilization of the estimated mean and empirical confidence interval bounds over iterations. For each output year, the MC ensemble was summarized using the iteration mean and an empirical confidence interval of 90%, consistent with the plotted outputs.

The MC simulation shuffled a set of key model inputs and parameters (≥16) to determine the triangular distribution from which the range of random proportions were drawn, with one proportion drawn from each parameter per iteration (Bonate, 2001). To improve sampling efficiency and representative coverage across distributions, the model used Latin Hypercube Sampling to generate the underlying uniform random draws, which were then transformed to triangular distributions for each parameter.

Across iterations, uncertainty was propagated through the full HWP-C vR workflow (e.g., inputs, product ratios, disposal, etc.). For select parameter sets where uncertainty was expected to be systematically related (e.g., multi-year blocks for product ratios, paired discard parameters), correlation amongst the associated random variables was imposed with a moderate positive relationship using a Pearson correlation of 0.5, implemented via a Cholesky-based procedure.

QA/QC Activities

A comprehensive literature search found no published alternative attempts to estimate California statewide harvested wood product (HWP) carbon stocks. Although a range of alternative methodologies exist, time and resource constraints limited the scope of this inventory iteration to implementing a single approach (Lucey et al. 2024). As a result, no external or internal benchmarks were available for comparison with the total HWP inventory estimate. However, numerous stepwise verification activities were conducted throughout the inventory development process.

QA/QC for the HWP inventory emphasized step-wise mass balance and reconciliation checks from raw data intake through final modeled fates, to ensure that wood and carbon were neither inadvertently created nor lost across processing steps. At the data collection stage, harvest, production, and trade inputs were screened for completeness (coverage by year, units, and product type), harmonized to consistent units and classifications, and checked for internal consistency (e.g., totals equaled the sum of component categories after crosswalks and unit conversions). Within the modeling workflow, mass balance was verified

at each transformation through unit conversions, allocation through ratio structures (e.g., TPR/PPR/EUR where applicable), and subsequent partitioning into PIU and SWDS pathways. Additional checks compared annual trajectories and category shares against validation data and confirmed that boundary treatments preserved accounting identity across the full system. Collectively, these procedures provided a transparent audit trail linking reported HWP stock changes to underlying datasets and ensured that final estimates were mass-conserving, reproducible, and consistent with the inventory boundary definition.

2018 Methods

Harvested wood products were not included in the 2018 NWL Carbon Inventory.

Future Work

Field-Based Measurements

Field-based measurements provide the empirical foundation needed to calibrate and validate model and satellite-derived estimates. They anchor inventory results in direct observations and improve the accuracy of carbon stock and GHG flux estimates. The current inventory leveraged a curated database of approximately 3,000 soil carbon measurements from across California. It also incorporated tree inventory data and field-based measurements of woody and herbaceous biomass from the USDA FIA-DB program, the BLM AIM program, and other agency, academic, and non-profit partners. In addition, published, annual eddy covariance flux tower budgets were used alongside chamber-based data to estimate regional emission factors for wetland GHG fluxes. However, additional field-based data are needed to help maintain robust temporal coverage, capture underrepresented regions and land types (e.g., the Mojave Desert), improve representation of management and disturbance effects (e.g., cropland management), and expand estimates to include other GHG fluxes and carbon pools (e.g., soil inorganic carbon), as appropriate. Ongoing and future efforts aim to address these data gaps through coordinated field data collection campaigns. These campaigns will expand temporal and spatial coverage of biomass, soil carbon, and GHG fluxes in ways that support integration with remote sensing products and models.

Remote Sensing

Remote sensing offers consistent, statewide observations that are essential for tracking wall-to-wall changes in land cover, vegetation, and carbon dynamics over time. It detects and measures what has occurred on the land surface based on satellite and airborne imagery, often at daily or weekly intervals. The current inventory relied on Landsat, MODIS, and NAIP-derived remote sensing products to map land cover, monitor disturbances, and help

estimate biomass and soil carbon over the inventory period. Going forward, The NWL Carbon Inventory will incorporate new remote sensing products that expand the ability to detect and attribute ecological disturbances, track vegetation dynamics, and characterize fine-scale changes in land cover using tailored, higher-resolution NAIP imagery, LiDAR, and Sentinel-2 data products. These efforts will help support more detailed accounting of carbon and GHG fluxes within California's land base over time. Multiple projects and partnerships are currently underway with academic, state, and federal organizations towards this end.

Activity Tracking

Accurately estimating and attributing changes in carbon stocks and GHG fluxes requires not only robust field-based measurements and remote sensing, but also systematic tracking of disturbances and land management activities occurring across the landscape. In practice, this kind of tracking involves documenting and compiling spatially explicit records of when, where, and what types of land management and disturbance activities occur on the ground. This information is essential for validating remote sensing data, capturing and quantifying the effects of disturbance and management on carbon stocks and GHG fluxes, and attributing observed changes to their underlying drivers. The current inventory used LANDFIRE disturbance data to identify areas affected by wildfire, prescribed fire, and vegetation management. Some additional disturbance dynamics (e.g., livestock grazing) were implicitly represented through the remote sensing inputs described above; however, comparable reported datasets related to other land management activities (such as the application of fertilizers and other soil amendments to croplands, or the physical restoration of streams and wetlands) were not incorporated due to the absence of consistent, temporally resolved, and spatially explicit data sources. Efforts are underway to coordinate tracking of additional disturbance and land management information across agencies and partners, enabling this critical information to be incorporated into future inventory updates.

Beyond documenting where and when disturbances and land management occur, tracking the downstream fate of harvested biomass is essential for quantifying how activities such as forest and fuels management and perennial cropland management influence carbon storage and emissions over time. Accurately representing HWP and other harvested biomass requires tracing the journey from removal to use, capturing how the biomass is processed, transformed, and stored within California—whether sourced from within the state's borders or imported from elsewhere. The current inventory combines available state and federal data to estimate harvest volumes, product allocation, and material fate, providing insight into how harvested biomass contributes to durable and non-durable carbon pools. Ongoing and future work aims to strengthen these linkages by improving data integration and chain-of-custody tracking, supporting a more complete representation of harvested biomass flows and associated carbon dynamics within California.

Modeling

This inventory update has made many strides in improving accuracy, functionality, transparency, reproducibility, and inclusion of more ecosystems and carbon pools. Ultimately, for carbon neutrality accounting, the NWL Carbon Inventory will require a strengthened ability to not only quantify carbon stocks, but also sequestration and emissions in terms of CO_2e. This can only be done through incorporating more advanced modeling into the inventory. Models serve as a tool for integrating field-based data, remote sensing products, and reported activity information to generate and scale up ecosystem carbon stock and GHG flux estimates. Process-based models simulate the underlying physical and biological processes that control carbon cycling and GHG dynamics (e.g., plant growth and decomposition), while empirical models derive relationships directly from measured data to estimate spatial and temporal trends. Both kinds of models vary in complexity, with, for instance, empirical models ranging from simple mathematical relationships to complex data-driven frameworks that can approximate process-based dynamics. The current inventory applied a suite of empirical models to estimate biomass and soil carbon stocks statewide. This included use of the LANDFIRE-C model for forest and shrubland biomass carbon, a machine learning model for mineral soil carbon, and the Harvested Wood Products Carbon Model for HWPs. Future work will focus on refining models by incorporating new field data, remote sensing products, and tracked activity data to improve training, validation, and temporal consistency. In parallel, open-source process-based models will be integrated to support more detailed assessment of disturbance and land management impacts, strengthen the empirical soil carbon modeling framework, refine existing GHG flux estimates from wetlands, and add a GHG component to other land types such as croplands. Combined, these efforts will continue to improve the temporal and spatial accuracy of modeled carbon dynamics while expanding the inventory's capacity to quantify GHG fluxes across California's landscapes.

References

Anderson, C. B., Joseph, M. B., Söthe, C., Mendes, F. D. S., Maschler, T., McCarthy, R. C., Mascaro, J., O'Shea, T., Rosenthal, A., & Marvin, D. C. (2025). Forest Carbon Diligence: Digital MRV for Jurisdictional and Voluntary Offsets Markets.

Arias-Ortiz, A., Wolfe, J., Bridgham, S. D., Knox, S., McNicol, G., Needelman, B. A., ... & Holmquist, J. R. (2024). Methane fluxes in tidal marshes of the conterminous United States. *Global change biology*, *30*(9), e17462.

Battles, J. J., Gonzalez, P., Robards, T., Collins, B. M. & Saah, D.S. (2013). California Forest and Rangeland Greenhouse Gas Inventory Development. Final Report, CARB Contract 10-778. California Air Resources Board.

Battles, J. J., Bell, D. M., Kennedy, R. E., Saah, D. S., Collins, B. M., York, R. A., Sanders, J. E. & Lopez-Ornelas, F. (2018). Innovations in measuring and managing forest carbon stocks in California. Rep California's Fourth Clim Change Assess, 99.

Bergamaschi, B., & Windham-Myers, L. (2018). *AmeriFlux AmeriFlux US-Srr Suisun marsh-Rush Ranch*. Lawrence Berkeley National Laboratory (LBNL), Berkeley, CA (United States). AmeriFlux; United States Geological Survey; USGS.

Bjorkman, J., Thorne, J. H., Hollander, A., Roth, N. E., Boynton, R. M., de Goede, J., ... & Quinn, J. (2015). Biomass, Carbon Sequestration, and Avoided Emissions: Assessing the Role of Urban Trees in California. Information Center for the Environment, University of California, Davis.

Bogard, M. J., Bergamaschi, B. A., Butman, D. E., Anderson, F., Knox, S. H., & Windham-Myers, L. (2020). Hydrologic export is a major component of coastal wetland carbon budgets. *Global Biogeochemical Cycles*, *34*(8), e2019GB006430.

Bonate, P. L. (2001). A brief introduction to Monte Carlo simulation. *Clinical pharmacokinetics*, *40*(1), 15-22.

Bureau of Land Management (BLM). (2025). Natl AIM TerrADat Hub. U.S. Department of the Interior Bureau of Land Management. Retrieved from https://gbp-blm-egis.hub.arcgis.com/datasets/BLM-EGIS::blm-natl-aim-terradat-hub/about

CAL FIRE. (2015). Vegetation (fveg) - CALFIRE FRAP [ds1327]. Retrieved from https://map.dfg.ca.gov/metadata/ds1327.html

CAL FIRE. (2025). Historical Wildland Fire Perimeters. Fire and Resource Assessment Program. Retrieved from https://calfire-forestry.maps.arcgis.com/home/item.html?id=c3c10388e3b24cec8a954ba10458039d

California Air Resources Board (CARB). (2018a). An inventory of ecosystem carbon for California's natural & working lands. Retrieved from https://ww2.arb.ca.gov/california-natural-and-working-lands-inventory

California Air Resources Board (CARB) (2018b). Technical support document for the natural & working lands inventory. Retrieved from https://ww2.arb.ca.gov/california-natural-and-working-lands-inventory

California Air Resources Board (CARB). (2022). 2022 Scoping Plan: Appendix I – Natural and Working Lands technical support document.

California Air Resources Board (CARB). (2025). California greenhouse gas emissions from 2000 to 2023: Trends of emissions and other indicators.

California Department of Water Resources (DWR). (2022). Statewide Crop Mapping—California Natural Resources Agency Open Data. Retrieved January 1, 2026, from *https://data.cnra.ca.gov/dataset/statewide-crop-mapping*.

California Natural Resources Agency (CNRA). (2022). Natural and Working Lands Climate Smart Strategy. Retrieved from https://resources.ca.gov/-/media/CNRA-Website/Files/Initiatives/Expanding-Nature-Based-Solutions/CNRA-Report-2022---Final_Accessible.pdf

California Natural Resources Agency (CNRA). (2024). California's Nature-Based Solutions Climate Targets 2024. Retrieved from https://resources.ca.gov/-/media/CNRA-Website/Files/Initiatives/Expanding-Nature-Based-Solutions/Californias-NBS-Climate-Targets-2024.pdf

Christensen, G. A., Gray, A. N., Kuegler, O., Tase, N. A., & Rosenberg, M. (2017). AB 1504 California forest ecosystem and harvested wood product carbon inventory: 2006–2015. Final Report. California Department of Forestry and Fire Protection agreement, (7CA02025).

Christensen, G. A., Gray, A. N., Kuegler, O., Tase, N. A., & Rosenberg, M. (2021). AB 1504 California forest ecosystem and harvested wood product carbon inventory: 2019 Reporting Period Data update. Final Report. California Department of Forestry and Fire Protection agreement, (8CA04056).

Deverel, S. J., Dore, S., & Schmutte, C. (2020). Solutions for subsidence in the California Delta, USA, an extreme example of organic-soil drainage gone awry. *Proceedings of the International Association of Hydrological Sciences*, *382*, 837-842.

Dewitz, J. (2025). LANDFIRE 2001 Base Map. Department of the Interior U.S. Geological Survey. doi:10.5066/P13KXTGM

Doraisami, M., Kish, R., Paroshy, N., Domke, G., Thomas, S., & Martin, A. (2022). GLOWCAD: A global database of woody tissue carbon concentrations and fractions. DRYAD.

EarthDefine. (2012). California Urban Tree Canopy (2012), Version 1. Retrieved from https://www.fs.usda.gov/r05/state-tribal-forestry/californias-urban-tree-canopy

Fonseca, M. (2005). The measurement of roundwood: methodologies and conversion ratios. CABI Publishing.

Gao, X., Koven, C. D., & Kueppers, L. M. (2024). Allometric relationships and trade-offs in 11 common M editerranean-climate grasses. *Ecological Applications*, *34*(4), e2976.

Gonzalez, P., Battles, J. J., Collins, B. M., Robards, T., & Saah, D. S. (2015). Aboveground live carbon stock changes of California wildland ecosystems, 2001–2010. *Forest Ecology and Management*, *348*, 68-77.

Groom, J., & Tase, N. (2022). Harvested wood products carbon model, version R documentation. California Department of Forestry and Fire Protection.

i-Tree. (2024). i-Tree Eco (version 6.0.38) . i-Tree / USDA Forest Service. Retrieved from https://www.itreetools.org/tools/i-tree-eco.

Intergovernmental Panel on Climate Change (IPCC). (2006). IPCC Guidelines for National Greenhouse Gas Inventories. Retrieved from https://www.ipcc-nggip.iges.or.jp/public/2006gl/

Intergovernmental Panel on Climate Change (IPCC). (2014). 2013 Supplement to the 2006 IPCC Guidelines for National Greenhouse Gas Inventories: Wetlands. Retrieved from https://www.ipcc.ch/site/assets/uploads/2018/03/Wetlands_Supplement_Entire_Report.pdf

Jones, M. O., Robinson, N. P., Naugle, D. E., Maestas, J. D., Reeves, M. C., Lankston, R. W., & Allred, B. W. (2021). Annual and 16-day rangeland production estimates for the western United States. *Rangeland Ecology & Management*, *77*, 112-117.

Kummerow, J., J.D. Krause, and W. Jow. 1977. Root systems of chaparral shrubs. Oecologia 29:163–177.

LANDFIRE. (2021). LF 2016 Remap Project Close-Out Report. Department of the Interior U.S. Geological Survey. Retrieved from https://landfire.gov/sites/default/files/documents/LF2016%20Remap_Project_Closeout_Report_Final%20PDF.pdf

LANDFIRE. (2022a). Annual Disturbance - Dist. Department of the Interior, Geological Survey, and U.S. Department of Agriculture. Retrieved from https://landfire.gov/data

LANDFIRE. (2022b). Existing Vegetation Cover. Department of the Interior, Geological Survey, and U.S. Department of Agriculture. Retrieved from https://landfire.gov/data

LANDFIRE. (2022c). Existing Vegetation Height. Department of the Interior, Geological Survey, and U.S. Department of Agriculture. Retrieved from https://landfire.gov/data

LANDFIRE. (2022d). Existing Vegetation Type. Department of the Interior, Geological Survey, and U.S. Department of Agriculture. Retrieved from https://landfire.gov/data

Li, C., Frolking, S., & Frolking, T. A. (1992). A model of nitrous oxide evolution from soil driven by rainfall events: 1. Model structure and sensitivity. *Journal of Geophysical Research: Atmospheres*, *97*(D9), 9759-9776.

Liu, H., Jin, Y., Roche, L. M., T O'Geen, A., & Dahlgren, R. A. (2021). Understanding spatial variability of forage production in California grasslands: delineating climate, topography and soil controls. *Environmental Research Letters*, *16*(1), 014043.

Lucey, T. K., Tase, N., Nepal, P., Bergman, R. D., Nicholls, D. L., Khatri, P., Sahoo, K., & Gray, A. N. (2024). A synthesis of harvested wood product carbon models. U.S. Department of Agriculture, Forest Service, Pacific Northwest Research Station.

McBratney, A. B., Santos, M. M., & Minasny, B. (2003). On digital soil mapping. *Geoderma*, *117*(1-2), 3-52.

McPherson, E. G. (2010). Selecting reference cities for i-Tree Streets. Arboriculture and Urban Forestry 36 (5): 230-240, 36(5), 230-240.

Miller, P.C.. and E. Ng. 1977. Root:shoot biomass ratios in shrubs in southern California USA and central Chile. Madrono 24:215–223.

Morandé, J. A., Stockert, C. M., Liles, G. C., Williams, J. N., Smart, D. R., & Viers, J. H. (2017). From berries to blocks: carbon stock quantification of a California vineyard. Carbon balance and management, 12(1), 5.

Ocean Protection Council (OPC). (2024). Blue Carbon Ecosystem Data and Model Assessment Report. Retrieved from https://opc.ca.gov/wp-content/uploads/2024/07/Blue-carbon-model-assessment-report-508.pdf

Office of Energy Infrastructure Safety. (2025). Energy Infrastructure Map. Personal Communications.

Ohmann, J. L., & Gregory, M. J. (2002). Predictive mapping of forest composition and structure with direct gradient analysis and nearest-neighbor imputation in coastal Oregon, USA. Canadian Journal of Forest Research, 32(4), 725-741.

Oliphant, A., Graham, N., Monohan, C. (2024). Greenhouse Gas Fluxes at the Clover Valley Ranch Meadow Restoration Project. The Sierra Fund Technical Report (2024) Prepared for California Department of Fish and Wildlife (CDFW).

O'Riordan, R., Davies, J., Stevens, C., & Quinton, J. N. (2021). The effects of sealing on urban soil carbon and nutrients. *Soil*, *7*(2), 661-675.

Pereira, M. C., O'Riordan, R., & Stevens, C. (2021). Urban soil microbial community and microbial-related carbon storage are severely limited by sealing. *Journal of Soils and Sediments*, *21*(3), 1455-1465.

Point Blue Conservation Science (2023). Evidence for the Multiple Benefits of Wetland Conservation in North America: Carbon, Biodiversity, and Beyond. Retrieved from https://www.pointblue.org/wetland-multiple-benefits.

Raciti, S. M., Hutyra, L. R., & Finzi, A. C. (2012). Depleted soil carbon and nitrogen pools beneath impervious surfaces. *Environmental Pollution*, *164*, 248-251.

Reed, C. C., Merrill, A. G., Drew, W. M., Christman, B., Hutchinson, R. A., Keszey, L., ... & Sullivan, B. W. (2021). Montane meadows: a soil carbon sink or source?. *Ecosystems*, *24*(5), 1125-1141.

Reeves, M., & Frid, L. (2016). The Rangeland Vegetation Simulator: A user-driven system for quantifying production, succession, disturbance and fuels in non-forest environments. In Iwaasa, Alan; Lardner, HA (Bart); Schellenberg, Mike; Willms, Walter; Larson, Kathy, eds. Proceedings of the 10th International Rangelands Congress: The Future Management of Grazing and Wild Lands in a High-Tech World; 16-22 July, 2016; Saskatoon, Saskatchewan. The International Rangeland Congress. p. 1062-1063.

Riley, K. L., Grenfell, I. C., Shaw, J. D., & Finney, M. A. (2022). TreeMap 2016 dataset generates CONUS-wide maps of forest characteristics including live basal area, aboveground carbon, and number of trees per acre. Journal of Forestry, 120(6), 607-632.

Rocha, A. V., & Goulden, M. L. (2010). Drought legacies influence the long-term carbon balance of a freshwater marsh. *Journal of Geophysical Research: Biogeosciences*, *115*(G3).

Saah D., J. Battles, J. Gunn, T. Buchholz, D. Schmidt, G. Roller, and S. Romsos. (2016). Technical Improvements to the Greenhouse Gas (GHG) Inventory for California Forests and Other Lands. Final Report, CARB Contract 14-757. California Air Resources Board.

San Francisco Estuary Institute (SFEI). (2024). EcoAtlas. Retrieved from https://www.ecoatlas.org/

Scott, S., Dillon, T., & Morgan, T. (2024). California's Forest Products Industry and Timber Harvest, 2021. Bureau of Business and Economic Research, University of Montana.

Shahan, J., Chu, H., Windham-Myers, L., Matsumura, M., Carlin, J., Eichelmann, E., ... & Oikawa, P. (2022). Combining eddy covariance and chamber methods to better constrain CO2 and CH4 fluxes across a heterogeneous restored tidal wetland. *Journal of Geophysical Research: Biogeosciences*, *127*(9), e2022JG007112.

Skog, K. E. (2008). Sequestration of carbon in harvested wood products for the United States. *Forest products journal. Vol. 58, no. 6 (June 2008): Pages 56-72*.

Stenzel, J. E., Bartowitz, K. J., Hartman, M. D., Lutz, J. A., Kolden, C. A., Smith, A. M., ... & Hudiburg, T. W. (2019). Fixing a snag in carbon emissions estimates from wildfires. *Global change biology*, *25*(11), 3985-3994.

Stockman, K., Anderson, N., Young, J., Skog, K., Healey, S., Loeffler, D., . . . Morrison, J. (2014). Estimates of carbon stored in harvested wood products from United States Forest Service Pacific Southwest Region, 1909-2012. United States Forest Service.

Thorne, J.H., Hollander, A., Shapiro, K. D., Boynton, R.M. 2023. Change Analysis of California's Urban Forests. Information Center for the Environment, University of California, Davis.

Treyz, G. I., Rickman, D. S., & Shao, G. (1991). The REMI economic-demographic forecasting and simulation model. *International Regional Science Review*, *14*(3), 221-253.

Ugbaje, S. U., Karunaratne, S., Bishop, T., Gregory, L., Searle, R., Coelli, K., & Farrell, M. (2024). Space-time mapping of soil organic carbon stock and its local drivers: Potential for use in carbon accounting. *Geoderma*, *441*, 116771.

U.S. Census Bureau. (2021). 2010 Census Urban Area Reference Map. Geography Division. Retrieved from https://www.census.gov/geographies/reference-maps/2010/geo/2010-census-urban-areas.html

U.S. Census Bureau. (2023a). 2020 Census Urban Areas Wall Map. Geography Division. Retrieved from https://www.census.gov/geographies/reference-maps/2020/geo/2020-census-urban-areas.html

U.S. Census Bureau. (2023b). 2022 TIGER/Line® Shapefiles: Roads. Geography Division, U.S. Department of Commerce. Retrieved from https://www.census.gov/cgi-bin/geo/shapefiles/index.php?layergroup=Roads&year=2022

U.S. Department of Agriculture (USDA). (2010). *CropScape -Cropland Data Layer.* [Online] Available at: https://nassgeodata.gmu.edu/CropScape/ USDA, 2012. *CropScape -Cropland Data Layer.* [Online] Available at: https://nassgeodata.gmu.edu/CropScape/

U.S. Environmental Protection Agency (EPA). (2024). Inventory of U.S. Greenhouse Gas Emissions and Sinks: 1990-2022. Retrieved from https://www.epa.gov/system/files/documents/2024-04/us-ghg-inventory-2024-main-text_04-18-2024.pdf

U.S. Forest Service (USFS). (2012). Forest inventory and analysis database of the United States of America (FIA). Biodiversity and Ecology, 4: 225-231.

U.S. Forest Service (USFS). (2025). California Urban Canopy Data 2018, 2022. Retrieved from https://www.fs.usda.gov/r05/state-tribal-forestry/california-urban-canopy-data

Urban Forest Ecosystem Institute. (2025). California Urban Forest Inventory. Cal Poly State University, San Luis Obispo. Retrieved from https://lookerstudio.google.com/u/0/reporting/880d448d-de26-48d3-b563-0c6317e456e4/page/jWHKB

Ventura, J., Pawlak, C., Honsberger, M., Gonsalves, C., Rice, J., Love, N. L., ... & Ritter, M. (2024a). Individual tree detection in large-scale urban environments using high-resolution multispectral imagery. International Journal of Applied Earth Observation and Geoinformation, 130, 103848.

Ventura, J., Pawlak, C., Honsberger, M., Gonsalves, C., Rice, J., Love, N. L., ... & Ritter, M. (2024b). Results: Individual tree detection in large-scale urban environments using high-

resolution multispectral imagery [dataset]. Open Science Framework. DOI 10.17605/OSF.IO/4S859

Wang, Y. H., Shi, Y. M., Sun, G. D., Li, J. T., Chen, H., Chow, A. T., ... & Wang, J. J. (2020). Soil organic carbon signature under impervious surfaces. *ACS Earth and Space Chemistry*, *4*(10), 1785-1792.

Williams, C. A., Collatz, G. J., Masek, J., & Goward, S. N. (2012). Carbon consequences of forest disturbance and recovery across the conterminous United States. Global Biogeochemical Cycles, 26(1).

Xu, Q., Man, A., Fredrickson, M., Hou, Z., Pitkänen, J., Wing, B., ... & Greenberg, J. A. (2018). Quantification of uncertainty in aboveground biomass estimates derived from small-footprint airborne LiDAR. *Remote sensing of environment*, *216*, 514-528.

Yu, Y., Saatchi, S. S., Walters, B. F., Ganguly, S., Li, S., Hagen, S., Melendy, L., Nemani, R. R., Domke, G. M., & Woodall, C. W. (2021). Carbon Pools across CONUS using the MaxEnt Model, 2005, 2010, 2015, 2016, and 2017 (Version 1). ORNL Distributed Active Archive Center. https://doi.org/10.3334/ORNLDAAC/1752.

Yu, Y., Saatchi, S., Domke, G. M., Walters, B., Woodall, C., Ganguly, S., Li, S., Kalia, S., Park, T., Hagen, S. C., & Melendy, L. (2022). Making the US national forest inventory spatially contiguous and temporally consistent. Environmental Research Letters, 17(6), 065002.